NOTE TO USERS

This reproduction is the best copy available.

UMI°

•

Mathematical Modeling of Airflow, Heat and Mass Transfer during Forced Convection Cooling of Produce in Ventilated Packages

By

Jalal Dehghannya

Department of Bioresource Engineering

McGill University, Montreal

Canada

December 2008

A thesis submitted to McGill University in partial fulfillment of the requirements of the degree of

Doctor of Philosophy



Library and Archives Canada

Published Heritage Branch

395 Wellington Street Ottawa ON K1A 0N4 Canada Bibliothèque et Archives Canada

Direction du Patrimoine de l'édition

395, rue Wellington Ottawa ON K1A 0N4 Canada

> Your file Votre référence ISBN: 978-0-494-66271-7 Our file Notre référence ISBN: 978-0-494-66271-7

NOTICE:

The author has granted a non-exclusive license allowing Library and Archives Canada to reproduce, publish, archive, preserve, conserve, communicate to the public by telecommunication or on the Internet, loan, distribute and sell theses worldwide, for commercial or non-commercial purposes, in microform, paper, electronic and/or any other formats.

The author retains copyright ownership and moral rights in this thesis. Neither the thesis nor substantial extracts from it may be printed or otherwise reproduced without the author's permission.

AVIS:

L'auteur a accordé une licence non exclusive permettant à la Bibliothèque et Archives Canada de reproduire, publier, archiver, sauvegarder, conserver, transmettre au public par télécommunication ou par l'Internet, prêter, distribuer et vendre des thèses partout dans le monde, à des fins commerciales ou autres, sur support microforme, papier, électronique et/ou autres formats.

L'auteur conserve la propriété du droit d'auteur et des droits moraux qui protège cette thèse. Ni la thèse ni des extraits substantiels de celle-ci ne doivent être imprimés ou autrement reproduits sans son autorisation.

In compliance with the Canadian Privacy Act some supporting forms may have been removed from this thesis.

While these forms may be included in the document page count, their removal does not represent any loss of content from the thesis.

Conformément à la loi canadienne sur la protection de la vie privée, quelques formulaires secondaires ont été enlevés de cette thèse.

Bien que ces formulaires aient inclus dans la pagination, il n'y aura aucun contenu manquant.



ABSTRACT

Forced convection cooling process is the most widely used method of cooling to extend shelf life of horticultural produce after harvest. However, heterogeneous cooling of produce inside different parts of ventilated packages is a serious problem. Therefore, it is essential to design packages that facilitate air circulation throughout the entire package to provide uniform cooling. Selection of appropriate combinations of air temperature and velocity for a given vent design is currently done largely by experimental trial and error approach. A more logical approach in designing new packages, to provide uniform cooling, is to develop mathematical models that would be able to predict package performance without requiring costly experiments.

In this study, mathematical models of simultaneous airflow, heat and mass transfer during forced convection cooling process were developed and validated with experimental data. The study showed that produce cooling is strongly influenced by different ventilated package designs. Generally, cooling uniformity was increased by increasing number of vents from 1 (2.4% vent area) to 5 (12.1% vent area). More uniform produce cooling was obtained at less cooling time when vents were uniformly distributed on package walls with at least 4.8% opening areas. Aerodynamic studies showed that heterogeneity of airflow distribution during the process is strongly influenced by different package vent configurations. The highest cooling heterogeneity index (108%) was recorded at 2.4% vent area whereas lowest heterogeneity index (0%) was detected in a package with 12.1% vent area.

The magnitudes of produce evaporative cooling (EC) and heat generation by respiration (HG) as well as the interactive effects of EC, HG and package vent design on produce cooling time were also investigated. Considerable differences in cooling times were obtained with regard to independent and simultaneous effects of EC and HG in different package vent configurations. Cooling time was increased to about 47% in a package with 1 vent compared to packages with 3 and 5 vents considering simultaneous effects of EC and HG. Therefore, the effects of EC and

HG can be influential in designing the forced-air precooling system and consequently, in the accurate determination of cooling time and the corresponding refrigeration load.

RÉSUMÉ

Le refroidissement par convection forcée est la méthode de refroidissement après-récolte préférée lorsqu'une prolongation de la durée de conservation à l'étalage est visée. Cependant, le refroidissement hétérogène de fruits et légumes frais à divers endroits dans un emballage ventilé pose un important problème. Il devient donc essentiel de concevoir un emballage qui facilite la circulation d'air à travers l'ensemble du contenu, afin de permettre son refroidissement uniforme. La sélection de combinaisons appropriées de température et de vitesse de l'air circulé, pour un agencement spécifique de fentes, est présentement faite selon une méthode d'essais et erreurs. De prédire la performance d'un emballage par modélisation mathématique, plutôt que de compléter une série d'expériences coûteuses, représenterait une démarche plus logique lors de la conception de nouveaux emballages livrant un refroidissement uniforme.

Dans cette étude une modélisation mathématique simultanée du débit d'air, du transfert thermique et du transfert de masse durant le processus de refroidissement par convection forcée fut développé et validé avec des données expérimentales. Cette étude démontra que l'agencement de différents emballages, particulièrement des fentes, a une importante influence sur le refroidissement des denrées qui y sont contenus. En général, l'uniformité de refroidissement fut améliorée par une hausse du nombre de fentes de 1 à 5, soit une hausse de 2.4% à 12.1% de la surface de l'emballage occupée par les fentes. Des fentes couvrant au moins 4.8% de la surface et disposées uniformément sur les côtés de l'emballage donnèrent un refroidissement plus uniforme et plus rapide. Des études aérodynamiques indiquèrent que la non-homogénéité de la distribution du débit d'air durant le refroidissement était fortement liée a l'agencements des fentes. L'indice de hétérogénéité du refroidissement le plus élevé (108%) fut enregistré pour un pourcentage de la surface en fentes de 2.4%, tandis que pour des fentes couvrant 12.1% de la surface, l'indice fut à son plus bas niveau (0%).

De même, l'effet de l'ampleur du refroidissement par évaporation (REF), du réchauffement lié à la respiration (REC) de la denrée, de leur l'interaction, et de l'agencement des fentes, sur le temps de refroidissement de la denrée, fut étudié. Pour différents agencements de fentes, d'importantes différences en temps de refroidissement furent liés aux effets indépendants et simultanées du REF et REC. Prenant compte des effets simultanés du REF et REC, le temps de refroidissement en emballage fut 47% plus long pour un emballage avec une seule fente, qu'un emballage ayant 3 ou 5 fentes. Il est donc important de tenir en compte les effets du REF et REC lors de la conception d'un système de pré-réfrigération par convection forcée, et donc aussi dans un calcul précis du temps de refroidissement et de la charge calorifique correspondante.

ACKNOWLEDGEMENTS

First and foremost, I humbly praise the potent God for His will and divine providence during the entire period of my Ph.D. studies. I also wish to express my deepest heartful gratitude to my family for emotional companionship and supports as well as my father, mother, sisters and brother for their affection and words of encouragement.

I would like to sincerely appreciate my principal supervisor, Dr. Michael Ngadi, for his endless patience, great humor, continued encouragements and valuable comments. No doubt, I mainly owe my professional development to his insightful leadership, respectful manner to his profession, strong work ethic, never-discouraging attitude, and indeed to his willingness to listen. I am honestly thankful for his vast confidence on me throughout the course of my Ph.D. program that allowed this research to come true.

My acknowledgement is also extended to my thesis co-supervisor, Dr. Clement Vigneault, for his motivational criticisms and discussions. I would also like to sincerely thank Dr. Shiv O. Prasher, chair of the Department of Bioresource Engineering, for his kind support, valuable advice and honest help during the course of my studies. I realize the value of honest help and this makes me more appreciative of his supports. I wish to acknowledge my Ph.D. program committee members, Dr. Vijaya Raghavan and Dr. Hosahalli S. Ramaswami for their constructive criticisms and suggestions during my comprehensive exam.

I would also like to appreciate Dr. Yousef Karimi for his encouragement, kind support and our valuable discussions. Appreciation also goes to all students in the Food Engineering Group especially Mr. Akinbode Adedeji and Mr. Bob Xiang for their understanding and for building a friendly environment during my stay at McGill.

I am thankful to the Graduate Studies Coordinator and Administrative Assistant of the Department of Bioresource Engineering, Ms. Susan Gregus, for her kind support and always-ready-to-assist character. I would also like to acknowledge the

support of the department secretarial staff, Ms. Trish Singleton and Ms. Abida Subhan.

The acknowledgement is extended to the Natural Sciences and Engineering Research Council of Canada (NSERC) for funding a part of this study. And last but not least, I acknowledge the financial support of the Ministry of Science, Research and Technology of Iran for a research award for my Ph.D. program.

PART OF THE THESIS HAS BEEN PUBLISHED

Dehghannya, J., Ngadi, M. and Vigneault, C. Simultaneous aerodynamic and thermal analysis during cooling of stacked spheres inside ventilated packages. Chemical Engineering and Technology 31(11):1651-1659.

PARTS OF THE THESIS HAVE BEEN SUBMITTED FOR PUBLICATION

Dehghannya, J., Ngadi, M. and Vigneault, C. Mathematical modeling of airflow and heat transfer during forced convection cooling of produce intended for optimal package design. Transactions of the Institution of Chemical Engineers (IChemE) - Part C, Food and Bioproducts Processing. Submitted for publication.

Dehghannya, J., Ngadi, M. and Vigneault, C. Direct numerical simulation of produce cooling in ventilated packages. Journal of Food Engineering. Submitted for publication.

Dehghannya, J., Ngadi, M. and Vigneault, C. Influence of ventilated package design, evaporative cooling and heat generation on cooling of bulk produce using simultaneous modeling of airflow, heat and mass transfer. Manuscript prepared for submission.

PARTS OF THE THESIS HAVE BEEN PRESENTED AT SCIENTIFIC AND TECHNICAL CONFERENCES

Dehghannya, J., Ngadi, M. and Vigneault, C. (2008). Optimization of cooling performance in vented packages containing stacked spherical produce. Northeast Agricultural and Biological Engineering Conference (NABEC), July 27 - July 30, 2008, Aberdeen, Maryland, USA.

Dehghannya, J., Ngadi, M. and Vigneault, C. (2008). Mathematical modeling of transport phenomena as a package design tool for forced-air precooling of produce. American Society of Agricultural and Biological Engineers (ASABE) Annual International Meeting, June 29 - July 2, 2008, Providence, Rhode Island, USA.

Dehghannya, J., Ngadi, M. and Vigneault, C. (2008). Simulation of airflow during forced-air precooling of bulk produce in vented package. International Congress of Engineering and Food (ICEF 10), April 20-24, 2008, Vina del Mar, Chile.

Dehghannya, J., Ngadi, M. and Vigneault, C. (2007). Mathematical modeling of momentum, heat, and mass transfer for optimal package design in forced-air precooling of fruits and vegetables. Northeast Agricultural and Biological Engineering Conference (NABEC), July 29 - August 1, 2007, Wooster, Ohio, USA. Paper # 07-010.

Dehghannya, J., Ngadi, M. and Vigneault, C. (2007). Prediction of airflow pattern for bulk fruits and vegetables in a vented package. Northeast Agricultural and Biological Engineering Conference (NABEC), July 29 - August 1, 2007, Wooster, Ohio, USA. Paper # 07-011.

CONTRIBUTION OF AUTHORS

The role and contribution made by different authors are as follows:

The principal author is Mr. Jalal Dehghannya. He is the Ph.D. candidate who planned, designed, and executed all the stages in model development, data analysis and wrote the manuscripts for scientific publications. Dr. Michael Ngadi is the thesis supervisor, who guided the candidate in planning, design and execution of the stages in model development and analysis of the data during the course of the entire program. He corrected, edited, and reviewed all the manuscripts sent for publication. Dr. Clement Vigneault is the thesis co-supervisor who also contributed in guiding the candidate in planning and execution of the project. He provided raw data for model validation and also corrected, edited and reviewed the manuscripts sent for publication.

TABLE OF CONTENTS

ABSTRACT	I
RÉSUMÉ	III
ACKNOWLEDGEMENTS	V
PART OF THE THESIS HAS BEEN PUBLISHED	VII
PARTS OF THE THESIS HAVE BEEN SUBMITTED FOR PUBLICATION	N VII
PARTS OF THE THESIS HAVE BEEN PRESENTED AT SCIENTIFIC AN TECHNICAL CONFERENCES	-
CONTRIBUTION OF AUTHORS	IX
TABLE OF CONTENTS	X
LIST OF FIGURES	XV
LIST OF TABLES	XXI
NOMENCLATURE	XXII
I. GENERAL INTRODUCTION	1
1.1 BACKGROUND	1
1.2 OBJECTIVES	2
II. GENERAL LITERATURE REVIEW	3
2.1 THE IMPORTANCE OF PRODUCE PRECOOLING	3
2.2. FORCED-AIR PRECOOLING PROCESS	4
2.3 MATHEMATICAL MODELING OF FORCED-AIR PRECOOLING	
PROCESS	6
2.3.1 Porous Medium Approach	
2.3.1.1 Airflow in porous media	7

2.3.1.2 Confined flows in finite packings	9
2.3.1.3 Conduction heat transfer in porous media	11
2.3.1.3.1 Local thermal equilibrium assumption	11
2.3.1.3.1.1 Criteria for the validity of the local thermal equilibration	ium 12
2.3.1.3.2 Local volume averaged conduction heat transfer	13
2.3.1.4 Convection heat transfer in porous media	14
2.3.1.4.1 Dispersion in porous media	14
2.3.1.4.2 Local volume averaged convection heat transfer	15
2.3.1.5 Two-medium treatment in porous media	16
2.3.1.6 Limitations of porous media approach	17
2.3.2 Direct Numerical Simulation	18
2.3.2.1 Background	18
2.3.2.2 Airflow, heat and mass transfer models	19
2.3.2.3 Heat generation by respiration	20
2.3.2.4 Mass transfer	20
2.4 MODELS AVAILABLE IN THE LITERATURE	22
CONNECTING TEXT	28
III. AERODYNAMIC ANALYSIS DURING COOLING OF STACKED	
PRODUCE INSIDE VARIOUS VENTILATED PACKAGES	20
3.1 ABSTRACT	
3.2 INTRODUCTION	
3.3 MATERIALS AND METHODS	32
3.3.1 Model Formulation	32
3.3.2 Numerical Method	33
3.3.3 Experimental and Simulation Setups	36
3.3.4 Heterogeneity Index	38
3.4 RESULTS AND DISCUSSION	38
3.4.1 Effect of Package Vent Configuration on Velocity Distribution	38

3.4.2 Heterogeneity Indexes Created in Different Package Vent Configuration	rations
•••••	39
3.4.3 Temperature Profiles in Different Package Vent Areas	
3.5 CONCLUSIONS	41
3.6 REFERENCES	42
CONNECTING TEXT	59
IV. COOLING OF STACKED PRODUCE INSIDE VARIOUS VENTILATI	E D
PACKAGES: THERMAL ANALYSIS	60
4.1 ABSTRACT	60
4.2 INTRODUCTION	
4.3 MATERIALS AND METHODS	62
4.3.1 Heterogeneity Index	62
4.4 RESULTS AND DISCUSSION	62
4.4.1 Temperature Distribution in Different Ventilated Package Configuration	rations
	62
4.4.2 Heterogeneity Indexes Obtained at Different Positions of the Venti	lated
Packages	63
4.5 CONCLUSIONS	65
4.6 REFERENCES	66
CONNECTING TEXT	75
V. SENSITIVITY OF PRODUCE COOLING EFFICIENCY AS INFLUENCE	CED
BY DIFFERENT PACKAGE VENT CONFIGURATIONS	76
5.1 ABSTRACT	76
5.2 INTRODUCTION	76
5.3 MATERIALS AND METHODS	77
5.4 RESULTS AND DISCUSSIONS	78
5.4.1 Temperature Distribution inside Different Package Vent Designs	70

5.4.2 Cooling Heterogeneity Obtained in Different Package Vent	
Configurations	80
5.4.3 Cooling Time Obtained in Different Ventilated Packages	81
5.5 CONCLUSIONS	82
5.6 REFERENCES	83
CONNECTING TEXT	103
VI. INFLUENCE OF VENTILATED PACKAGE DESIGN, EVAPORATI	VE
COOLING AND HEAT GENERATION ON PRODUCE COOLING	104
6.1 ABSTRACT	104
6.2 INTRODUCTION	
6.3. MATERIALS AND METHODS	107
6.3.1 Model Overview	107
6.3.1.1 Model parameters	107
6.3.1.1.1 Heat generation by respiration	107
6.3.1.1.2 Mass transfer	107
6.3.1.1.2.1 Calculation of k	108
6.3.1.1.2.2 Calculation of pw, pa and ps	109
6.3.1.1.3 Latent heat of evaporation	109
6.3.1.2 Simulation setups	110
6.4 RESULTS AND DISCUSSIONS	110
6.4.1 Effect of Different Package Vent Designs and Relative Humidity	on
Produce Evaporative Cooling	110
6.4.2 Effect of Different Package Vent Designs on Produce Heat General	ration
	112
6.4.3 Effect of Evaporative Cooling and Heat Generation on Cooling T	'ime 113
6.5 CONCLUSIONS	115
6.6 REFERENCES	116
VIII CUD D (A DV A VIII CID VIII A VIII CID VIII A VIII CID VIII C	
VII SUMMARY AND GENERAL CONCLUSIONS	121

VIII. CONTRIBUTIONS TO KNOWLEDGE AND SUGGESTIONS FOR	
FUTURE RESEARCH	133
8.1 CONTRIBUTIONS TO KNOWLEDGE	133
8.2 SUGGESTIONS FOR FUTURE RESEARCH	134
GENERAL REFERENCES	135

LIST OF FIGURES

FIGURE 3.1 (A): A COMPUTATIONAL GEOMETRY REPRESENTING CROSS-SECTIONAL
AREA OF A PACKAGED PRODUCE WITH INLET AND OUTLET VENT POSITIONS
SHOWN IN LEFT AND RIGHT SIDES AND NUMBERED FROM #1 TO #5 FROM TOP TO
BOTTOM, EXACT LOCATIONS OF THE 21 POINTS CONSIDERED FOR THE AIR
VELOCITY AND HETEROGENEITY INDEX EVALUATIONS, AS WELL AS PRODUCE
POSITIONS (P1, P2, P3 AND P4) USED FOR MODEL VALIDATION46
FIGURE 3.1 (B): PACKAGE SIDE VIEW ILLUSTRATING DIFFERENT PACKAGE VENT
CONFIGURATIONS DESCRIBED IN TABLE 3.1
FIGURE 3.2: EXPERIMENTAL SETUP SHOWING FORCED AIR TUNNEL, BALL MATRIX,
FAN, AND THE AIRFLOW MEASURING DEVICE48
FIGURE 3.3: AIR VELOCITY AT 21 POSITIONS FOR THREE DIFFERENT PACKAGE VENT
AREAS49
FIGURE 3.4: HETEROGENEITY INDEX (HI) AT 21 POSITIONS FOR THREE DIFFERENT
PACKAGE VENT CONFIGURATIONS50
FIGURE 3.5 (A): SIMULATED (SIM) AND EXPERIMENTAL (EXP) TEMPERATURE
PROFILES BASED ON CENTER TEMPERATURES OF THE POSITIONS P1 AND P2,
DEMONSTRATED IN FIGURE 3.1 (A), IN THE PACKAGE WITH 1 VENT51
FIGURE 3.5 (B): SIMULATED (SIM) AND EXPERIMENTAL (EXP) TEMPERATURE
PROFILES BASED ON CENTER TEMPERATURES OF THE POSITIONS P3 AND P4,
DEMONSTRATED IN FIGURE 3.1 (A), IN THE PACKAGE WITH 1 VENT52

FIGURE 3.5 (C): SIMULATED (SIM) AND EXPERIMENTAL (EXP) TEMPERATURE
PROFILES BASED ON CENTER TEMPERATURES OF THE POSITIONS P1 AND P2,
DEMONSTRATED IN FIGURE 3.1 (A), IN THE PACKAGE WITH 3 VENTS53
FIGURE 3.5 (D): SIMULATED (SIM) AND EXPERIMENTAL (EXP) TEMPERATURE
PROFILES BASED ON CENTER TEMPERATURES OF THE POSITIONS P3 AND P4,
DEMONSTRATED IN FIGURE 3.1 (A), IN THE PACKAGE WITH 3 VENTS54
FIGURE 3.5 (E): SIMULATED (SIM) AND EXPERIMENTAL (EXP) TEMPERATURE
PROFILES BASED ON CENTER TEMPERATURES OF THE POSITIONS P1 AND P2,
DEMONSTRATED IN FIGURE 3.1 (A), IN THE PACKAGE WITH 5 VENTS55
FIGURE 3.5 (F): SIMULATED (SIM) AND EXPERIMENTAL (EXP) TEMPERATURE
PROFILES BASED ON CENTER TEMPERATURES OF THE POSITIONS P3 AND P4,
DEMONSTRATED IN FIGURE 3.1 (A), IN THE PACKAGE WITH 5 VENTS56
FIGURE 3.6: OVERALL MODEL PERFORMANCE BASED ON REGRESSION PLOT OF THE
EXPERIMENTAL VS. PREDICTED TEMPERATURES FOR ALL THREE DIFFERENT VENT
CONFIGURATIONS57
FIGURE 4.1: CROSS-SECTIONAL AREA OF A PACKAGED PRODUCE WITH INLET AND
OUTLET VENT POSITIONS SHOWN IN LEFT AND RIGHT SIDES, RESPECTIVELY
(TABLE 3.1)69
FIGURE 4.2 (A): PRODUCE TEMPERATURE DISTRIBUTION AFTER 30 MIN COOLING IN
THE PACKAGE WITH ONE VENT70
FIGURE 4.2 (B): PRODUCE TEMPERATURE DISTRIBUTION AFTER 30 MIN COOLING IN
THE PACK AGE WITH THREE VENTS 71

FIGURE 4.2 (C): PRODUCE TEMPERATURE DISTRIBUTION AFTER 30 MIN COOLING IN
THE PACKAGE WITH FIVE VENTS
FIGURE 4.3: HETEROGENEITY INDEXES AT 64 POSITIONS, SHOWN IN FIGURE 4.1, FOR
THREE DIFFERENT PACKAGE VENT CONFIGURATIONS AFTER 30 MIN COOLING 73
FIGURE 4.4: COOLING HETEROGENEITIES AT DIFFERENT COOLING TIMES IN THREE
DIFFERENT PACKAGE VENT CONFIGURATIONS74
FIGURE 5.1: PACKAGE INLET AND OUTLET VENT POSITIONS SHOWN IN LEFT AND RIGHT
SIDES, RESPECTIVELY (TABLE 5.1) AS WELL AS PRODUCE POSITIONS (P1, P2, P3
AND P4) USED FOR INVESTIGATION OF PRODUCE TEMPERATURE DISTRIBUTIONS
AT NINE DIFFERENT PACKAGE VENT CONFIGURATIONS
FIGURE 5.2 (A): PRODUCE TEMPERATURE DISTRIBUTION AFTER 120 MIN COOLING IN
THE PACKAGE VENT CONFIGURATION OF "A" DESCRIBED IN TABLE 5.1
FIGURE 5.2 (B): PRODUCE TEMPERATURE DISTRIBUTION AFTER 120 MIN COOLING IN
THE PACKAGE VENT CONFIGURATION OF "B" DESCRIBED IN TABLE 5.1
FIGURE 5.2 (C): PRODUCE TEMPERATURE DISTRIBUTION AFTER 120 MIN COOLING IN
THE PACKAGE VENT CONFIGURATION OF "C" DESCRIBED IN TABLE 5.1
FIGURE 5.2 (D): PRODUCE TEMPERATURE DISTRIBUTION AFTER 120 MIN COOLING IN
THE PACKAGE VENT CONFIGURATION OF "D" DESCRIBED IN TABLE 5.190
FIGURE 5.2 (E): PRODUCE TEMPERATURE DISTRIBUTION AFTER 120 MIN COOLING IN
THE PACKAGE VENT CONFIGURATION OF "E" DESCRIBED IN TABLE 5.191
FIGURE 5.2 (F): PRODUCE TEMPERATURE DISTRIBUTION AFTER 120 MIN COOLING IN
THE PACKAGE VENT CONFIGURATION OF "F" DESCRIBED IN TABLE 5.1 92

FIGURE 5.2 (G): PRODUCE TEMPERATURE DISTRIBUTION AFTER 120 MIN COOLING IN
THE PACKAGE VENT CONFIGURATION OF "G" DESCRIBED IN TABLE 5.193
FIGURE 5.2 (H): PRODUCE TEMPERATURE DISTRIBUTION AFTER 120 MIN COOLING IN
THE PACKAGE VENT CONFIGURATION OF "H" DESCRIBED IN TABLE 5.194
FIGURE 5.2 (I): PRODUCE TEMPERATURE DISTRIBUTION AFTER 120 MIN COOLING IN
THE PACKAGE VENT CONFIGURATION OF "I" DESCRIBED IN TABLE 5.195
FIGURE 5.3 (A): PRODUCE TEMPERATURE PROFILES BASED ON CENTER TEMPERATURE
OF THE POSITIONS P1 DEMONSTRATED IN FIGURE 5.1 CONSIDERING VARIOUS
VENT CONFIGURATIONS96
FIGURE 5.3 (B): PRODUCE TEMPERATURE PROFILES BASED ON CENTER TEMPERATURE
OF THE POSITIONS P2 DEMONSTRATED IN FIGURE 5.1 CONSIDERING VARIOUS
VENT CONFIGURATIONS97
FIGURE 5.3 (C): PRODUCE TEMPERATURE PROFILES BASED ON CENTER TEMPERATURE
OF THE POSITIONS P3 DEMONSTRATED IN FIGURE 5.1 CONSIDERING VARIOUS
VENT CONFIGURATIONS98
FIGURE 5.3 (D): PRODUCE TEMPERATURE PROFILES BASED ON CENTER TEMPERATURE
OF THE POSITIONS P4 DEMONSTRATED IN FIGURE 5.1 CONSIDERING VARIOUS
VENT CONFIGURATIONS99
FIGURE 5.4: COOLING HETEROGENEITY IN 9 DIFFERENT PACKAGE VENT DESIGNS, AS
DEMONSTRATED IN TABLE 5.1, DURING 180 MIN COOLING
FIGURE 5.5: MAXIMUM TIME REQUIRED FOR COOLING OF THE SLOWEST COOLED
PRODUCE TO BEACH 7°C IN DIFFERENT VENTULATED BACKAGES 101

FIGURE 6.1: CROSS-SECTIONAL AREA OF A PACKAGED PRODUCE WITH INLET AND
OUTLET VENT POSITIONS SHOWN IN LEFT AND RIGHT SIDES, RESPECTIVELY
(Table 3.1) as well as produce positions (P1, P2, P3 and P4) used for
INVESTIGATION OF EVAPORATIVE COOLING AND HEAT GENERATION
FIGURE 6.2 (A): PRODUCE EVAPORATIVE COOLING AT THE POSITION P1 SHOWN IN
FIGURE 6.1 AT RH=60% AND RH=95% IN DIFFERENT PACKAGE VENT
CONFIGURATIONS
FIGURE 6.2 (B): PRODUCE EVAPORATIVE COOLING AT THE POSITION P2 SHOWN IN
FIGURE 6.1 AT RH=60% AND RH=95% IN DIFFERENT PACKAGE VENT
CONFIGURATIONS
FIGURE 6.2 (C): PRODUCE EVAPORATIVE COOLING AT THE POSITION P3 SHOWN IN
FIGURE 6.1 AT RH=60% AND RH=95% IN DIFFERENT PACKAGE VENT
CONFIGURATIONS
FIGURE 6.2 (D): PRODUCE EVAPORATIVE COOLING AT THE POSITION P4 SHOWN IN
FIGURE 6.1 AT RH=60% AND RH=95% IN DIFFERENT PACKAGE VENT
CONFIGURATIONS
FIGURE 6.3 (A): PRODUCE HEAT GENERATION AT THE POSITION P1 SHOWN IN FIGURE
6.1 AT RH=60% AND RH=95% IN DIFFERENT PACKAGE VENT CONFIGURATIONS
125
FIGURE 6.3 (B): PRODUCE HEAT GENERATION AT THE POSITION P2 SHOWN IN FIGURE
6.1 AT RH=60% AND RH=95% IN DIFFERENT PACKAGE VENT CONFIGURATIONS

FIGURE 6.3 (C): PRODUCE HEAT GENERATION AT THE POSITION P3 SHOWN IN FIGURE
6.1 AT RH=60% AND RH=95% IN DIFFERENT PACKAGE VENT CONFIGURATIONS
FIGURE 6.3 (D): PRODUCE HEAT GENERATION AT THE POSITION P4 SHOWN IN FIGURE
6.1 AT RH=60% AND RH=95% IN DIFFERENT PACKAGE VENT CONFIGURATIONS
FIGURE 6.4: MAXIMUM TIME REQUIRED FOR COOLING OF THE SLOWEST-COOLED
PRODUCE TO REACH 7°C IN DIFFERENT VENTILATED PACKAGES REGARDING
INDEPENDENT AND SIMULTANEOUS EFFECTS OF EVAPORATIVE COOLING (EC
AND HEAT GENERATION (HG)

LIST OF TABLES

TABLE	3.1: P.	ACKAGE VE	NT CON	FIGURATIO	NS BASEI	ON DIFFERE	NT VEN	T POSITIONS
DE	EMONS	TRATED IN F	GURE	1 (A)	••••••	•••••••••••	•••••	58
						CONSIDEREI		
SIN	MULAT	TIONS BASED	ON DIF	FERENT V	ENT POSIT	TIONS DEMON	STRATE	d in Figure
5.	1	••••••	••••••	•••••	•••••	••••••	•••••	102
TABLE	6.1: E	EFFECT OF E	VAPORA	ATIVE COO	LING (EC	C), HEAT GENI	ERATIO	n (HG) and
PA	CKAG	E VENT CON	FIGURA	TION ON P	RODUCE 1	TEMPERATURE	(°C) A	r different
PO	MOITIZ	IS AFTER 60	MIN CO	OLING				130

NOMENCLATURE

A: surface area (m²)

Ao: volumetric or specific surface area (1/m)

A_{fs}: interfacial area between fluid and solid phases (m²)

c: diffusivity in element Peclet number (Pa.s or W/m K)

cart: coefficient of artificial diffusion (Pa.s or W/m K)

c_{p,a}: air specific heat capacity (J/kg K)

c_{p,p}: produce specific heat capacity (J/kg K)

d: hydraulic diameter (m) or pore-level linear length scale (m)

d_{eff}: effective produce diameter (m)

D: diffusivity of water vapor in air (m²/s) or total diffusivity (m²/s)

D^d: dispersion coefficient (m²/s)

f and g: respiration constants

h: element size (m)

h_{sf}: interstitial convection heat transfer coefficient (W/m² K)

I: second-order identity tensor

k: mass transfer coefficient (kg/m².s. Pa)

kair: air film mass transfer coefficient (kg/m².s. Pa)

k'air: air film mass transfer coefficient (m/s)

k_{skin}: skin mass transfer coefficient (kg/m².s. Pa)

k_a: air thermal conductivity (W/m K)

k_p: produce thermal conductivity (W/m K)

K₁ and K₂: constants in Darcy - Forchheimer equation

Ke: effective thermal conductivity (W/m K)

 ℓ : linear length scale for representative elementary volume (m)

L: latent heat of evaporation (J/kg) or system dimension (m)

m: rate of produce moisture loss (kg/s.m²)

 Nu_d : Nusselt number (dimensionless); $Nu_d = \frac{h_{sf} d}{k_a}$

P: pressure (Pa)

pa: water vapor pressure in air (Pa)

ps: water vapor pressure at produce surface (Pa)

pw: saturation water vapor pressures (Pa)

Pe_{el}: element Peclet number (dimensionless); Pe_{el} = $\frac{h|\beta|}{c}$

Pr: Prandtl number (dimensionless); $Pr = \frac{\mu_a c_{p,a}}{k_a}$

q_{resp}: respiratory heat generation per unit mass of commodity (W/kg)

Q_{resp}: respiratory heat generation per unit package volume (W/m³)

R_{H2O}: gas constant for water vapor (m³ Pa/kg K)

Re: Reynolds number (dimensionless); Re = $\frac{\rho_a u d}{\mu_a}$

RH: relative humidity

Sc: Schmidt number (dimensionless); Sc = $\frac{\mu_a}{\rho_a D}$

Sh: Sherwood number (dimensionless); Sh = $\frac{\mathbf{k}'_{air}\mathbf{d}}{\mathbf{D}}$

t: time (s)

Ta: air temperature at different positions inside ventilated packages (°C)

T_p: produce temperature at different positions inside ventilated packages (°C)

u: velocity vector (m/s)

v: intrinsic air velocity (m/s)

V: volume (m³)

Greek

 α : thermal diffusivity (m²/s)

β: convection coefficient (kg/m² s or W/m² K) or Forchheimer coefficient

 δ_{id} : tuning parameter

ε: porosity

 κ : permeability of porous medium (m²)

 μ_a : air dynamic viscosity (Pa.s)

 μ_{eff} : effective dynamic viscosity (Pa.s)

v: kinematic viscosity (m²/s)

 ρ_a : air density (kg/m³)

 ρ_p : produce density (kg/m³)

Subscripts and Superscripts

f: fluid

s: solid

Others

⟨ ⟩: volume average

O(): order of magnitude

I. GENERAL INTRODUCTION

1.1 BACKGROUND

Reducing postharvest losses of fresh produce is a topic of major interest all over the world. This is because fresh fruits and vegetables continue to deteriorate and shrivel after harvest and their freshness is only short-lived (Amirante et al., 2000; Banks et al., 2000; Rodriguez-Bermejo et al., 2007). To minimize their ultimate loss of quality, the crops are cooled from field temperature to an optimal storage temperature (Beukema et al., 1982; Kumar et al., 2008). The cooling process retards ripening, suppresses the spoiling physiological, biochemical, and microbiological processes, and extends the preservation of the natural properties such as appearance, texture, and flavor during storage (Amos et al., 1993; Fikiin et al., 1999). Since the maintenance of market quality has a fundamental importance to the success of the agricultural industry, it is necessary not only to cool the produce but to cool it as quickly as possible after harvest (Brosnan and Sun, 2001).

Forced-air precooling process is the most widely used method of cooling to extend produce shelf life (Kader, 2002). However, complete or partial losses of fresh fruits and vegetables occur as a result of poor temperature management during the process (Alvarez and Flick, 1999a; Alvarez et al., 2003). This is mainly due to the non-uniform nature of produce cooling (Hoang et al., 2000; Nahor et al., 2005), resulting in under-cooling or over-cooling of fresh produce located at different parts of ventilated packages. Quality losses of agricultural produce can be reduced by using improved forced-air precooling systems along with suitable temperature maintenance throughout the marketing channels (de Castro et al., 2004b). In practice, combinations of air temperature and velocity are chosen by designers through experience to rapidly cool the produce to a suitable temperature inside ventilated packages. A more logical approach in designing new packages is to develop a model that would be able to predict influence of important variables on produce cooling. This approach should help in improving current forced-air precooling systems to maintain the produce quality for a longer period of time.

1.2 OBJECTIVES

The overall objective of this study was to develop a system of mathematical models of airflow, heat and mass transfer that can be used to predict temperature and velocity distribution inside ventilated packages during forced air-precooling process. This is to provide homogeneous temperature distribution and therefore, uniform produce cooling inside different ventilated packages resulting in increased produce shelf life.

To contribute to the overall objective of the study, the following specific objectives were set for the proposed research as follows:

- 1) Investigate airflow distributions by aerodynamic analysis during cooling of stacked produce inside ventilated packages with different vent areas and positions. Air velocities at different locations of the package are to be predicted by considering different package vent configurations.
- 2) Conduct thermal analysis during forced-air precooling of stacked produce inside ventilated packages with different package vent areas and positions.
- 3) Assess the sensitivity of produce cooling uniformity and cooling time as influenced by different package vent designs during forced convection cooling of produce. Effect of different package designs including various vent areas and positions on produce cooling are to be considered.
- 4) Investigate the relative magnitudes of produce evaporative cooling and heat generation considering different package vent configurations as well as to study the interactive effects of evaporative cooling, heat generation and package vent design on produce temperature and cooling time. The model is to predict produce transient temperature, evaporative cooling and heat generation at any position inside different ventilated packages.

II. GENERAL LITERATURE REVIEW

2.1 THE IMPORTANCE OF PRODUCE PRECOOLING

Postharvest treatment is a very important step in quality maintenance and shelf life extension of agricultural crops. There are a variety of different postharvest technologies available, among them precooling is likely the most important of all the operations in the maintenance of a desirable, fresh and salable produce (Baird and Gaffney, 1976). The term "Precooling" is defined as the removal of field heat from freshly harvested produce in order to slow down metabolism and reduce deterioration prior to transport or storage (Janick, 1986). The optimum storage temperature is usually slightly higher than the product freezing point and it is highly important that the temperature be held fairly constant; because large temperature fluctuations promote the product deterioration (Tashtoush, 2000).

Precooling is among the most cost-effective and efficient quality preservation methods available to commercial crops and that is the most essential of all the value-added marketing services demanded by increasingly more sophisticated consumers (Sullivan et al., 1996). There are a variety of precooling techniques available for use in the agricultural industry. Room cooling, forced-air cooling, hydro-cooling, vacuum cooling and liquid icing are common methods of precooling systems among others (Dincer, 1995; Carroll et al., 1996; Rennie et al., 2001; Vigneault and Goyette, 2002; Rennie et al., 2003; He and Li, 2003; Allais et al., 2006; Fricke, 2006). These various precooling systems transfer heat from the commodity to a cooling medium such as water, air or ice. Cooling times may be required from several minutes to more than 24 hours for proper precooling of commodities (Fricke, 2006). The choice of precooling method is greatly influenced by produce type, since different commodities have different cooling requirements (Edeogu et al., 1997; Brosnan and Sun, 2001). Although no unique universal method among these methods exists as the most suitable for all of the crops, forcedair cooling is adaptable to a wider range of commodities than any other cooling method (Kader, 2002).

Precooling of fruits and vegetables is influenced by airflow rate, air temperature, relative humidity, produce geometry (size, shape, and surface area), packing configuration, thermal properties, produce initial temperature, final desired temperature, respiratory heat generation, evaporative cooling, package vent design (vent area and vent positions) and stacking arrangement which are important factors that affect airflow, heat and mass transfer processes during the process (Hass et al., 1976; Sastry et al., 1978; Gaffney et al., 1985a; Thompson, 1996; Emond et al., 1996; Becker et al., 1996a; Faubion and Kader, 1997; Wills, 1998; Ladaniya and Singh, 2000; Vigneault et al., 2004; de Castro et al., 2004a; Vigneault and de Castro, 2005; Cortbaoui et al., 2006).

2.2. FORCED-AIR PRECOOLING PROCESS

Forced-air precooling is accomplished by forcing cold air through stacked packages and through individual pieces of produce items. The airflow creates a pressure gradient across the containers, generating a driving force to draw air from the surroundings, through the container openings and commodity (Vigneault and Goyette, 2002). This system is the most common technology used to extend agricultural produce shelf life, reducing deterioration and water loss rates, especially for those crops sensitive to water exposure (Kader, 2002; de Castro et al., 2005a). Forced-air precooling does not wet produce as in hydrocooling or liquid icing, which is critical for some crops; it is cost effective and has a wide range of applications (Edeogu et al., 1997; Ladaniya and Singh, 2000; Brosnan and Sun, 2001; Anderson et al., 2004).

However, strong cooling heterogeneity is created during forced-air precooling due to poor temperature management (Alvarez and Flick, 1999a; Alvarez et al., 2003). Commodities located behind blind walls may not be sufficiently cooled while others exposed to higher velocities are over-cooled. The occurrence of the heterogeneous airflow during forced-air precooling is directly related to design of the ventilated packages to be used during the process. The design of these containers is largely based on the criterion of mechanical strength with minimal consideration of the effect of their venting pattern on cooling efficiency.

Unfortunately, many of the packages currently used by the industry remain inefficient in promoting rapid and uniform cooling of the packaged produce (Ferrua and Singh, 2007).

Ventilated packages used during the process should be designed in such a way that they can provide a uniform airflow distribution and consequently uniform produce cooling. The package must have enough openings to provide uniform airflow through the produce while providing suitable mechanical resistance (Vigneault and Goyette, 2002; de Castro et al., 2004b; Vigneault and de Castro, 2005). Percent vent area of the package is a very critical factor affecting the efficiency of a cooling system (Arifin and Chau, 1988; Baird et al., 1988; de Castro et al., 2005b). An increase in side ventilation from 2 to 6% increased airflow in corrugated fiber board packages in different stacking patterns and reduced cooling time (Ladaniya and Singh, 2000). Apart from the percent vent area of a package, the openings must be well distributed on the package walls in order to provide uniform airflow distribution during the process (de Castro et al., 2004a). Therefore, a proper package vent design including both vent area and vent positions is necessary to enhance the efficiency of forced-air precooling system (Stanley, 1989; Brosnan and Sun, 2001; Smale et al., 2003; de Castro et al., 2004a).

Several experimental studies have been reported in the literature to elucidate the influence of different package vent designs on the efficiency of the forced-air precooling process. However, these experimental studies are expensive and involve much time and labor. A more logical approach is to develop mathematical models capable of predicting airflow, heat and mass transfer within ventilated packages under different conditions and designs. This approach should help in improving current systems to maintain the produce quality for a longer period of time.

The complex and chaotic structure within agricultural produce packages during the forced-air precooling process complicates the numerical study of the thermal behavior of each individual produce within ventilated packages. The main obstacle that has limited this analysis is the determination of the airflow behavior around particles. Even in the case of uniformly distributed products in a package, measurement of fluid flow around individual products, by means of traditional

methods, is impossible without disturbing the packaging arrangement itself (Ferrua and Singh, 2007).

2.3 MATHEMATICAL MODELING OF FORCED-AIR PRECOOLING PROCESS

There are typically two methods for modeling forced-air precooling of produce, namely the porous medium approach (single-phase or two-phase) and direct numerical simulation (DNS).

2.3.1 Porous Medium Approach

A porous medium is a solid matrix permeated by an interconnected network of pores (voids) filled with a fluid (gas or liquid). Transport phenomena (the transport of fluid, heat and mass) in porous media play an important role in many areas of applied science and engineering fields. Some of these applications can be found in mechanics, biomechanics, geosciences, biology, biophysics, material science and food systems. In food systems, an enormous range of processes with different scales can be viewed as involving transport of fluid, heat and mass through porous media. Examples include extraction, drying, frying, meat roasting, rehydration of breakfast cereals, beans and dried vegetables as well as cooling of stacked bulk produce such as oranges and strawberries with or without packaging.

Other than the particle dimension d, the porous medium has a system dimension L, which is generally much larger than d. When $L/d \gg 1$ and the variation of temperature across d is negligible compared to that across L for both the solid and fluid phases, then it can be assumed that within a distance d both phases are in thermal equilibrium (local thermal equilibrium). When the solid matrix can not be fully described by considering the solid phase distribution over distance d, a representative elementary volume with a linear dimension larger than d is needed. The requirement of a negligible temperature variation also has to be considered over the linear dimension of the representative elementary volume ℓ . In addition to d, ℓ and L, a length scale equal to the square root of the permeability is also used.

This length scale $\kappa^{1/2}$ is smaller than d and is generally $O(10^{-2}\text{d})$, where κ is the permeability. Local thermal equilibrium assumption based on the length scales requires that (Kaviany, 1995):

$$\kappa^{1/2} \ll d \ll L \tag{2.1}$$

The ranges for the following length scales have been tabulated in Kaviany (1995).

Therefore, the approach taken in porous media is a continuum one in which all variables and parameters are averaged over a representative elementary volume. In this continuum approach, the actual multiphase porous medium is replaced by a fictitious continuum at any point of a "structureless" substance where all assigned variables and parameters are continuous functions of the spatial coordinates (Bear, 1972; Datta, 2007). In treatment of transport phenomena in porous media, a large number of unknowns are introduced in averaging methods that require experimental verifications. This is due to the complexity of the flow paths and the inter-pore and pore-to-pore fluid dynamic interactions. Therefore, although the local volume averaging involves integration of the conservation equations over the representative elementary volume, empiricism to various extents is applied in arriving at the local volume-averaged conservation equations (Kaviany, 1995).

The porous medium approach to airflow, heat and mass transfer has been until recently the only means of modeling transport phenomena inside a packed bed (Verboven et al., 2006). This space-averaging approach, where the fluid flow is characterized by an average (superficial) velocity, is required when computational resources do not allow individual modeling of each phase (solid and interstitial space). The fundamental theory of airflow in porous media together with important aspects related to heat and mass transfer based on the porous medium approach is discussed in the following sections.

2.3.1.1 Airflow in porous media

For small airflows in porous media, the airflow rate is proportional to the applied pressure drop expressed by Darcy's law. Darcy's law establishes a linear

relationship between the pressure gradient ∇p (Pa/m) and the flow velocity u (m/s) in porous media:

$$-\nabla p = \frac{\mu}{\kappa} u \tag{2.2}$$

where p is pressure, μ air dynamic viscosity and κ the permeability of porous medium which depends on various factors including pore size, produce diameter and pore geometry. The vector u is the air velocity averaged over the entire medium (pore space as well as solid matrix) and is known as the superficial velocity (Liu and Masliyah, 1996; Verboven et al., 2006). The intrinsic air velocity which is averaged only over the pore space is calculated from:

$$v = \frac{u}{\varepsilon} \tag{2.3}$$

where ε is the porosity.

Darcy's law expresses a linear relationship between pressure drop and velocity which does not hold for larger velocities. At higher velocities, the airflow is described by the Darcy - Forchheimer equation, which includes a quadratic term (Verboven et al., 2006):

$$-\nabla p = \frac{\mu_a}{\kappa} u + \beta \rho_a u |u| \tag{2.4}$$

where β is the Forchheimer coefficient mainly dependent on the geometry of pore space.

The permeability of the porous medium (κ) and the Forchheimer constant (β) can be computed for near spherical produce using the Ergun relations (Ergun, 1952):

$$\kappa = \frac{K_1 (1 - \varepsilon)^2}{d_{\text{eff}}^2 \varepsilon^3} \tag{2.5}$$

$$\beta = \frac{K_2(1-\varepsilon)}{d_{\text{eff}}\varepsilon^3} \tag{2.6}$$

where d_{eff} is the effective produce diameter and for nearly spherical items is expressed as (Bird et al., 2002):

$$d_{\text{eff}} = \frac{6V}{A} \tag{2.7}$$

where V and A are the volume (m³) and the surface area (m²) of produce, respectively. The values of the constants K₁ and K₂ for randomly stacked spheres differ from source to source, the original parameters being equal to 150 and 1.75 (Ergun, 1952), respectively, while others have suggested values of 180 and 1.8 (Macdonald et al., 1979; Van der Sman, 2002). However, for packed beds with objects having other shapes or rough surfaces, the parameters K₁ and K₂ can have other values (Comiti and Renaud, 1989). Chau et al. (1985) conducted some experiments to study the resistance of airflow through oranges in bulk and in simulated cartons. The Ergun equation was used to fit the experimental data. Fruit size, stacking pattern and porosity considerably affected the values of K₁ and K₂.

2.3.1.2 Confined flows in finite packings

Packages confine food materials inside a finite size. Any packing that is bounded by confining walls, an influence of the package-to-produce diameter ratio on the pressure drop is to be expected (Eisfeld and Schnitzlein, 2001). The Darcy - Forchheimer equation is essentially only valid for infinite porous media without walls (Verboven et al., 2006). Therefore, for flow through a confined packed bed, such as a vented packaging, the Darcy - Forchheimer equation is extended with the

Brinkman term, which is required for the description of the boundary layer at the solid/porous-media interface (Vafai & Tien, 1982):

$$-\nabla p = \frac{\mu_a}{\kappa} u + \beta \rho_a u |u| - \mu_{\text{eff}} \nabla^2 u$$
 (2.8)

which is implemented with the continuity equation:

$$\nabla \cdot \mathbf{u} = 0 \tag{2.9}$$

 $\mu_{\rm eff}$ is the effective dynamic viscosity in the boundary layer at the solid/porous-media interface. In practice, the Brinkman term does not have a significant influence on the pressure drop over the packed bed; however, the effect of the Brinkman term is that it will give rise to a boundary layer, where the velocity reduces to zero exactly at the solid wall (Van der Sman, 2002; Verboven et al., 2006). Therefore, the importance of the term is significant only in near-wall regions in the porous medium.

The effect of the Brinkman term on reducing the velocity in this layer is contradicted because of the increased velocity due to a higher porosity near package walls, where produce items can not be packed as tightly as in the interior of the porous medium. On the one hand, package walls offer an additional resistance due to the wall friction and on the other hand, they force the commodities to order in such a way that a region of increased void fraction is formed. Therefore, the resultant wall effect are contradictory (Eisfeld and Schnitzlein, 2001; Verboven et al., 2004; Verboven et al., 2006). Eisfeld and Schnitzlein (2001) stated that the counteracting effect of the wall friction and the increased local porosity near the package walls is Reynolds number dependent. In low Reynolds number regime, the pressure drop in a confined bulk increases as a result of wall friction. At high Reynolds number, however, the increased void fraction near the wall reduces resistance. For package-to-produce confinement ratios smaller than 10, the effect of

the confinement can be taken into account by the correlation proposed by Eisfeld and Schnitzlein (2001).

2.3.1.3 Conduction heat transfer in porous media

Heat transfer by conduction through porous media, as with heat conduction through any heterogeneous media, depends on the matrix structure and the thermal conductivity of each phase. Since the thermal conductivity of the solid phase is generally larger than that of fluid, the manner in which the solid is interconnected influences the conduction significantly (Kaviany, 1995). For the analysis of the macroscopic heat flow through heterogeneous media, the local volume-averaged (or effective) properties such as the effective thermal conductivity $\langle \mathbf{k} \rangle = \mathbf{k}_e$ are used.

2.3.1.3.1 Local thermal equilibrium assumption

In principle, determination of the effective thermal conductivity involves application of the energy equation in the representative elementary volume of the matrix and the integration over this volume. In doing so, at the pore level, there will be a difference ΔT_d between the temperature at a point in the solid and in the fluid. Similarly, across the representative elementary volume, there is a maximum temperature difference of ΔT_ℓ . However, it is assumed that these temperature differences are much smaller than those occurring over the system dimension ΔT_L . Therefore, the assumption of local thermal equilibrium is imposed by requiring that:

$$\Delta T_{\kappa^{1/2}} < \Delta T_{d} < \Delta T_{\ell} < \Delta T_{L} \tag{2.10}$$

Therefore, it is assumed that within the representative elementary volume $V = V_f + V_s$, the solid and fluid phases are in local thermal equilibrium:

$$\frac{1}{V_s} \int_{V_s} T_s dV = \frac{1}{V_s} \int_{V_s} T_s dV = \frac{1}{V} \int T dV$$
 (2.11)

2.3.1.3.1.1 Criteria for the validity of the local thermal equilibrium

The following criteria for the validity of the local thermal equilibrium approximation must be reached (Carbonell and Whitaker, 1984):

For time scale:

$$\frac{\varepsilon(\rho c)_{f} \ell^{2}}{t} \left(\frac{1}{k_{f}} + \frac{1}{k_{s}}\right) << 1$$
(2.12)

and

$$\frac{(1-\varepsilon)(\rho c)_{f} \ell^{2}}{t} \left(\frac{1}{k_{f}} + \frac{1}{k_{s}}\right) << 1$$
(2.13)

For length scale:

$$\frac{\varepsilon \, \mathbf{k}_{\mathsf{f}} \, \ell}{\mathbf{A}_{\mathsf{o}} \mathbf{L}^2} \left(\frac{1}{\mathbf{k}_{\mathsf{f}}} + \frac{1}{\mathbf{k}_{\mathsf{s}}} \right) << 1 \tag{2.14}$$

and

$$\frac{(1-\varepsilon)k_s \ell}{A_o L^2} \left(\frac{1}{k_f} + \frac{1}{k_s}\right) << 1 \tag{2.15}$$

where A_0 is the volumetric or specific surface area based on the solid volume, i.e., solid surface area divided by the solid volume defined by:

$$A_o = \frac{A_{fs}}{V_s} \tag{2.16}$$

where A_{fs} is the interfacial area between the fluid and the solid phases and V_s is the solid volume $(1-\epsilon)$.

2.3.1.3.2 Local volume averaged conduction heat transfer

In dealing with any quantity ϕ that has nonzero values in both phases, the intrinsic volume-averaged value is defined by:

$$\langle \phi_f \rangle^f = \frac{1}{V_f} \int_{V_f} \phi_f dV = \langle \phi \rangle^f$$
 (2.17)

By using the following equation under the local thermal equilibrium condition:

$$\langle T \rangle^{s} = \langle T \rangle^{f} = \langle T \rangle \tag{2.18}$$

with the representative elementary volume of:

$$V = V_f + V_s \tag{2.19}$$

the local volume-averaged energy equation becomes:

$$\left[\varepsilon\left(\rho c_{p}\right)_{f} + (1-\varepsilon)\left(\rho c_{p}\right)_{s}\right] \frac{\partial \langle T \rangle}{\partial t} = \nabla \cdot \left(K_{e} \cdot \nabla \langle T \rangle\right) \tag{2.20}$$

where the effective thermal conductivity tensor $K_{\rm e}$ is given by:

$$K_{c} = \left[\varepsilon k_{f} + (1 - \varepsilon)k_{s}\right]I + \frac{k_{f} - k_{s}}{V} \int_{A_{fs}} n_{fs} b_{f} dA$$
 (2.21)

b_f is a transformation vector (Kaviany, 1995).

2.3.1.4 Convection heat transfer in porous media

As simultaneous fluid flow and heat transfer in porous media is considered, the role of the macroscopic (Darcean) and microscopic (pore-level) velocity fields on the temperature field needs to be considered. Experiments have shown that the mere inclusion of $\mathbf{u} \cdot \nabla \langle \mathbf{T} \rangle$ in the energy equation does not accurately account for all the hydrodynamic effects. The pore level hydrodynamics also influence the temperature field. Inclusion of the effect of the pore-level velocity-non-uniformity on the temperature distribution (called the dispersion effect) is discussed in this section.

2.3.1.4.1 Dispersion in porous media

The dispersion in porous media is expected to have the following features (Kaviany, 1995):

- Dispersion should depend on the pore-level hydrodynamics. The pore structure, pore velocity and upstream conditions determine whether they are recirculation zones, dead ends, etc. The classification of the structure to ordered or disordered media allows for further specifications of the pore-level hydrodynamics. In ordered and isotropic media and when simple unit-cell structures with convenient symmetries are present, the flow field can be analyzed for various pore Reynolds numbers. The bulk of the available experimental results show that Pe = Re Pr can approximately express the pore-level hydrodynamics and heat transfer. This Pe dependence is characteristic of fully developed velocity and temperature fields and signifies the ratio of the momentum to thermal boundary-layer thicknesses $(Pr = \frac{v}{g})$.
- Dispersion should depend on the ratio of the molecular thermal resistances because the temperature field in the pore is influenced by the solid conductivity. Therefore, $\frac{k_s}{k_f}$ is expected to influence the dispersion tensor.

- Dispersion should depend on the ratio of the volumetric heat capacities, $\frac{\left(\rho c_{p}\right)_{s}}{\left(\rho c_{p}\right)_{f}}$. The transient temperature distribution in the unit cell (pore plus solid) depends on the extent of the ability of the solid to store or

release heat. Large values of $(\rho c_p)_s$ dampen the temporal temperature disturbances.

Based on this, the dispersion tensor is expected to have a functional form (Kaviany, 1995):

$$\frac{D^{d}}{\alpha_{f}} = \frac{D^{d}}{\alpha_{f}} \left(\text{Re, Pr, structure, } \frac{k_{s}}{k_{f}} \text{ and } \frac{\left(\rho c_{p} \right)_{s}}{\left(\rho c_{p} \right)_{f}} \right)$$
 (2.22)

Various analysis of the dispersion phenomena in porous media have been discussed by Kaviany (1995) where numerical and experimental methods were used for the determination of the dispersion tensor. In the following, the local volume averaging will be applied to convection as was already applied to conduction.

2.3.1.4.2 Local volume averaged convection heat transfer

In accordance with the definition of the representative elementary volume, the phase- averaged energy equation becomes:

$$\left[\varepsilon\left(\rho c_{P}\right)_{f} + \left(1 - \varepsilon\right)\left(\rho c_{P}\right)_{s}\right] \frac{\partial \langle T \rangle}{\partial t} + \left(\rho c_{P}\right)_{f} u \cdot \nabla \langle T \rangle = \left(\rho c_{P}\right)_{f} \nabla \cdot \left(D \cdot \nabla \langle T \rangle\right) \tag{2.23}$$

where the total diffusivity tensor, D is defined as:

$$D = \frac{K_e}{(\rho c_p)_f} + \varepsilon D^d \tag{2.24}$$

2.3.1.5 Two-medium treatment in porous media

When there is a significant heat generation occurring in any of the phases (solid or fluid), then the local (finite and small) volumes of the solid and fluid phases will be far from the local thermal equilibrium. In this section, the two-medium treatment of airflow and heat transfer in porous media is considered where the assumption of the local thermal equilibrium between the phases is not valid. In the two-medium treatment, no thermal equilibrium is assumed between the fluid and solid phases, but it is assumed that each phase is continuous and represented with an appropriate effective total thermal conductivity. Then thermal coupling between the phases is approached by a modeling parameter, h_{sf}, called the interfacial convective heat transfer coefficient.

Thus, two-temperature model is derived with the phase volume averaging of the energy equations, which shows how the fluid phase dispersion as well as the other convective and conductive effects appear as the coupling coefficients in the energy equations (Kaviany, 1995). The energy equations for each phase are written as:

$$\frac{\partial \langle T \rangle^{f}}{\partial t} = u_{ff} \cdot \nabla \langle T \rangle^{f} + u_{fs} \cdot \nabla \langle T \rangle^{s} = \nabla \cdot D_{ff} \cdot \nabla \langle T \rangle^{f} + \nabla \cdot D_{fs} \cdot \nabla \langle T \rangle^{s}
+ \frac{A_{fs}}{V_{f} (\rho c_{p})_{f}} h_{sf} (\langle T \rangle^{s} - \langle T \rangle^{f})$$
(2.25)

$$\frac{\partial \langle T \rangle^{s}}{\partial t} = \mathbf{u}_{sf} \cdot \nabla \langle T \rangle^{f} + \mathbf{u}_{ss} \cdot \nabla \langle T \rangle^{s} = \nabla \cdot \mathbf{D}_{sf} \cdot \nabla \langle T \rangle^{f} + \nabla \cdot \mathbf{D}_{ss} \cdot \nabla \langle T \rangle^{s}
+ \frac{\mathbf{A}_{fs}}{\mathbf{V}_{s} (\rho \mathbf{c}_{P})_{s}} \mathbf{h}_{sf} (\langle T \rangle^{f} - \langle T \rangle^{s})$$
(2.26)

These models require the determination of four thermal diffusivity tensors, D_{ff} , D_{ss} , D_{fs} , D_{sf} , the interfacial convective heat transfer coefficient, h_{sf} , and the closure vectors involving u_{uu} , u_{fs} , u_{sf} and u_{ss} . The coefficients in the following equations have been computed for some geometry and range of parameters (Quintard et al., 1997). The solution of this complicated system of equations is

difficult to attain and therefore, a more practical equation system is typically used (Quintard et al., 1997):

$$\varepsilon \left(\rho c_{P} \right)_{f} \left[\frac{\partial \langle T \rangle^{f}}{\partial t} + u \cdot \nabla \langle T \rangle^{f} \right] = \nabla \cdot K_{ff} \cdot \nabla \langle T \rangle^{f} + A_{fs} h_{sf} \left(\langle T \rangle^{s} - \langle T \rangle^{f} \right)$$
 (2.27)

$$(1 - \varepsilon)(\rho c_{P})_{s} \frac{\partial \langle T \rangle^{s}}{\partial t} = \nabla \cdot K_{ss} \cdot \nabla \langle T \rangle^{s} + A_{fs} h_{sf} (\langle T \rangle^{f} - \langle T \rangle^{s})$$
(2.28)

Different simplified versions of the energy equations have been used in determination of the interfacial convective heat transfer coefficient and therefore, the literature on the reported values of h_{sf} are rather incoherent (Kaviany, 1995). For example, the h_{sf} for a single heated particle is expected to be significantly different than that for particles in packed beds. Wakao and Kaguei (1982) have critically examined experimental results for determination of the interfacial convective heat transfer coefficients. They have found the following correlation for spherical particles:

$$Nu_d = \frac{h_{sf}d}{k_f} = 2 + 1.1Re^{0.6} Pr^{1/3}$$
 (2.29)

2.3.1.6 Limitations of porous media approach

Despite extensive efforts, no agreement has been reached for modeling transport phenomena during forced-air precooling process using the porous medium approach. The approach neglects the internal produce gradient. This is questionable when the difference between center and surface temperature of produce are sufficiently large; as the case in transient forced-air precooling process (Verboven et al., 2006). Another main drawback of the porous medium approach is the breakup of the continuous medium assumption when the package-to-product diameter is under 10 (Eisfeld and Schnitzlein, 2001; Verboven et al., 2006), which

is a common case in forced-air precooling process (Ferrua and Singh, 2008). Furthermore, when modeling the heat transfer process within packages using the two-treatment porous medium approach, complex two-equation models involving a series of model parameters are created whose determination of the parameters has seriously limited the accuracy of the model. The numerical calculation of these parameters for complex structures as well as experimental research to estimate them from experimental data has not been successful despite over 50 years of efforts (Ferrua and Singh, 2007). Some efforts have been done by lumping of different transport processes in the two-medium treatment; however, they obscure the physical basis of the models leading to considerable errors (Nijemeisland and Dixon, 2004; Verboven et al., 2006).

2.3.2 Direct Numerical Simulation

2.3.2.1 Background

Direct numerical simulation (DNS) performs a complete time-dependent solution of the Navier-Stokes and continuity equations. The value of such simulations is obvious. The method is targeted at obtaining a more fundamental understanding of how a local behavior of the fluid flow affects the heat and mass transfer processes. This is especially desirable in obtaining information about essentially immeasurable properties such as pressure and velocity fluctuations (Wilcox, 1993). For example, the difficulty in measuring air velocity within ventilated packages has caused limited progress in improving the design and efficiency of the forced-air precooling process. Some of the previously attempted strategies can not accurately measure or predict air velocity inside ventilated packages during the process (Alvarez and Flick, 1999a; Vigneault and de Castro, 2006; de Castro et al., 2004a). However, recent advances in computational resources have provided powerful tools to obtain detailed aerodynamic and thermal analysis by modeling coupled airflow, heat and mass transfer during the process.

In direct numerical simulation, the geometrical complexities are not simplified by the effective medium that is used in the porous medium approach (Kaviany, 1995; Nijemeisland and Dixon, 2004). Because this approach deals with local quantities, it is not constrained to any container-to-particle diameter ratio and it does not require any additional model parameters (Ferrua and Singh, 2007). In addition, the governing equations for the fluid flow and heat transfer include both laminar and turbulent flows, and are not restricted by fluid type or by flow rate; however, the geometric modeling and grid generation become complicated and the computational demands increase significantly (Ranade, 2002; Nijemeisland and Dixon, 2004). The enhanced computational requirements are mainly due to the extremely fine mesh necessary to carry out the simulation. Because of the significant computing costs and numerical difficulties, DNS is typically performed at low and moderate Reynolds number near laminar and transition regimes (Kim et al., 1987; Natarajan and Acrivos, 1993; Hetsroni et al., 2001; Portela et al., 2002; Ferrua and Singh, 2008).

2.3.2.2 Airflow, heat and mass transfer models

For a transient two-phase air-produce mathematical model of simultaneous airflow, heat and mass transfer inside ventilated packages the following equations are applied for air and produce domains. For air domain, the governing equations in Cartesian coordinates for incompressible airflow are as follows:

$$\nabla \cdot \mathbf{u} = 0 \tag{2.30}$$

$$\rho_{a} \frac{\partial \mathbf{u}}{\partial t} + \rho_{a} (\mathbf{u} \cdot \nabla \mathbf{u}) = -\nabla \mathbf{p} + \nabla \cdot \left[\mu_{a} \left(\nabla \mathbf{u} + (\nabla \mathbf{u})^{\mathsf{T}} \right) \right]$$
(2.31)

$$\rho_{\mathbf{a}} \mathbf{c}_{\mathbf{p},\mathbf{a}} \frac{\partial \mathbf{T}_{\mathbf{a}}}{\partial \mathbf{t}} + \rho_{\mathbf{a}} \mathbf{c}_{\mathbf{p},\mathbf{a}} (\mathbf{u} \cdot \nabla \mathbf{T}_{\mathbf{a}}) = \nabla \cdot (\mathbf{k}_{\mathbf{a}} \nabla \mathbf{T}_{\mathbf{a}})$$
(2.32)

For produce domain, the respiratory heat generation can be incorporated into the energy conservation equation as follows:

$$\rho_{p}c_{p,p}\frac{\partial T_{p}}{\partial t} = \nabla \cdot (k_{p}\nabla T_{p}) + Q_{resp}$$
(2.33)

2.3.2.3 Heat generation by respiration

Becker et al. (1996a) developed correlations that relate a commodity's rate of carbon dioxide production to its temperature. The carbon dioxide production rate can then be related to the commodity's heat generation rate due to respiration. An interpretation of the correlation is as follows:

$$Q_{resp} = \rho_p q_{resp} \tag{2.34}$$

where q_{resp} is given by:

$$q_{resp} = \frac{10.7f}{3600} (1.8 T_p - 459.67)^g$$
 (2.35)

T_p is transient produce temperature in K and the respiration constants (f and g) have been given in Becker et al. (1996a) for different crops.

2.3.2.4 Mass transfer

The rate of moisture loss from fruits and vegetables is expressed by the basic equation of the following form:

$$\dot{\mathbf{m}} = \mathbf{k}(\mathbf{p}_{s} - \mathbf{p}_{a}) \tag{2.36}$$

where the mass transfer coefficient (k) is given as follows (Becker et al., 1996a):

$$k = \frac{1}{\frac{1}{k_{\text{air}}} + \frac{1}{k_{\text{skin}}}} \tag{2.37}$$

The air film mass transfer coefficient (k_{air}) can be estimated by using the Sherwood-Reynolds-Schmidt correlations (Sastry and Buffington, 1982; Gaffney et al., 1985a; Becker et al., 1996a; Geankoplis, 2003):

$$Sh = 2 + 0.552 Re^{0.53} Sc^{0.33}$$
 (2.38)

The Sherwood number yields k'_{air} with a driving force in concentration unit (kg/m^3) ; however, the driving force in the mass transfer model is vapor pressure. Therefore, a conversion from concentration to vapor pressure is made by use of the ideal gas law:

$$\mathbf{k_{air}} = \frac{1}{\mathbf{R_{H,O}}} \mathbf{K'_{air}} \tag{2.39}$$

where T is the transient boundary layer temperature in K.

The skin mass transfer coefficient, k_{skin} , describing the resistance to moisture migration through the skin of a produce, is related to the structure and properties of the produce skin. Becker et al. (1996a) have tabulated skin mass transfer coefficients for different commodities.

The saturation partial water vapor pressure (p_w) can be approximated from the Antoine equation (Chuntranuluck et al., 1998; Hu and Sun, 2000):

$$p_w \approx \exp\left[23.4795 - \frac{3990.5}{T - 39.317}\right]$$
 (2.40)

where T is the transient boundary layer temperature in K.

Assuming water vapor to follow the ideal gas law, the partial pressure of water vapor in the air (p_a) is given by the standard psychrometric principle:

$$p_a = RH \cdot p_w \tag{2.41}$$

where RH denotes the relative humidity.

The partial pressure of water vapor at the evaporating surface (p_s) is defined as (Becker et al., 1996a):

$$p_s = VPL \cdot p_w \tag{2.42}$$

where VPL is vapor pressure lowering effect of the produce. The water vapor pressure lowering effect for various fruits and vegetables has also been provided in Becker et al. (1996a) obtained from Chau et al. (1987).

2.4 MODELS AVAILABLE IN THE LITERATURE

There are few mathematical models of airflow, heat and mass transfer during forced-air precooling in the literature considering packaged bulk produce.

Talbot et al. (1990) developed a porous-medium-approach model to investigate airflow behavior through oranges packed in shipping containers. The study applied a commercial finite element package to predict pressure and velocity distribution using the Darcy-Forchheimer and Ergun equations. Local velocity in free spaces between produce items as affected by different ventilated package designs and their resultant effects on produce temperature distribution was not considered in the study.

Alvarez and Trystram (1995) introduced a 1-D heat transfer model in order to control the cooling process of fruits and vegetables packed in bins piled on a pallet. The study showed strong variation of produce cooling with respect to different positions inside the bins for the same airflow conditions. The variation between the lowest and the highest produce surface temperature was almost 320% considering 30 different produce simulators (PVC spheres). The heterogeneity of produce moisture loss with 50% difference between the so-called "coldest point" and "hottest point" was also observed as a result of significant temperature heterogeneity between the produce simulators. Thus, a serious local quality loss (by moisture loss) and "freezing risk" due to the temperature heterogeneity inside different positions of a bin was monitored. They concluded that in order to prevent

surface freezing of produce, surface temperature of the coldest point should be controlled. No airflow equation was considered in the study to predict the air velocity distribution in the interstices of the bins.

Becker et al. (1996a and 1996b) developed a comprehensive model to estimate temperature distribution in the bulk cooling process of fruits and vegetables. However, the effect of package vents was not considered in the model. They applied the porous medium approach and the combined phenomena of airflow, heat and mass transfer were considered. The pertinent factors which govern the heat and mass transfer from fresh fruits and vegetables were taken into account including thermophysical properties of commodities such as transpiration and heat generation due to respiration as well as airflow parameters. A parametric study was performed to investigate the influence of bulk mass, airflow rate, skin mass transfer coefficient and relative humidity on the cooling time and moisture loss of a bulk load of apples. It was found that bulk mass and airflow rate were of primary importance to cooling time. Moisture loss was found to vary appreciably with regard to relative humidity, airflow rate and skin mass transfer coefficient. They also showed that an increase in airflow rate resulted in a decrease in moisture loss. They attributed this phenomenon to the fact that the increased airflow rate reduces the cooling time which quickly reduces the water vapor pressure deficit, thus lowering the transpiration rate.

Gowda et al. (1997) simulated the forced-air precooling of produce in bulk through mathematical modeling considering produce cooling variation in various layers. A number of additional factors such as the temperature variation of air along the height of a package were included in the model but the package vent effect on produce cooling was not considered. The model exhibited a transient behavior typical to bodies subjected to cooling at the surface; namely, rapid cooling followed by leveling off of temperature at larger times. They showed that the first layer; i.e., the produce layer nearest to the entry of air, cools faster and reaches the lowest temperature; whereas, the last layer cools slower and is at the highest temperature in the package. The layers in between reached intermediate temperatures in ascending order from the first to the last layer.

Van der Sman (2002) applied the Darcy-Forchheimer-Brinkman equation to predict airflow in ventilated packages by developing correlations between pressure drop and superficial velocity. The study used the porous medium approach and did not consider local velocities in free spaces between produce items at different positions inside the ventilated packages to investigate temperature heterogeneity.

Tanner et al. (2002a, 2002b, and 2002c) developed a modeling system to predict produce cooling rate by assessment of the relative effect of different package configurations on produce heat and mass transfer. They used a "zoned" approach, in which each package was subdivided into a number of zones with defined dependencies between them. Packaging, produce and fluid could be present in each zone with interactions between one another. However, a main drawback of the study was a "decoupled" modeling of heat and mass transfer processes. The assumptions of the model created a heat transfer-only and a mass transfer-only model. The effects of package vents and their locations as well as the evaporative cooling effect were also not considered in this study.

A three-dimensional two-phase air-produce model of airflow, heat and mass transfer has been developed to predict cooling rate and weight loss of chicory roots in a wind tunnel using the porous medium approach (Hoang et al., 2003). The model consisted of a system of conservation equations of airflow, heat and mass transfer for the air phase, and heat and mass transfer for the produce phase without considering the internal gradient in temperature in the produce phase. The effects of package vents were also not considered in the model. The interaction between the airflow and the porous media was described by an Ergun-type equation based on experimental data. Heat of respiration was included in the model as an empirically derived function of temperature. Some of the discrepancies between model prediction and experimental date were attributed to the non-ideal experimental conditions, the various sizes of the produce items, the small scale of the porous region compared to the size of the produce, assumption of uniform produce temperature and the estimation of transfer correlations. A good discussion was provided to explain some reasons for the difference between simulation and experimental data. They stated that the assumption of a two-phase flow in our case

of application may not hold. This is because of the large size of the produce items compared to the size of the package, which also increases the wall effect. The flow is, therefore, far from uniformly distributed over the whole domain.

Alvarez et al. (2003) proposed a semi-empirical model to predict the flow field through agricultural commodities stacked in packages by assuming the system as a continuous porous medium. The momentum equation was derived from the space averaging of Navier-Stokes equations. Calculation of the pressure and velocity fields was based on the Darcy-Forchheimer equation. Heat transfer between produce simulators (sphere) and the air was described by a correlation that linked the local Nusselt number to the modified Reynolds number and turbulence intensity. To verify the capability of the developed model, an experimental analysis of a two-dimensional system consisting of 75 mm diameter PVC spheres arranged in rectangular parallelepipeds within a rectangular air-blast tunnel was performed. Most characteristics of the measured heat transfer coefficients were reproduced and estimated with a relative accuracy of the order of 6%. However, the effect of package vent configuration on airflow and temperature distribution was not considered in this study.

Zou et al. (2006a and 2006b) developed a porous-medium-approach based modeling system for simulating airflow and heat transfer processes, and therefore to predict airflow patterns and temperature profiles in ventilated packages during forced-air precooling process. The ventilated packages were divided into two types, namely bulk and layered packages. In the bulk packages, produce items were held in a bin or carton without any other packaging materials and in the layered packages, produce items were placed on a stack of trays. The areas inside the packages were categorized as solid, plain air, and produce-air regions. The produce-air regions inside the bulk packages or between trays in the layered packages were treated as porous media, in which volume-averaged transport equations were applied. The authors noted that the approach used in the study does not completely satisfy the conditions for the porous medium approach due to the existence of trays as well as the small package-to-produce diameter ratio. In addition, the study considered only one central vent and, therefore, the effects of different package vent

area and its position on airflow and produce temperature distribution were not considered in the study. Opara and Zou (2007) applied sensitivity analysis of the same model to study the effect of variation in package vent areas and positions during forced convection cooling process. The authors noticed some considerable effects of the variation on produce cooling rate; however, the effect of multiple vents on airflow pattern and temperature profile considering different vent area and position was not reflected in the study.

Ferrua and Singh (2008) applied direct numerical simulation of laminar airflow in a ventilated package during forced convection cooling. A typical 0.5-kg strawberry package used for retail marketing was considered in this study. The packed test section consisted of 22 spheres of 1.63 cm diameter inside a basket of 5.3×5.3×4.3 cm³ with the container-to-produce diameter ratio of 2.96. The packed structure was constrained by a pair of ventilated walls with a typical shape, size and distribution of the vents in a strawberry package. The vented area represented 16.1% of the total cross-sectional wall area. The horizontal vent accounted for 54% of the total vented area in the wall. The vertical vents, uniformly distributed at the bottom and top of the perforated wall, represented 26% and 20% of the total vented area, respectively. The flow field developed within this packed structure was numerically and experimentally investigated when air at 0°C was forced through it at 0.000034 m³/s. The Reynolds number was 50, which was calculated based on the mean fluid velocity. The results showed a significantly heterogeneous airflow distribution within the flow domain. The flow within the packed structure accelerated as its pathway was narrowed between spheres, and it significantly slowed down as it approached solid surfaces. The standard deviation of the velocity field within any of the horizontal planes under study was larger than 60% of the averaged velocity within it. The study is one of the recent attempts of its kind in detailed understanding of the behavior of flow field within a packed structure without disturbing the flow; however, the influence of different package vent designs on airflow pattern and its resultant temperature distribution was not considered.

Delele et al. (2008) applied the porous medium approach for modeling airflow through stacked produce in vented packages. Two layers of 32 spheres with a diameter of 7.5cm each randomly stacked in packages of dimensions $30 \times 40 \times 16 \,\mathrm{cm}^3$ with the container-to-produce diameter ratio of 2.4 was considered. The percent vent area of the side, front and bottom surfaces of the packages were 11.03%, 14.36% and 19.10%, respectively. The aerodynamic study showed very heterogeneous airflow inside the ventilated packages and considerable effects of the vented packages on the flow resistance was also noted. Due to applying the porous medium approach, the study did not consider local velocities in free spaces between produce items at different positions inside the ventilated packages. Also, the effect of the heterogeneous airflow inside the stack on temperature distribution was not studied.

CONNECTING TEXT

In order to design an optimized package to be used during forced-air precooling, it is necessary to start with a detailed understanding of the aerodynamic behavior occurring inside different ventilated packages during the process. In many cases, this understanding has been limited to only few experimental studies that attempt to link the local fluid flow behavior to the heat transfer process. The difficulty in measuring the local flow field inside ventilated packages is the main drawback that has limited the application of this approach. This is because the measurement of the fluid flow inside the packages without disturbing produce packaging arrangement becomes impossible by means of conventional measurement methods. As an alternative approach, mathematical modeling of airflow and heat transfer during forced convection cooling of produce can provide a tool to investigate airflow pattern and the resultant temperature distribution during the process. This tool can predict air velocity at any position inside ventilated packages during the process to investigate a detailed aerodynamic behavior and, therefore, to optimize package design.

III. AERODYNAMIC ANALYSIS DURING COOLING OF STACKED PRODUCE INSIDE VARIOUS VENTILATED PACKAGES

3.1 ABSTRACT

Aerodynamic analysis during forced convection cooling of produce was conducted by modeling coupled airflow and heat transfer. Air velocities and heterogeneity indexes were predicted for different configurations of package openings at an airflow rate of 0.022 m³/s. Predicted temperature profiles were compared with experimental data for model validation. Good agreement between model prediction and measured data was obtained. The results showed that airflow distribution during the process was not homogeneous. More uniform airflow distribution was obtained by increasing vent area from 2.4 to 12.1%. The highest cooling heterogeneity index (108%) was recorded at 2.4% vent area whereas lowest heterogeneity index (0%) was detected in a package with 12.1% vent area. Proper package vent design is necessary to provide more uniform cooling operation during forced convection cooling process.

Keywords: Mathematical modeling, Airflow and heat transfer, Forced convection cooling, Airflow heterogeneity, Package design, Heterogeneity index

3.2 INTRODUCTION

Fruits and vegetables are cooled from ambient temperature to an optimal temperature before storage or shipment in order to minimize their deterioration after harvest. Forced convection cooling is the most common technology used for this purpose (de Castro et al., 2005). However, it induces strong heterogeneities of the thermal treatment due to heterogeneous airflow distribution at different locations in ventilated packages (Alvarez and Flick, 1999; de Castro et al., 2004; Alvarez and

Flick, 2007). Commodities located behind blind walls may not be sufficiently cooled while others exposed to higher velocities are over-cooled. Therefore, package vent design is a very critical factor influencing airflow and heat transfer patterns during forced convection cooling and, therefore, affecting the efficiency of the system (de Castro et al., 2004; Vigneault and de Castro, 2006).

The difficulty in measuring air velocity within ventilated packages has caused limited progress in improving the design and efficiency of the forced convection cooling process. Some of the previously attempted strategies can not accurately measure or predict air velocity inside ventilated packages during the process (Alvarez and Flick, 1999; de Castro et al., 2004; Vigneault and de Castro, 2006). However, recent advances in computational resources have provided powerful tools to obtain detailed aerodynamic and thermal analysis by modeling coupled airflow and heat transfer during the process.

There are two typical methods for modeling forced convection cooling of produce, namely the porous medium approach (single-phase or two-phase) and direct numerical simulation (DNS). Severe simplifications of the porous medium approach, such as the assumption of local thermal equilibrium in single-phase models and continued lumping of transport processes in the two-phase models obscure the physical basis of the models, leading to considerable errors (Kaviany, 1995; Nijemeisland and Dixon, 2004). Additionally, the two-phase porous medium approach neglects the internal produce gradient. This is questionable when the difference between center and surface temperature of the produce are sufficiently large, as is the case in the transient forced-air precooling process (Verboven et al., 2006). The porous medium assumption is also questionable when the package-to-product diameter ratio is below 10 (Eisfeld and Schnitzlein, 2001) which is a common case for fruit and vegetable packages (Ferrua and Singh, 2008).

Direct numerical simulation performs a complete time-dependent solution of the Navier-Stokes and continuity equations. This is especially desirable in obtaining information about essentially immeasurable properties such as pressure and velocity fluctuations (Wilcox, 1993). In DNS, the geometrical complexities are not simplified by the effective medium that is used in the porous medium approach

(Kaviany, 1995; Nijemeisland and Dixon, 2004). The governing equations for the fluid flow and heat transfer include both laminar and turbulent flows, and are not restricted by fluid type or by flow rate; however, the geometric modeling and grid generation become complicated and the computational demands increase significantly (Ranade, 2002; Nijemeisland and Dixon, 2004). The enhanced computational requirements are mainly due to the extremely fine mesh necessary to carry out the simulation. Because of the significant computing costs and numerical difficulties, DNS is typically performed at low and moderate Reynolds numbers near laminar and transition regimes (Kim et al., 1987; Natarajan and Acrivos, 1993; Hetsroni et al., 2001; Portela et al., 2002; Ferrua and Singh, 2008).

There are few models in the literature about airflow distribution through stacked items inside ventilated packages. Van der Sman (2002) applied the Darcy-Forchheimer-Brinkman equation to predict airflow in ventilated packages by developing correlations between pressure drop and superficial velocity. The authors used the porous medium approach and did not consider local velocities in free spaces between produce items at different positions inside the ventilated packages to investigate air velocity heterogeneity. Additionally, heat transfer modeling was not considered to describe produce temperature profiles. Alvarez et al. (2003) developed a semi-empirical model to predict the flow field in porous media. The momentum equation was derived from the Navier-Stokes equations, leading to the Darcy-Forchheimer equations. The authors showed air velocity heterogeneity inside a bin of stacked spheres; however, the effect of package vents and their location on velocity distribution were not considered.

Ben Amara et al. (2004) proposed an empirical model of convective heat transfer as a function of velocity in a stack of spheres without considering the vent effect. Ferrua and Singh (2008) applied DNS for simulation of laminar airflow in a ventilated package during forced convection cooling without considering the effect of different vent designs on cooling uniformity. Delele et al. (2008) used the porous medium approach for modeling airflow through stacked produce in vented packages. The aerodynamic study showed very heterogeneous airflow inside the ventilated packages and considerable effects of the vented packages on the flow

resistance was also noted. Due to applying the porous medium approach, the study did not consider local velocities in free spaces between produce items at different positions inside the ventilated packages. Also, the effect of the heterogeneous airflow inside the stack on temperature distribution was not studied.

The aim of the present study was to mathematically model simultaneous airflow and heat transfer during forced convection cooling of produce to investigate airflow pattern and the resultant temperature distribution during the process. Air velocities at different locations of the package are to be predicted and coupled to heat transfer models by considering different vent areas and positions on package walls.

3.3 MATERIALS AND METHODS

3.3.1 Model Formulation

A transient two-phase air-produce mathematical model of simultaneous airflow and heat transfer inside a ventilated package containing spherical produce was considered (Figure 3.1). For the air domain, the governing equations in Cartesian coordinates were applied for incompressible airflow as follows:

$$\nabla \cdot \mathbf{u} = 0 \tag{3.1}$$

$$\rho_{a} \frac{\partial \mathbf{u}}{\partial t} + \rho_{a} (\mathbf{u} \cdot \nabla \mathbf{u}) = -\nabla \mathbf{p} + \nabla \cdot \left[\mu_{a} (\nabla \mathbf{u} + (\nabla \mathbf{u})^{\mathsf{T}}) \right]$$
(3.2)

$$\rho_{a}c_{p,a}\frac{\partial T_{a}}{\partial t} + \rho_{a}c_{p,a}(u \cdot \nabla T_{a}) = \nabla \cdot (k_{a}\nabla T_{a})$$
(3.3)

where u denotes the velocity field (m/s) at different positions inside the package, ρ_a air density (kg/m³), t time (s), P pressure (Pa), μ_a air dynamic viscosity (Pa.s), $c_{p,a}$ air specific heat capacity (J/kg K), T_a air temperature at different positions inside ventilated packages (°C) and k_a air thermal conductivity (W/m K).

For the produce domain, the respiratory heat generation can be incorporated into the energy conservation equation as follows:

$$\rho_{p} c_{p,p} \frac{\partial T_{p}}{\partial t} = \nabla \cdot (k_{p} \nabla T_{p}) + Q_{resp}$$
(3.4)

where ρ_p represents produce density (kg/m³), $c_{p,p}$ produce specific heat capacity (J/kg K), T_p produce temperature at different positions inside ventilated packages (°C), k_p produce thermal conductivity (W/m K) and Q_{resp} respiratory heat generation (W/m³).

The following boundary conditions were applied for airflow and heat transfer equations in package inlet, outlet, wall and air-produce interfaces:

Inlet:
$$u = u_0$$
; $T_a = T_{a0}$ (3.5)

Outlet:
$$p = p_0$$
; $(-k_a \nabla T_a) \cdot n = 0$ (3.6)

Wall:
$$u = 0$$
; $(-k_a \nabla T_a + \rho_a c_{p,a} T_a u) \cdot n = 0$ (3.7)

Interface:
$$\mathbf{u} = \mathbf{0}$$
; $\mathbf{T}_{\mathbf{a}} = \mathbf{T}_{\mathbf{p}}$; $(-\mathbf{k}_{\mathbf{p}}\nabla\mathbf{T}_{\mathbf{p}} + \mathbf{k}_{\mathbf{a}}\nabla\mathbf{T}_{\mathbf{a}}) \cdot \mathbf{n} = \dot{\mathbf{m}}\mathbf{L}$ (3.8)

where m is the rate of produce moisture loss (kg/s.m²) and L is the latent heat of evaporation (J/kg).

3.3.2 Numerical Method

A two-dimensional (2-D) model of airflow and heat transfer was considered. Three-dimensional (3-D) modeling of airflow and heat transfer inside a ventilated package containing few hundred spheres extensively increases the computational demands both in mesh size and number of iterations. To be able to solve for certain details in a 3-D model, such as areas where spheres are close to each other or to

package walls, a high level of detail is necessary for the required accuracy of the simulation. Such a large computational capacity is currently neither affordable nor manageable. Although the computational requirement is at the limit of today's computing power, it is predictable that within a few years, 3-D modeling of fluid flow and heat transfer for some hundred spheres will be considered a normal situation.

The COMSOL MultiphysicsTM software (COMSOL, Inc.), version 3.4 (2007), was used to solve the simultaneous airflow and heat transfer models using the finite element method. Quadratic Lagrange elements with a triangular mesh were used to solve the nonlinear system of equations at each time step. It is well known that in discretization of the convection-dominated convection-diffusion flows, the finite element computation of incompressible flows involves potential numerical instabilities. The instabilities are associated with the Galerkin formulation resulting in spurious oscillations in the studied fields primarily where steep gradients are present (Tezduyar, 1992). The oscillations can even be large enough to prevent the solution from converging.

In particular, if the element Peclet number (Pe_{el}) is greater than one, the discrete solution may exhibit non-physical instabilities (Elman and Ramage, 2002). There is a mesh resolution, at least in theory, beyond which the discretization is stable by decreasing the element size (h) to a required value. However, the element size is determined by available memory in a computer implying that a given mesh may not properly resolve small-scale effects. Different stabilized finite element formulations such as turbulent isotropic diffusion (isotropic diffusion), streamline diffusion, crosswind diffusion and pressure-stabilization are used to prevent the numerical instabilities (Tezduyar, 1992; Codina, 1993; Elman and Ramage, 2002; Galeao et al., 2004; Lube and Rapin, 2006; John and Knobloch, 2007).

Isotropic diffusion (Codina, 1993; Elman and Ramage, 2002; John and Knobloch, 2007) was used in the present study to address the numerical oscillations. In this approach, a coefficient of artificial diffusion, c_{art}, is added to the diffusion already present in the problem:

$$c_{art} = \delta_{id} h |\beta| \tag{3.9}$$

The tuning parameter, δ_{id} , controls the amount of artificial diffusion. Turek (1999) discusses the value of the parameter and indicates its practical values in the range [0.1...2]. By considering $\delta_{id} = 0.5$, the local Peclet number was changed to:

$$\operatorname{Pe}_{\mathsf{el}} = \frac{\mathbf{h}|\beta|}{(\mathbf{c} + \mathbf{c}_{\mathsf{art}})} = \frac{2\mathbf{h}|\beta|}{2\mathbf{c} + \mathbf{h}|\beta|} \tag{3.10}$$

The added turbulent isotropic diffusion can damp the effects of oscillations and impedes their propagation to other parts of the domain. It should however be stressed that the added diffusion only influences the solution to an appreciable extent where β and h are both large, i.e. where the element Peclet number is large.

To establish an optimal mesh, different mesh densities were extensively investigated so that it could represent the flow specifics of the geometry as accurately as possible. Several setups were defined and tested, changing mesh densities in the whole domain or a specific subdomain, and with near-wall treatments using different mesh sizes with different element growth rates. For example, the element growth rate of 1.1 determines the maximum rate of 10% at which the element size can grow from a region with small elements to a region with larger elements. A finer mesh was used at the package inlets and outlets so that velocity and temperature gradients did not become too large in these areas, which could lead to instability of the solution. A finer mesh was also used in vicinities where the produce items were close to each other or the package walls. Mesh quality (q_{mesh}) was calculated as:

$$q_{\text{mesh}} = \frac{4\sqrt{3} A}{h_1^2 + h_2^2 + h_3^2}$$
 (3.11)

where A is triangle area, and h_1 , h_2 and h_3 are side lengths of the triangle. The value of mesh quality ranges from 0 to 1. When $h_1 = h_2 = h_3$, mesh quality is equal to 1. If $q_{mesh} > 0.3$, mesh quality is unlikely to affect the solution's quality (COMSOL MultiphysicsTM, 2007). In all the simulations, mesh consisted of 152,236 elements resulting in 516,309 degrees of freedom with $q_{mesh} = 0.95$ and mean element size of 0.002 m in the whole domain and average $Pe_{el} \approx 74$ in the air domain considering three different package vent configurations. Solution time on a workstation with 2 dual core processors (3.00 GHz, 4 MB L2, 1333 MHz) and 32 GB RAM was about 55 min.

3.3.3 Experimental and Simulation Setups

For experimental model validation, solid polymer balls with 5.24 cm diameter and 125.55 g weight were used to simulate spherical produce inside a ventilated package (Figure 3.1). However in the simulation, due to the 2-D modeling, produce diameter was decreased to 5.14 cm in order to provide a free path for airflow. Thermal conductivity and heat capacity of the balls were 0.6839 W/m K and 1125 J/kg °C, respectively (Vigneault and de Castro, 2005). The balls were used for model validation due to their uniform nature in terms of size, shape and thermophysical properties.

Because the balls neither respire nor loose moisture, the terms Q_{resp} and $\dot{m}L$ appearing in the right-hand side of equations 4 and 8, respectively, were set to zero during the simulation. However, for real produce, effects of produce heat generation and evaporative cooling can be incorporated into the model. It should be noted that the primary objective of this study was to find not absolute but relative values of cooling efficiency that allow the comparison among different vent areas and positions during forced convection cooling process. These results were obtained under the same circumstances in terms of both materials and procedure.

In the physical experimental setup, 512 balls were uniformly distributed on a columnar pattern to form a cubic matrix of 8-ball-side dimension. Four out of 512 balls were instrumented with a 30-gage insulated copper-constantan thermocouple

wire placed in their center and located in the fourth z plane (z=4) parallel to airflow. Figure 3.1 (a) represents produce positions in which their center temperatures were used for model validation.

A forced convection cooling system (Figure 3.2) was set up by assembling four acrylic plates to form a tunnel of 42 cm square cross section and 125 cm length. The portion of the tunnel containing the balls was insulated with 2.5 cm-thick polystyrene foam to reduce heat conduction. Two sides of the package were simulated by placing a pair of perforated polypropylene square plates (42 cm wide and 0.3 cm thick) next to the first and eighth columns of balls, perpendicular to airflow. The polypropylene plates were drilled with five 33.75 cm × 1.25 cm grooves spaced at 10.125 cm (Figure 3.1 (b)). For each individual test, some of these grooves were covered with sealing tape to obtain the specific vent configuration demonstrated in Table 3.1. The air inlet was connected to a static heat-exchanger and the air outlet to an aspiration chamber.

Various package opening configurations with different vent area and position can be tested with different airflow rates by the system. Three different vent configurations including 1, 3 and 5 vents (see Tab. 1) corresponding to different vent areas of 2.4, 7.2, and 12.1%, respectively, were simulated at the airflow rate of 0.022 m³/s and the Reynolds number of 2157. The Re number was calculated considering the hydraulic diameter of the cross-section of the air domain (free space) demonstrated in Figure 3.1 (a). The mean air velocity (0.51 m/s) used to determine Re number was also calculated based on the same free space (Vigneault and de Castro, 2006).

Prior to starting a test, the forced-air tunnel containing the balls was placed in a warm chamber maintained at a prescribed temperature ranging from 26.4 to 38.7°C with standard deviation of 0.3°C. An axial fan forced the air to circulate through the ball matrix to provide a uniform initial temperature. Then, a pair of perforated plates was installed and the tunnel was placed in the cold chamber kept at 2.2±0.7°C. The system simultaneously recorded the temperature inside the instrumented balls along with air temperature before and after crossing the ball

matrix, the temperature in the center of the cold chamber, the pressure drop through the ball matrix and plates, and the airflow rate, at 20 s intervals.

3.3.4 Heterogeneity Index

In order to demonstrate the deviation of estimated air velocity at different positions from average velocity inside the ventilated packages, a heterogeneity index (HI) was defined as:

$$HI = \frac{\sqrt{(u - \overline{u})^2}}{\overline{u}} \times 100 \tag{3.12}$$

where \overline{u} is the average velocity obtained at 21 different positions and u is the velocity obtained at a specific position. The 21 positions were chosen after the 2^{nd} , 4^{th} , and 6^{th} columns of produce (Figure 3.1 (a)). In each column, 7 different positions were considered and numbered from top to bottom.

3.4 RESULTS AND DISCUSSION

This section presents the airflow distribution and temperature profiles predicted from the coupled airflow and heat transfer models during forced convection cooling of produce. The predicted temperature profiles were compared with experimental data for model validation.

3.4.1 Effect of Package Vent Configuration on Velocity Distribution

Figure 3.3 demonstrates air velocity distributions at 21 different positions inside ventilated packages with 1, 3 and 5 vents. As can be seen from the figure, more uniform airflow distribution was achieved by increasing vent area from 2.4 to 12.1%. In the package with only 1 vent, more heterogeneous velocity distribution was obtained with an average velocity of 0.62±0.26 m/s considering the 21 different

positions illustrated in Figure 3.1(a). At the positions after the 2nd column, the air velocity was gradually decreased from 1.30 at position 1 to 0.26 m/s at position 7. Then, a relatively uniform velocity ranging from 0.55 to 0.63 m/s was obtained for positions 8 to 14 located after the 4th column. However, velocity distribution was again heterogeneous for the positions placed after the 6th column where the velocity progressively increased from 0.31 m/s at position 15 to 1.16 m/s at position 21. This result shows that the velocity is higher near the only inlet and outlet of the package compared to the positions far from inlet and outlet vents. It should also be stressed that the minimum and maximum velocity, considering all the 21 positions, was obtained at positions 7 and 1 with the values of 0.26 and 1.30 m/s, respectively suggesting the most heterogeneous cooling near the package inlet vent.

In the package with 3 vents, homogeneous velocity distribution was obtained with an average velocity of 0.53±0.02 m/s considering 21 different points. The difference between the maximum velocity (0.57 m/s at positions 1 and 7) and minimum velocity (0.48 m/s at positions 3 and 5) was 0.09 m/s, where both of these values were estimated for locations after the 2nd column of the commodities, resulting in more heterogeneous cooling compared to the positions after the 4th and 6th columns. The difference between the maximum and minimum velocity for the positions after the 4th and 6th columns were 0.02 and 0.05 m/s suggesting the highest cooling uniformity in the middle of the package with 3 vents. On the other hand, in the package with 5 vents, the velocity magnitudes were in the range 0.54±0.01 m/s. The difference between the maximum and minimum velocity for the positions after the 2nd, 4th and 6th columns was 0.05, 0.03 and 0.02 m/s, respectively. As the case in the packages with 1 and 3 vents, the highest velocity heterogeneity was seen at the positions after the 2nd column.

3.4.2 Heterogeneity Indexes Created in Different Package Vent Configurations

The heterogeneity of air velocity inside the ventilated packages was further investigated by evaluation of the heterogeneity index at 21 different positions. Figure 3.4 shows that airflow distribution inside the ventilated packages is not

homogeneous during forced convection cooling of produce. Generally, by increasing vent area, more uniform airflow or less heterogeneity was obtained. The values of heterogeneity indexes in three different ventilated packages ranged from 108 to 0%. While the highest heterogeneity index (108%) was simulated for the vent configuration with only 2.4% vent area at position 1, the lowest heterogeneity index (0%) was simulated in the package with 12.1% vent area at position 2. The better cooling uniformity of the package with 5 vents can be related to better vent distribution on package walls and therefore, the better air circulation through the commodities during forced convection cooling.

Additionally, the highest heterogeneity indexes were generally observed after the 2nd (positions 1 and 7) and 6th (positions 15 and 21) columns. In all ventilated packages with 1, 3 and 5 vents, the highest heterogeneity indexes were seen at positions located near inlet and/or outlet vents. On the other hand, the highest uniformity of air velocities was observed in the middle of the ventilated packages in all three vent configurations. This could explain more uniform produce cooling in the middle of the packages (positions 8-14) during forced convection cooling.

3.4.3 Temperature Profiles in Different Package Vent Areas

Figure 3.5 (from a to f) shows the simulated and experimental temperature profiles in the center of commodities at four different positions (P1, P2, P3 and P4), shown in Figure 3.1 (a), inside three different packages with 1, 3 and 5 vents, respectively. Overall, good agreement between simulation and experimental data was obtained. The mean absolute error for the four positions was 2.2°C, considering all the three packages. The deviation could be considered satisfactory regarding various simulation and experimental parameters influencing the model performance such as variations in experimental inlet air velocity, air temperature and the balls' thermophysical properties, as well as numerical oscillations.

Figure 3.6 shows the overall model performance based on regression plot of the experimental vs. predicted temperatures for the three vent configurations. The

regression equation shows an intercept of 0.33 and a slope of 1.02 with $R^2 = 0.92$. The full identity between predicted and experimental temperature in the regression requires a null intercept and a slope of 1. The deviations of intercept and slope from 0 and 1, respectively, are not statistically significant at an alpha level of 5%.

3.5 CONCLUSIONS

Coupled mathematical models of airflow and heat transfer were developed for aerodynamic analysis during forced convection cooling of produce. Air velocity, heterogeneity indexes and produce temperature profiles were investigated in three different package opening configurations. The results showed that airflow distribution during the forced convection cooling process is not homogeneous. The larger the vent area the better the air uniformity during the process; however, the vent area can not exceed a certain limit due to the risk of compromising package structural resistance. As a result, suitable package vent design is necessary to provide more uniform produce cooling.

3.6 REFERENCES

- Alvarez, G., and D. Flick. 1999. Analysis of heterogeneous cooling of agricultural products inside bins Part I: Aerodynamic study. Journal of Food Engineering 39:227-237.
- Alvarez, G., P.E. Bournet, and D. Flick. 2003. Two-dimensional simulation of turbulent flow and transfer through stacked spheres. International Journal of Heat and Mass Transfer 46:2459-2469.
- Alvarez, G., and D. Flick. 2007. Modelling turbulent flow and heat transfer using macro-porous media approach used to predict cooling kinetics of stack of food products. Journal of Food Engineering 80:391-401.
- Ben Amara, S., O. Laguerre, and D. Flick. 2004. Experimental study of convective heat transfer during cooling with low air velocity in a stack of objects.

 International Journal of Thermal Sciences 43:1213-1221.
- Codina, R. 1993. A discontinuity-capturing crosswind-dissipation for the finite element solution of the convection-diffusion equation. Computer Methods in Applied Mechanics and Engineering 110:325-342.
- COMSOL Multiphysics TM. 2007. COMSOL Multiphysics User's Guide. COMSOL Inc., Burlington, Massachusetts.
- de Castro, L.R., C. Vigneault, and L.A.B. Cortez. 2004. Container opening design for horticultural produce cooling efficiency. Journal of Food, Agriculture & Environment 2:135-140.
- de Castro, L.R., C. Vigneault, and L.A.B. Cortez. 2005. Cooling performance of horticultural produce in containers with peripheral openings. Postharvest Biology and Technology 38:254-261.

- Delele, M.A., E. Tijskens, Y.T. Atalay, Q.T. Ho, H. Ramon, B.M. Nicolai, and P. Verboven. 2008. Combined discrete element and CFD modelling of airflow through random stacking of horticultural products in vented boxes. Journal of Food Engineering 89:33-41.
- Eisfeld, B., and K. Schnitzlein. 2001. The influence of confining walls on the pressure drop in packed beds. Chemical Engineering Science 56:4321-4329.
- Elman, H.C., and A. Ramage. 2002. An analysis of smoothing effects of upwinding strategies for the convection-diffusion equation. SIAM Journal on Numerical Analysis 40:254-281.
- Ferrua, M.J., and R.P. Singh. 2008. A nonintrusive flow measurement technique to validate the simulated laminar fluid flow in a packed container with vented walls. International Journal of Refrigeration-Revue Internationale Du Froid 31:242-255.
- Galeao, A.C., R.C. Almeida, S.M.C. Malta, and A.E. Loula. 2004. Finite element analysis of convection dominated reaction-diffusion problems. Applied Numerical Mathematics 48:205-222.
- Hetsroni, G., C.F. Li, A. Mosyak, and I. Tiselj. 2001. Heat transfer and thermal pattern around a sphere in a turbulent boundary layer. International Journal of Multiphase Flow 27:1127-1150.
- John, V., and P. Knobloch. 2007. On spurious oscillations at layers diminishing (SOLD) methods for convection-diffusion equations: Part I A review. Computer Methods in Applied Mechanics and Engineering 196:2197-2215.
- Kaviany, M. 1995. Principles of heat transfer in porous media. Springer-Verlag, New York.

- Kim, J., P. Moin, and R. Moser. 1987. Turbulence Statistics in Fully-Developed Channel Flow at Low Reynolds-Number. Journal of Fluid Mechanics 177:133-166.
- Lube, G., and G. Rapin. 2006. Residual-based stabilized higher-order FEM for advection-dominated problems. Computer Methods in Applied Mechanics and Engineering 195:4124-4138.
- Natarajan, R., and A. Acrivos. 1993. The Instability of the Steady Flow Past Spheres and Disks. Journal of Fluid Mechanics 254:323-344.
- Nijemeisland, M., and A.G. Dixon. 2004. CFD study of fluid flow and wall heat transfer in a fixed bed of spheres. AICHE Journal 50:906-921.
- Portela, L.M., P. Cota, and R.V.A. Oliemans. 2002. Numerical study of the nearwall behaviour of particles in turbulent pipe flows. Powder Technology 125:149-157.
- Ranade, V. 2002. Computational Flow Modeling for Chemical Reactor Engineering. Academic Press, New York.
- Tezduyar, T.E. 1992. Stabilized finite element formulations for incompressible flow computations, p. 1-44 Advances in Applied Mechanics, Vol. 28.
- Turek, S. 1999. Efficient solvers for incompressible flow problems / an algorithmic and computational approach. Springer-Verlag, Berlin, New York.
- Van der Sman, R.G.M. 2002. Prediction of airflow through a vented box by the Darcy-Forchheimer equation. Journal of Food Engineering 55:49-57.

- Verboven, P., D. Flick, B.M. Nicolai, and G. Alvarez. 2006. Modelling transport phenomena in refrigerated food bulks, packages and stacks: basics and advances. International Journal of Refrigeration-Revue Internationale Du Froid 29:985-997.
- Vigneault, C., and L.R. de Castro. 2005. Produce-simulator property evaluation for indirect airflow distribution measurement through horticultural crop package. Journal of Food, Agriculture & Environment 3:67-72.
- Vigneault, C., and L.R. de Castro. 2006. Indirect measurement method for laminar to turbulent airflow through horticultural produce simulators. Transactions of the ASABE 49:1455-1461.
- Wilcox, D.C. 1993. Turbulence modeling for CFD. DCW Industries, Inc., La Canada, California.

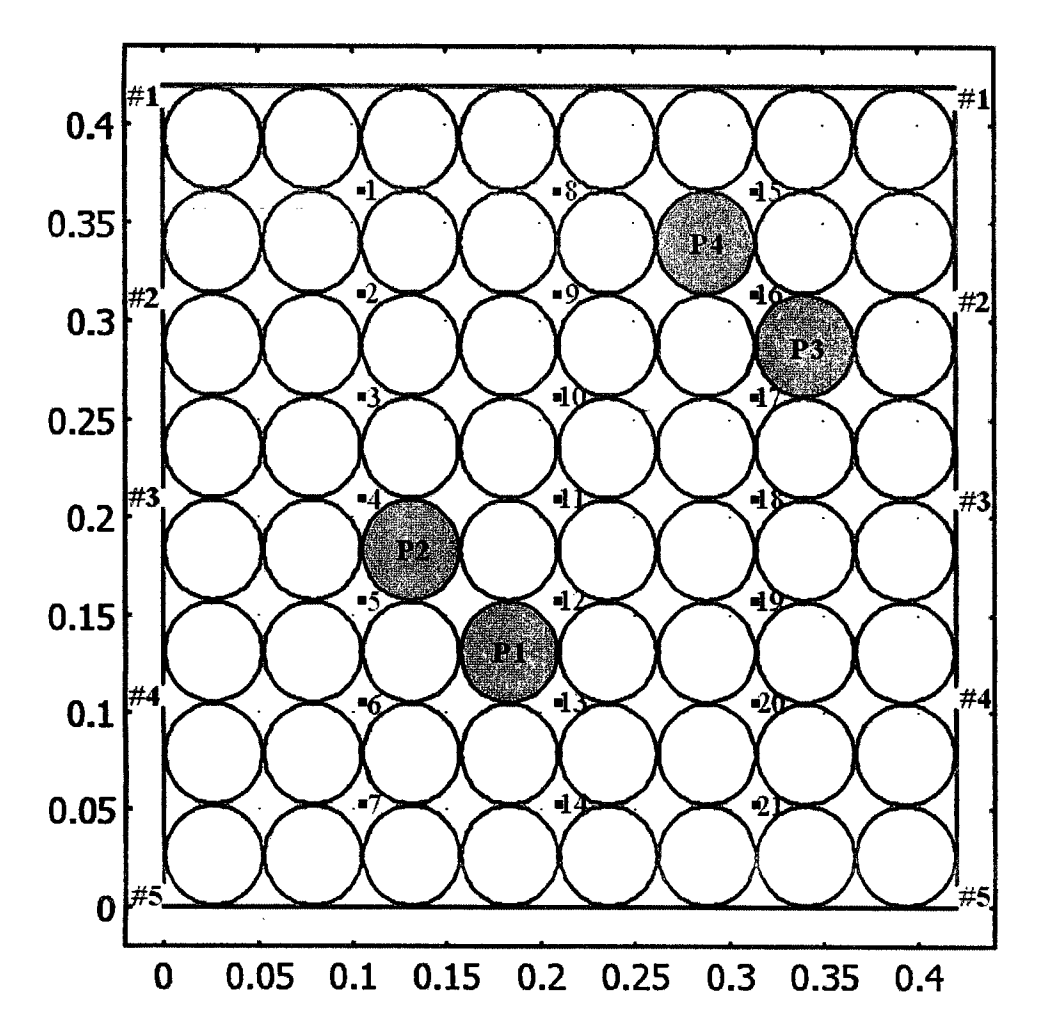


Figure 3.1 (a): A computational geometry representing cross-sectional area of a packaged produce with inlet and outlet vent positions shown in left and right sides and numbered from #1 to #5 from top to bottom, exact locations of the 21 points considered for the air velocity and heterogeneity index evaluations, as well as produce positions (P1, P2, P3 and P4) used for model validation.

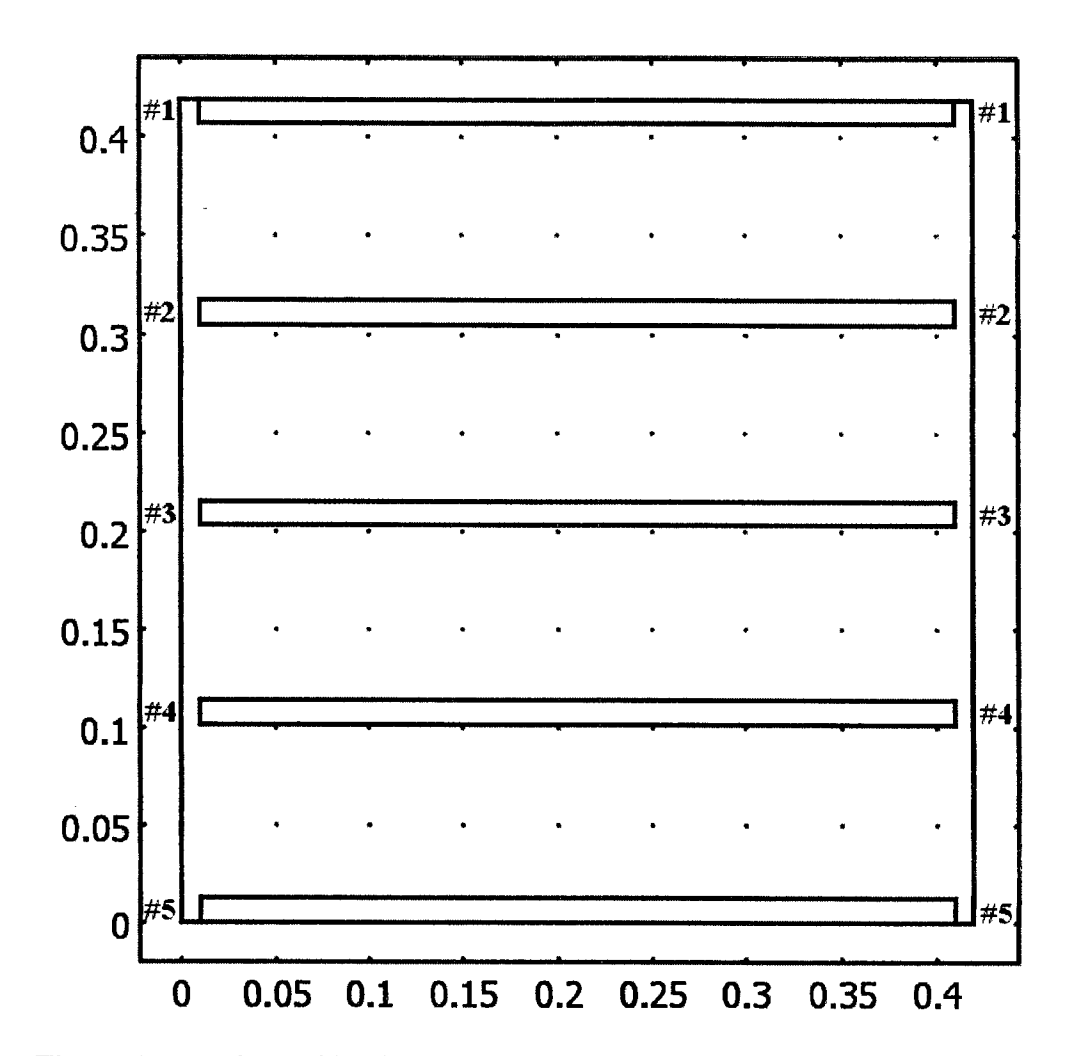


Figure 3.1: Package side view illustrating different package vent configurations described in Table 3.1

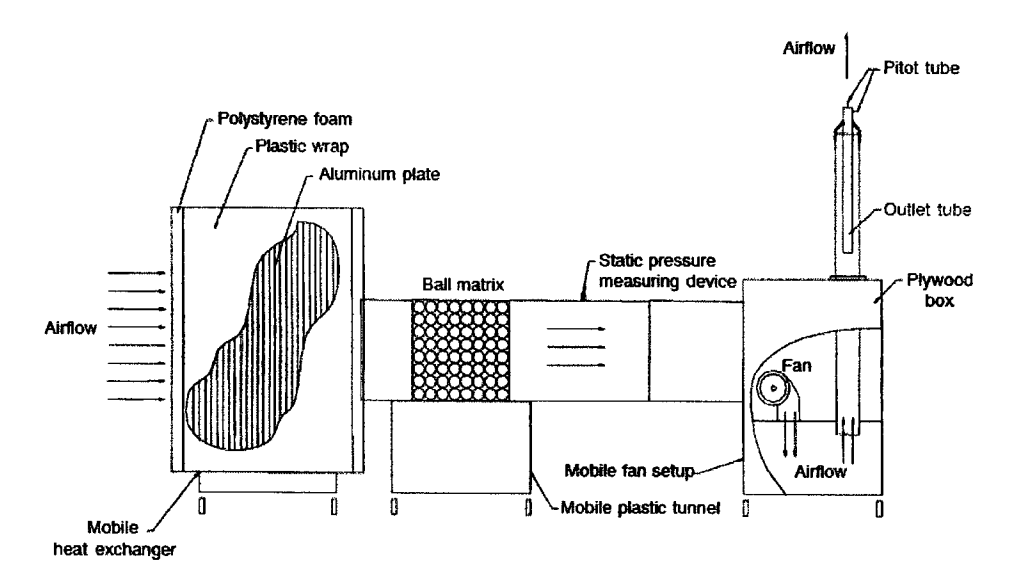


Figure 3.2: Experimental setup showing forced air tunnel, ball matrix, fan, and the airflow measuring device

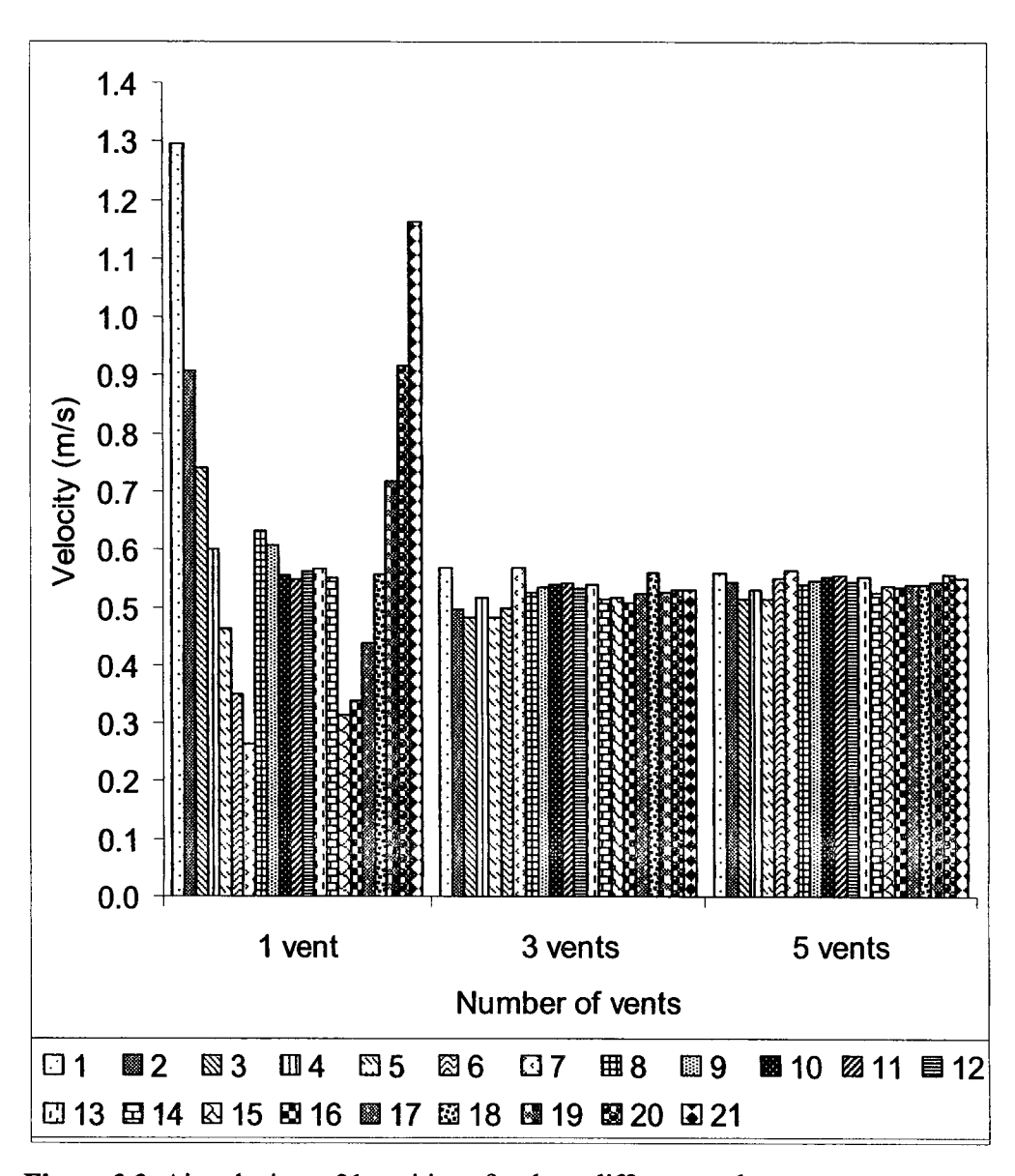


Figure 3.3: Air velocity at 21 positions for three different package vent areas

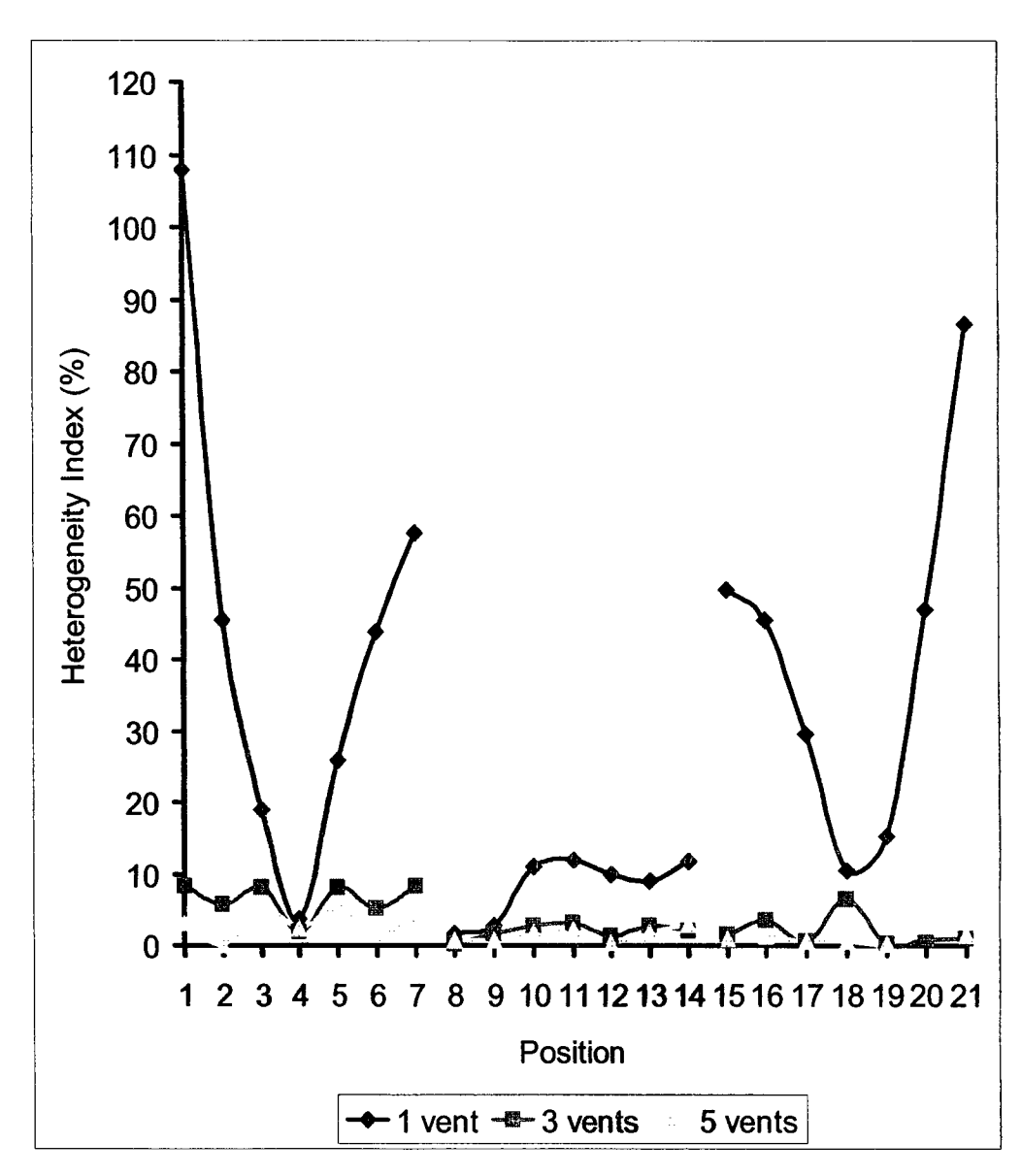
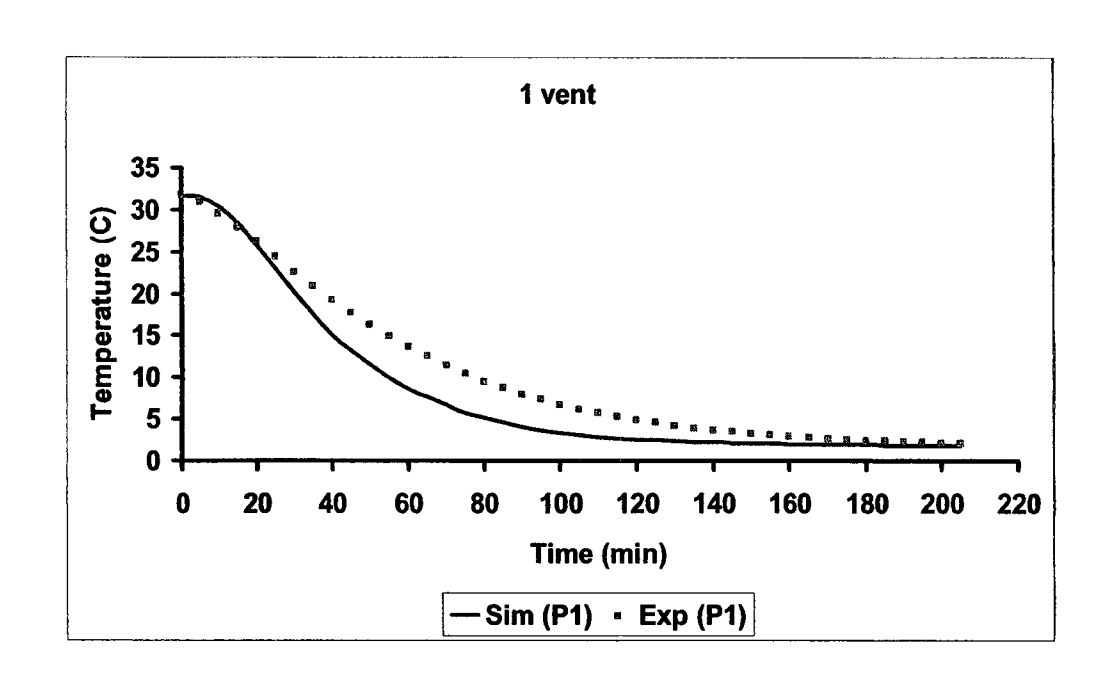


Figure 3.4: Heterogeneity index (HI) at 21 positions for three different package vent configurations



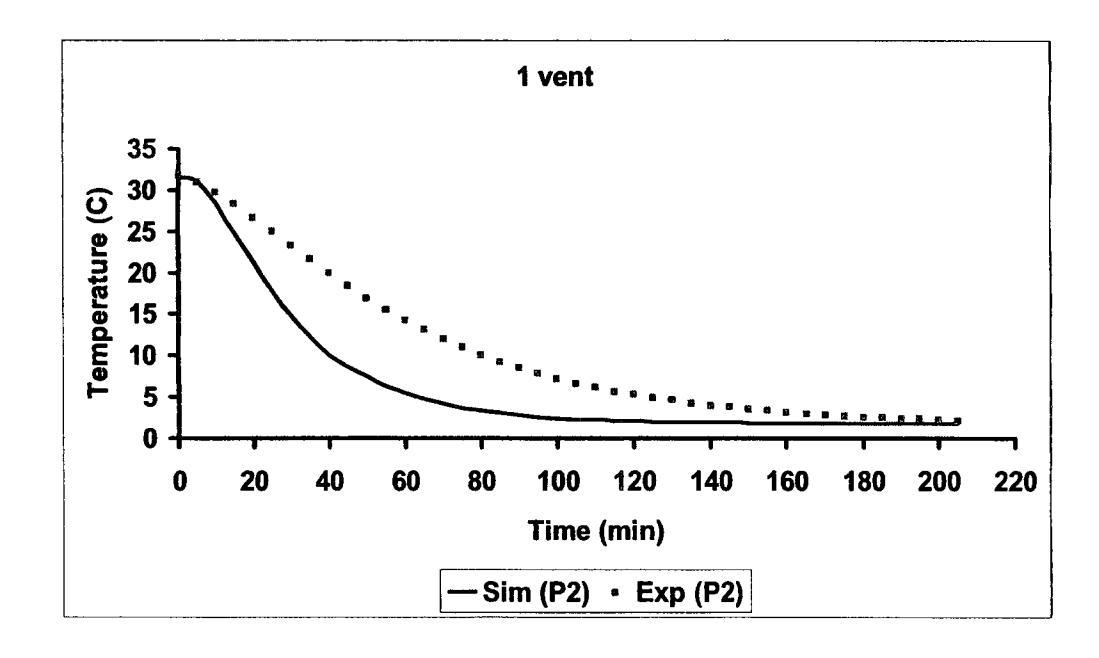
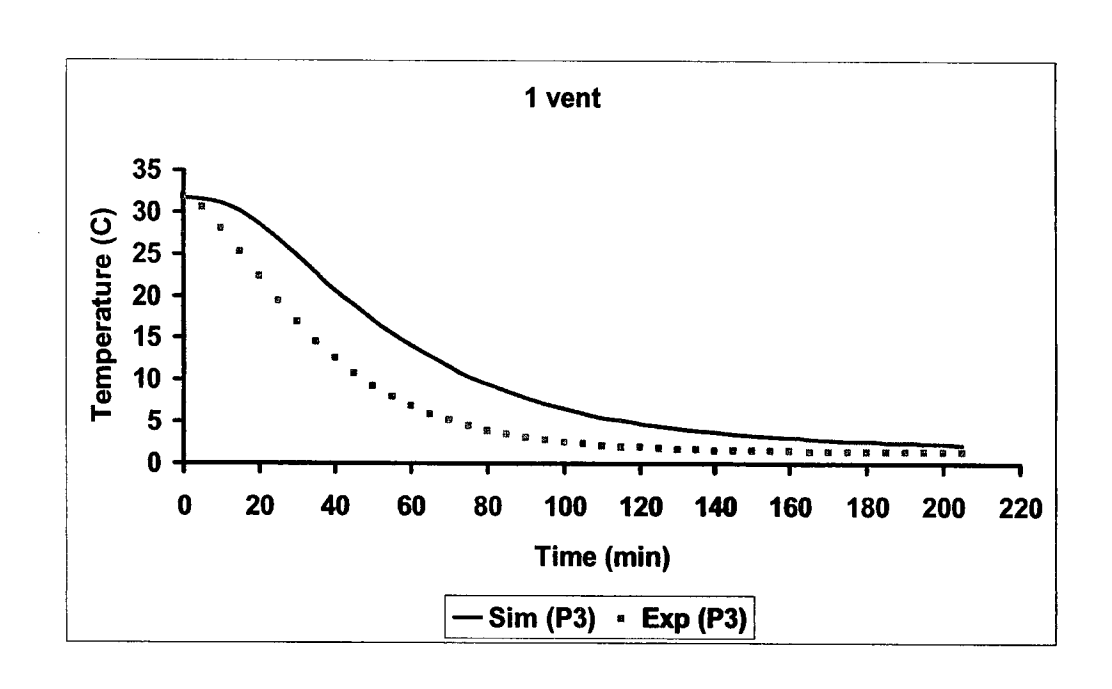


Figure 3.5 (a): Simulated (Sim) and Experimental (Exp) temperature profiles based on center temperatures of the positions P1 and P2, demonstrated in Figure 3.1 (a), in the package with 1 vent



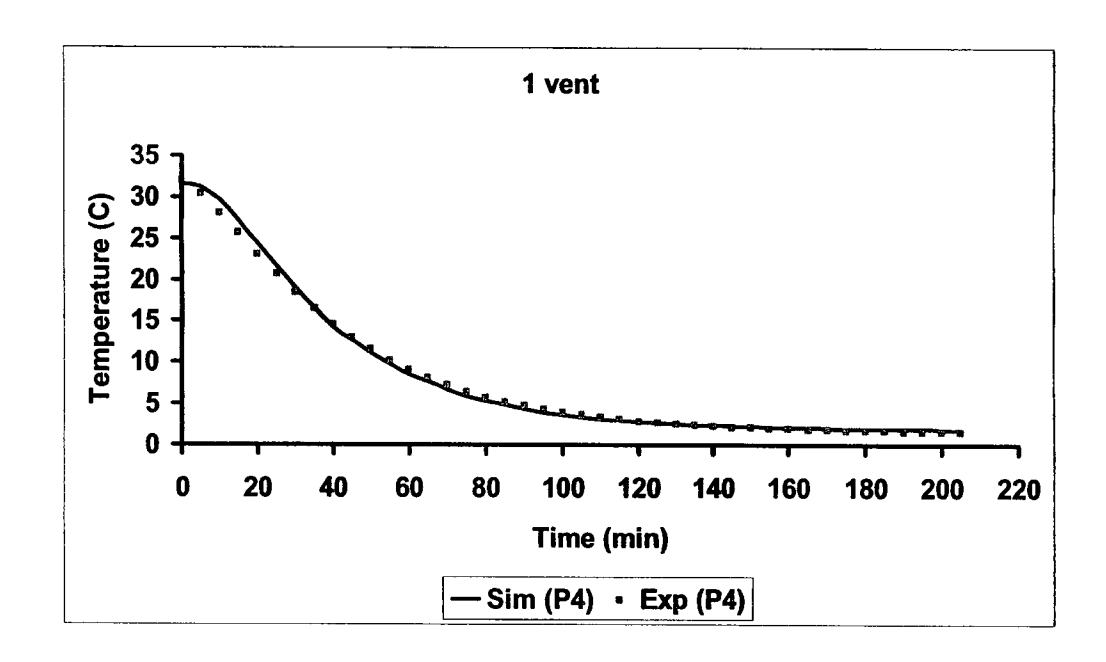
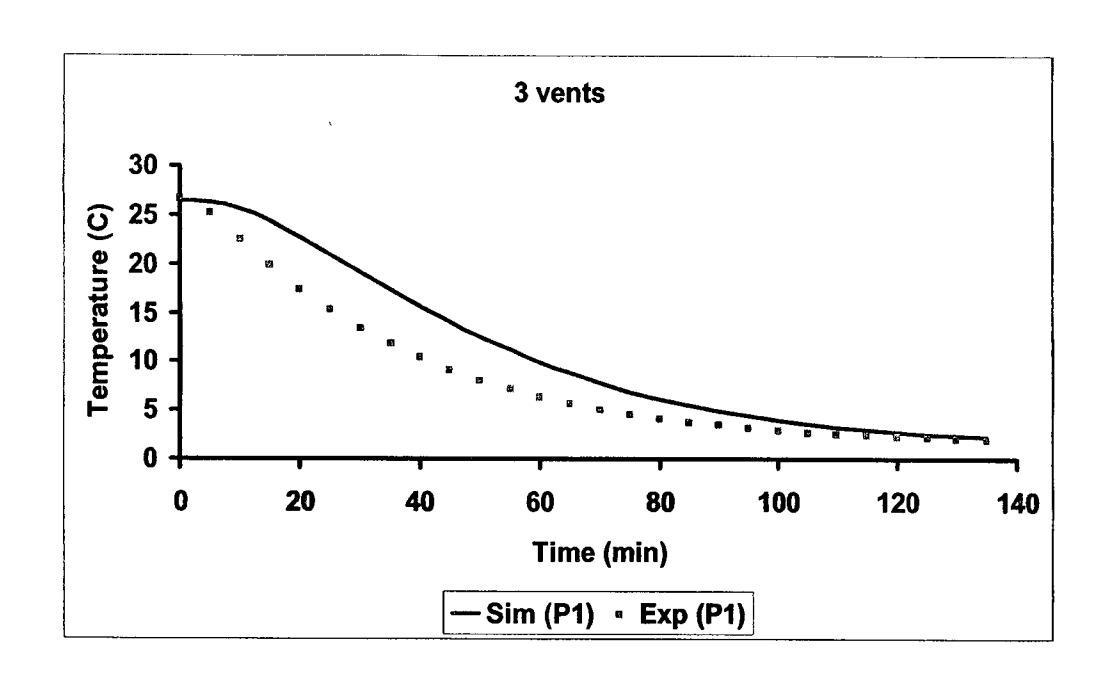


Figure 3.5 (b): Simulated (Sim) and Experimental (Exp) temperature profiles based on center temperatures of the positions P3 and P4, demonstrated in Figure 3.1 (a), in the package with 1 vent



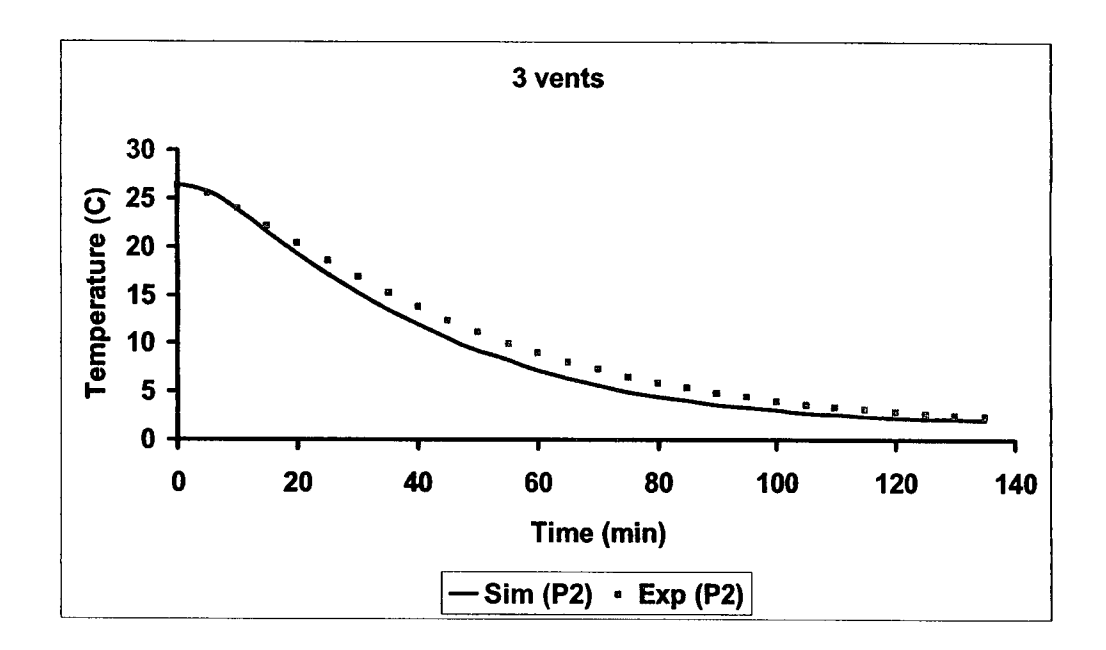
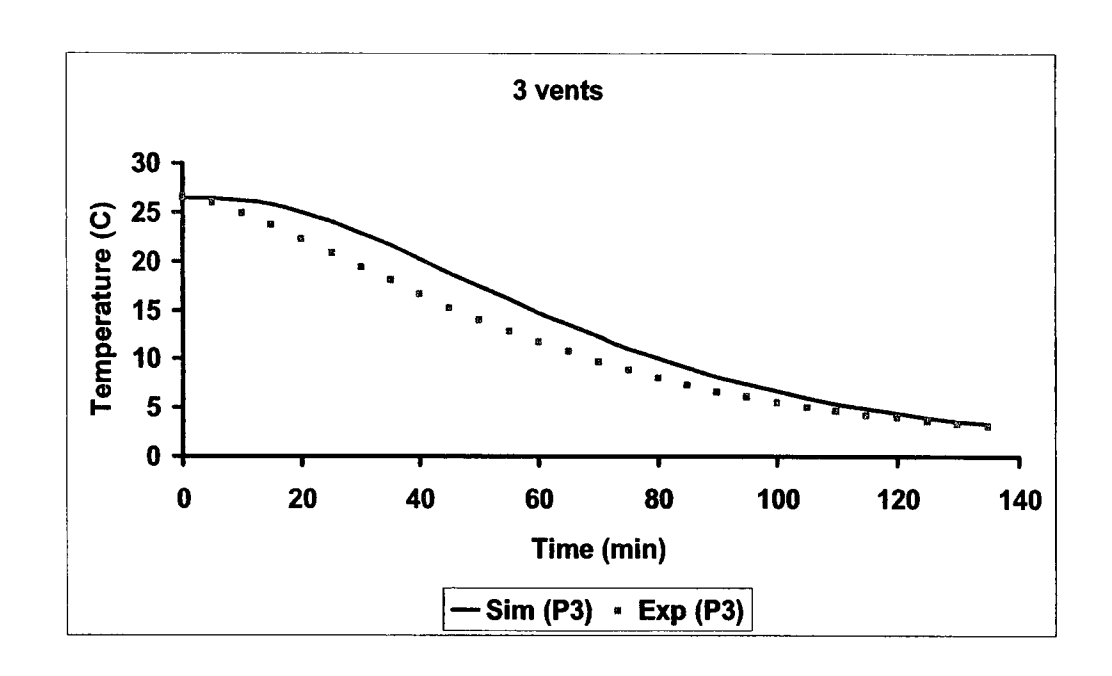


Figure 3.5 (c): Simulated (Sim) and Experimental (Exp) temperature profiles based on center temperatures of the positions P1 and P2, demonstrated in Figure 3.1 (a), in the package with 3 vents



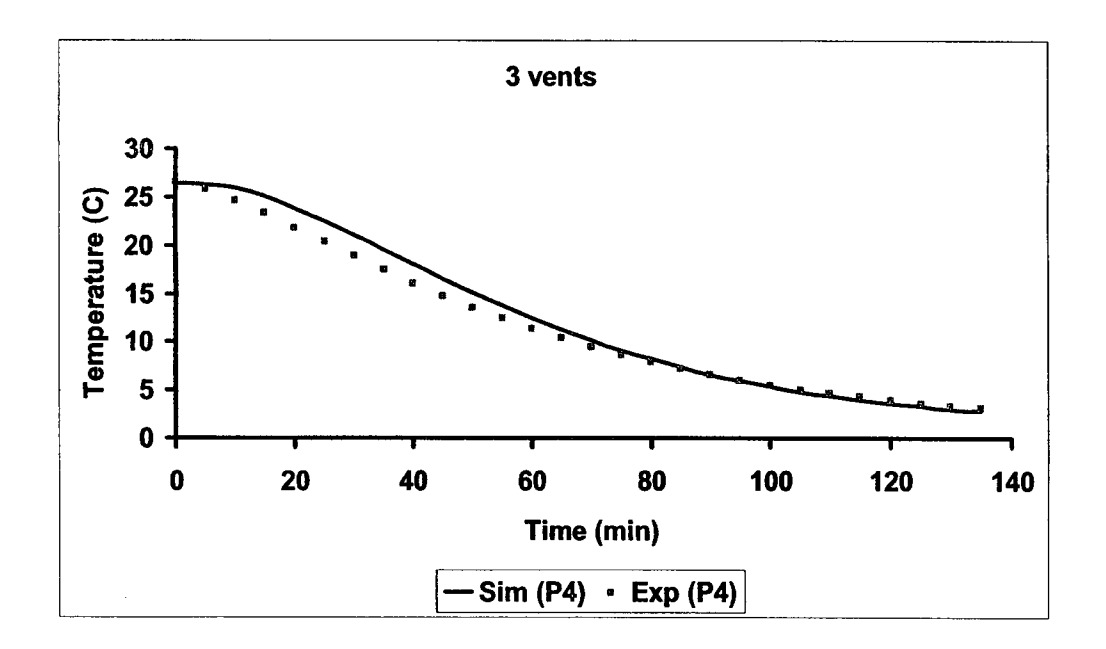
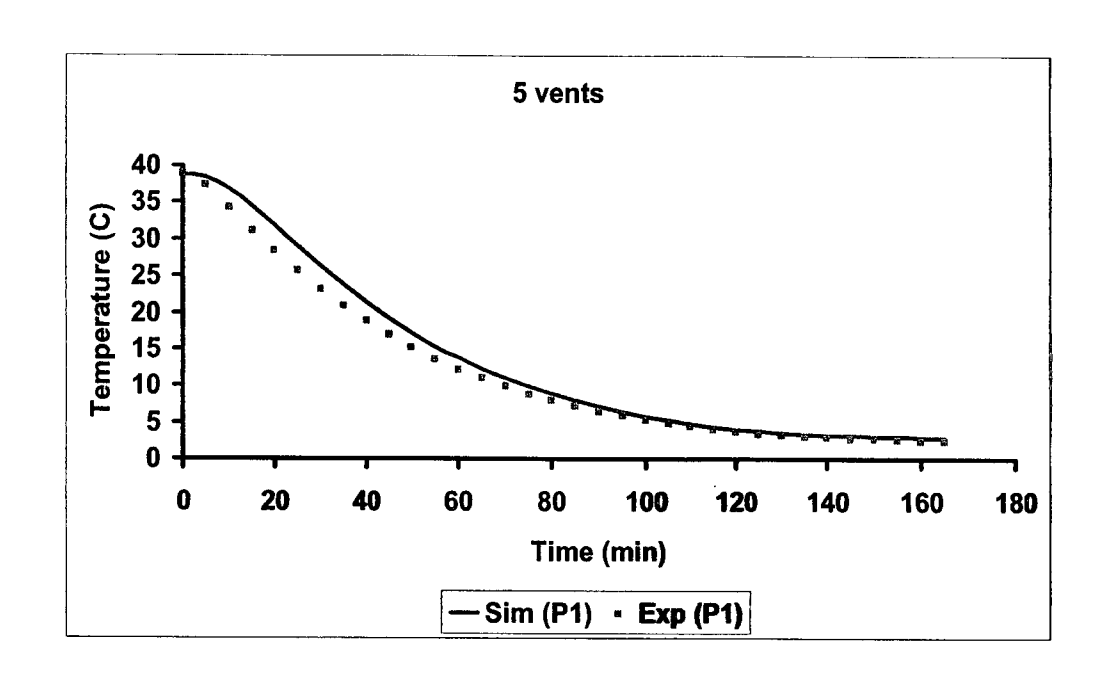


Figure 3.5 (d): Simulated (Sim) and Experimental (Exp) temperature profiles based on center temperatures of the positions P3 and P4, demonstrated in Figure 3.1 (a), in the package with 3 vents



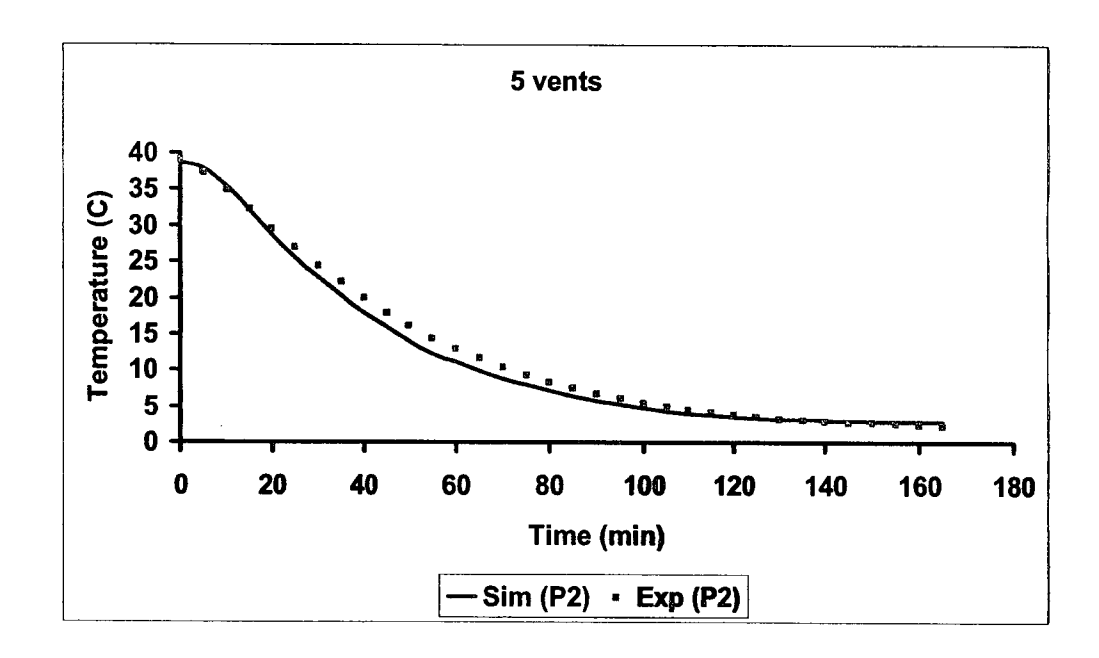
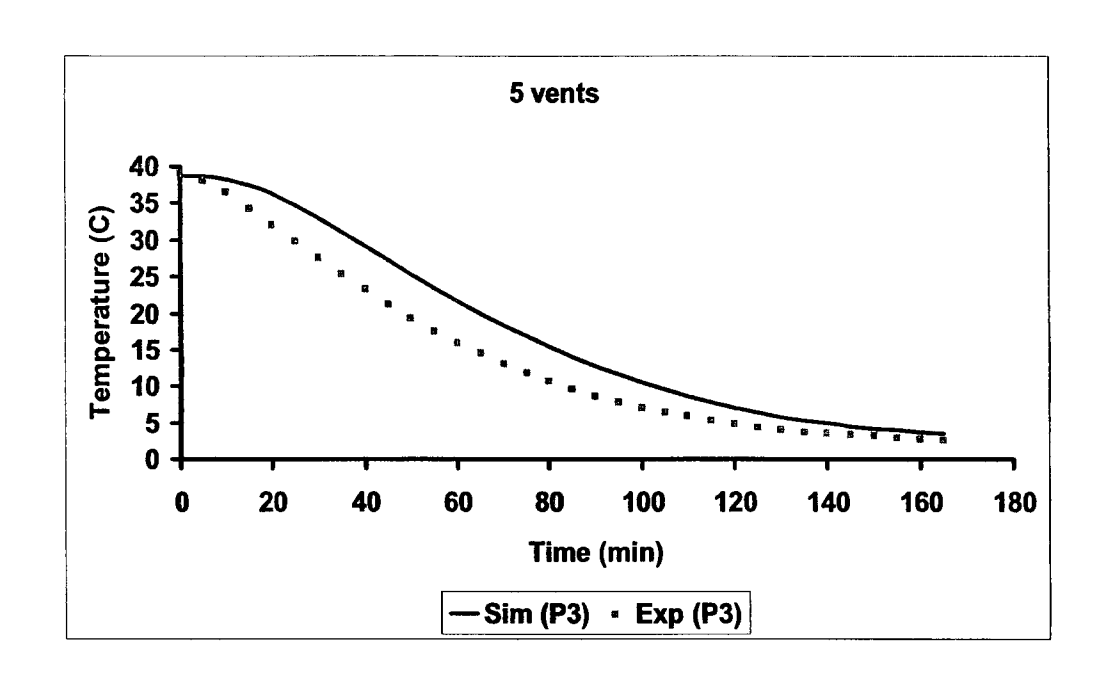


Figure 3.5 (e): Simulated (Sim) and Experimental (Exp) temperature profiles based on center temperatures of the positions P1 and P2, demonstrated in Figure 3.1 (a), in the package with 5 vents



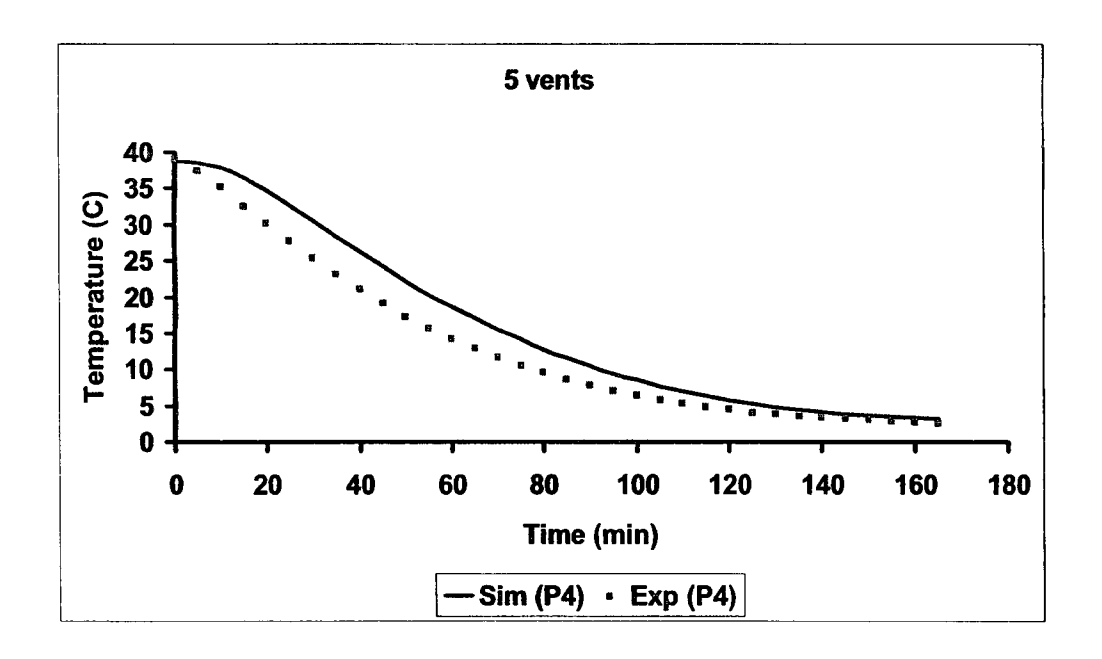


Figure 3.5 (f): Simulated (Sim) and Experimental (Exp) temperature profiles based on center temperatures of the positions P3 and P4, demonstrated in Figure 3.1 (a), in the package with 5 vents

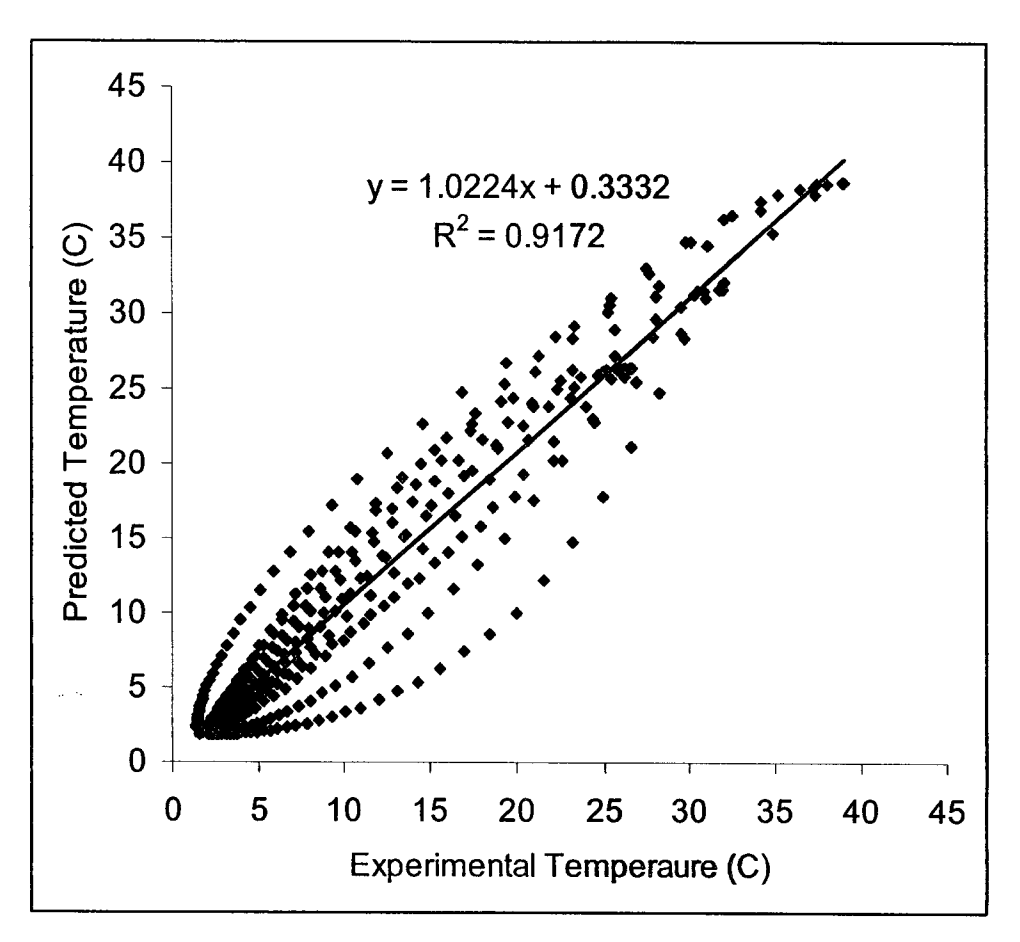


Figure 3.6: Overall model performance based on regression plot of the experimental vs. predicted temperatures for all three different vent configurations

Table 3.1: Package vent configurations based on different vent positions demonstrated in Figure 1 (a)

Vent configuration	Number of vent(s)	Inlet vent position(s)	Outlet vent position(s)	Vent area (%)
A	1	#1	#5	2.4
В	3	#1, #3, #5	#1, #3, #5	7.2
С	5	#1, #2, #3, # 4 , #5	#1, #2, #3, #4, #5	12.1

.....

CONNECTING TEXT

Aerodynamic analysis during forced convection cooling of produce was conducted in Chapter III. Air velocities and heterogeneity indexes were predicted for different configurations of package openings. The results showed that airflow distribution during the process is not homogeneous. In Chapter IV, the effect of the heterogeneous velocity distribution on produce temperature distribution will be investigated. The study is to simulate and analyze temperature distribution inside different ventilated packages to achieve uniform temperature during the process.

IV. COOLING OF STACKED PRODUCE INSIDE VARIOUS VENTILATED PACKAGES: THERMAL ANALYSIS

4.1 ABSTRACT

The influence of different package vent configurations, including ventilated packages with 1, 3 and 5 vents, on produce temperature distribution during forced convection cooling was investigated. Generally, produce cooling uniformity was increased by increasing the number of vents from 1 to 5. Produce cooling heterogeneity increased until about 90 min cooling and subsequently decreased with further cooling in all 3 ventilated packages. The methodology developed in this study can be used as a design tool to provide homogeneous temperature distribution in ventilated packages during forced convection cooling of produce.

Keywords: Direct numerical simulation; forced-air precooling; temperature distribution; cooling uniformity; ventilated package design

4.2 INTRODUCTION

Strong cooling heterogeneity is created during forced convection cooling process due to poor temperature management (Alvarez and Flick, 1999a; Alvarez and Flick, 1999b). Ventilated packages used during the process should be designed in such a way that they can provide a uniform temperature distribution during the process. Package vent design including different vent areas and locations on package walls are very critical factors influencing airflow and heat transfer patterns during forced convection cooling (de Castro et al., 2004; Vigneault and de Castro, 2006). Percent vent area of the package affects the efficiency of a cooling system (Baird et al., 1988). Increase in side ventilation from 2 to 6% increased airflow in corrugated fiber board packages in different stacking patterns and thus reduced cooling time

(Ladaniya and Singh, 2000). Package vents must also be well distributed on package walls to provide homogeneous airflow distribution and uniform cooling, ensuring adequate mechanical resistance (Smale et al., 2003).

There are numerous models in the literature on airflow, heat and mass transfer during precooling of agricultural produce. Baird and Gaffney (1976) developed a 1-D numerical procedure for predicting air and produce temperatures in bulk loads of fruits or vegetables. A 1-D heat transfer model to control the cooling process of fruits and vegetable was proposed by Alvarez and Trystram (1995). Moreover, Becker et al. (1996) developed a 1-D model to estimate temperature distribution in the bulk cooling process of fruits and vegetables. A mathematical model based on porous medium approach was also developed by Gowda et al. (1997) to describe simultaneous heat and mass transfer during forced convection cooling of spherical foods. Tanner et al. (2002a, 2002b) developed a 1-D modeling system to predict produce cooling rate by assessment of the relative effect of different packaging configuration design on produce heat transfer. A porous-medium-approach model of airflow, heat and mass transfer has also been developed to predict cooling rate and weight loss of chicory roots in a wind tunnel (Hoang et al., 2003). Furthermore, Zou et al. (2006a and 2006b) developed a modeling system for airflow and heat transfer based on porous medium approach in ventilated packages. However, none of these studies considered the effects of package vent configuration including different vent area and position on produce temperature distribution and cooling uniformity. Recently, Dehghannya et al. (2008) developed and experimentally validated a mathematical model of airflow and heat transfer for simultaneous aerodynamic and thermal analysis during forced-air precooling process inside ventilated packages. The study applied direct numerical simulation and analyzed velocity distributions and their resultant airflow heterogeneity indexes inside different ventilated packages; however, temperature distribution at different positions of the packages was not considered.

The aim of this study was to simulate and analyze temperature distribution inside different ventilated packages so that more uniform temperature distribution could be achieved during the process.

4.3 MATERIALS AND METHODS

A transient two-phase air-produce mathematical model of simultaneous airflow and heat transfer inside ventilated packages containing spherical produce (Figure 4.1) was developed and validated using experimental data (Dehghannya et al., 2008). Model description including the governing equations for air and produce domains, numerical method and experimental model validation are referred to Sections 3.3.1, 3.3.2 and 3.3.3, respectively.

4.3.1 Heterogeneity Index

In order to quantitatively compare the deviation of instantaneous temperature from average temperature at different package vent configurations, a heterogeneity index (HI) was defined as follows:

$$HI = \frac{\sqrt{\left(T_p - \overline{T}_p\right)^2}}{\overline{T}_p} \times 100 \tag{4.1}$$

where \overline{T}_p is the average temperature obtained at the center of all 64 positions, shown in Figure 4.1, after a specific time and T_p is the instantaneous temperature obtained at the center of a specific position.

4.4 RESULTS AND DISCUSSION

4.4.1 Temperature Distribution in Different Ventilated Package Configurations

Figure 4.2 (a, b and c) illustrates produce temperature distribution after 30 min cooling at different positions in three different package vent configurations including 1, 3 and 5 vents, respectively (Table 3.1). In all three vent configurations, the commodities near to airflow inlet are generally cooled faster compared to the commodities far from the inlet. Figure 4.2 (a) demonstrates that the cold air entering

from the only inlet of the package with 2.4% vent area creates a faster heat transfer for commodities placed in the top-left quarter of the package and a slower cooling rate for commodities located in the bottom and right sides of the package resulting in the most heterogeneous cooling compared to the packages with 3 and 5 vents. In the package with 7.2% vent area (Figure 4.2 (b)), more uniform cooling was achieved compared to the package with 2.4% vent area (Figure 4.2 (a)) for the commodities located in the middle of the package and near to the package outlets. However, more heterogeneous cooling was seen in the package with 3 vents, mainly in the first three columns near to airflow inlets. On the other hand, uniform cooling was achieved almost in whole parts of the package with 5 vents except in the first two columns (Figure 4.2(c)). In the package with 3 vents, in the last four columns (positions 33 - 64 shown in Figure 4.1), more homogeneous cooling was obtained with less than 2°C difference between maximum and minimum temperatures of each column. On the other hand, in the package with 5 vents, in addition to the last four columns, commodities located in the fourth column (positions 25 – 32 shown in Figure 4.1) also cooled homogeneously with less than 2°C difference between maximum and minimum temperatures. This result could suggest that homogeneous cooling is typically started somewhere from the middle toward outlet vents of the ventilated packages during forced-air precooling process.

4.4.2 Heterogeneity Indexes Obtained at Different Positions of the Ventilated Packages

Figure 4.3 illustrates the heterogeneity indexes of eight different columns after 30 min cooling based on center temperature of the 64 positions shown in Figure 4.1. As can be seen from the figure, more uniform cooling or less heterogeneity indexes were obtained by increasing number of vents from 1 to 5 considering eight different columns. The values of heterogeneity indexes regarding three different ventilated packages ranged from 0 to 83.9% in the packages with 5 vents and 1 vent, respectively. While the highest heterogeneity index (83.9%) was recorded for the vent configuration with only 2.4% vent area at position 1, the lowest heterogeneity index (0%) was detected in the package with 12.1% vent area at position 26. The

better cooling uniformity of the package with 5 vents can be related to better vent distribution on package walls and therefore, the better air circulation through the commodities during forced-air precooling.

A more comparative representation of the cooling heterogeneity (different from the heterogeneity index) for three different package vent configurations during 180 min cooling is shown in Figure 4.4. The cooling heterogeneity was calculated based on the ratio of the standard deviation to the mean instantaneous temperature (i.e., essentially coefficient of variation of cooling) obtained at the center of all the 64 positions. As can be seen from the figure, the cooling heterogeneity is increased until about 90 min cooling and then decreased by increasing cooling time in all three ventilated packages. The commodities located in the package with 1 vent, experienced the most heterogeneous cooling at different cooling times with 61.5% heterogeneity after 180 min cooling. In the packages with 3 and 5 vents, after an initial increase in the cooling heterogeneity until 80 min cooling, more uniform cooling was obtained by increasing the cooling time. After 180 min cooling, the cooling heterogeneity of 6.7 and 5.6% was obtained for commodities in the packages with 3 and 5 vents, respectively. Vigneault et al. (2006) also showed that cooling heterogeneity was not significantly different between packages with 7.2 and 12.1% opening areas at an alpha level of 5%.

The initial increase in cooling heterogeneity in the ventilated packages can be attributed to a very fast cooling of the commodities located in the columns near to airflow inlets. For example, in the package with 3 vents, after only 10 min cooling the maximum and minimum produce temperatures was 26.3 and 2.2° C, respectively (data is not shown). Therefore, more heterogeneous cooling is obtained for the commodities located in the columns near to package inlet vents. This result is in agreement with findings of Alvarez and Flick (1999a) who stated that following the airflow inside a ventilated package containing spheres, as the depth of spheres increases more homogeneous airflow is achieved. Analyzing heterogeneous cooling inside a ventilated package containing 35 (7×5) spheres, Alvarez and Flick (1999b) found that there is a heterogeneous cooling from the first to the fourth column of spheres, then uniform cooling from the fourth column onwards. After a

specific period of time, however, the temperature of other commodities located far from package inlets, reaches to the temperature of the commodities located near package inlets and therefore, the cooling heterogeneity is decreased.

4.5 CONCLUSIONS

Produce temperature distribution as influenced by different package vent designs was investigated during forced convection cooling. Produce temperature was predicted at various positions inside different ventilated packages. By simulating different vent configurations, the methodology developed in this study can be used to provide homogeneous temperature distribution in ventilated packages during forced convection cooling of produce. The tool can simulate velocity and temperature distributions for various combinations of package size and shape; size, number and location of vents; produce packing arrangements; size and shape of produce; airflow rate and air temperature.

4.6 REFERENCES

- Alvarez, G., and G. Trystram. 1995. Design of a new strategy for the control of the refrigeration process: Fruit and vegetables conditioned in a pallet. Food Control 6:347-355.
- Alvarez, G., and D. Flick. 1999a. Analysis of heterogeneous cooling of agricultural products inside bins Part I: Aerodynamic study. Journal of Food Engineering 39:227-237.
- Alvarez, G., and D. Flick. 1999b. Analysis of heterogeneous cooling of agricultural products inside bins Part II: Thermal study. Journal of Food Engineering 39:239-245.
- Baird, C.D., and J.J. Gaffney. 1976. A numerical procedure for calculating heat transfer in bulk loads of fruits and vegetables. ASHRAE Transactions 82:525-540.
- Baird, C., J. Gaffney, and M. Talbot. 1988. Design criteria for efficient and cost effective forced air cooling systems for fruits and vegetables. ASHRAE Transactions 94:1434-1454.
- Becker, B.R., A. Misra, and B.A. Fricke. 1996. Bulk refrigeration of fruits and vegetables Part I: Theoretical considerations of heat and mass transfer. HVAC&R Research 2:122-134.
- de Castro, L.R., C. Vigneault, and L.A.B. Cortez. 2004. Effect of container opening area on air distribution during precooling of horticultural produce.

 Transactions of the ASABE 47:2033-2038.

- Dehghannya, J., M. Ngadi, and C. Vigneault. 2008. Simultaneous aerodynamic and thermal analysis during cooling of stacked spheres inside ventilated packages. Chemical Engineering and Technology 31(11):1651-1659.
- Gowda, B.S., G.S.V.L. Narasimham, and M.V.K. Murthy. 1997. Forced-air precooling of spherical foods in bulk: A parametric study. International Journal of Heat and Fluid Flow 18:613-624.
- Hoang, M.L., P. Verboven, M. Baelmans, and B.M. Nicolai. 2003. A continuum model for airflow, heat and mass transfer in bulk of chicory roots. Transactions of the ASABE 46:1603-1611.
- Ladaniya, M.S., and S. Singh. 2000. Influence of ventilation and stacking pattern of corrugated fibre board containers on forced-air pre-cooling of 'Nagpur' mandarins. Journal of Food Science and Technology-Mysore 37:233-237.
- Smale, N.J., D.J. Tanner, N.D. Amos, and D.J. Cleland. 2003. Airflow properties of packaged horticultural produce - a practical study Acta Horticulturae (ISHS) 599:443-450.
- Tanner, D.J., A.C. Cleland, L.U. Opara, and T.R. Robertson. 2002a. A generalised mathematical modelling methodology for design of horticultural food packages exposed to refrigerated conditions: part 1, formulation. International Journal of Refrigeration-Revue Internationale Du Froid 25:33-42.
- Tanner, D.J., A.C. Cleland, and L.U. Opara. 2002b. A generalised mathematical modelling methodology for the design of horticultural food packages exposed to refrigerated conditions Part 2. Heat transfer modelling and testing. International Journal of Refrigeration-Revue Internationale Du Froid 25:43-53.

- Vigneault, C., B. Goyette, and L.R. De Castro. 2006. Maximum slat width for cooling efficiency of horticultural produce in wooden crates. Postharvest Biology and Technology 40:308-313.
- Vigneault, C., and L.R. de Castro. 2006. Indirect measurement method for laminar to turbulent airflow through horticultural produce simulators. Transactions of the ASABE 49:1455-1461.
- Zou, Q., L.U. Opara, and R. McKibbin. 2006a. A CFD modeling system for airflow and heat transfer in ventilated packaging for fresh foods: I. Initial analysis and development of mathematical models. Journal of Food Engineering 77:1037-1047.
- Zou, Q.A., L.U. Opara, and R. McKibbin. 2006b. A CFD modeling system for airflow and heat transfer in ventilated packaging for fresh foods: II. Computational solution, software development, and model testing. Journal of Food Engineering 77:1048-1058.

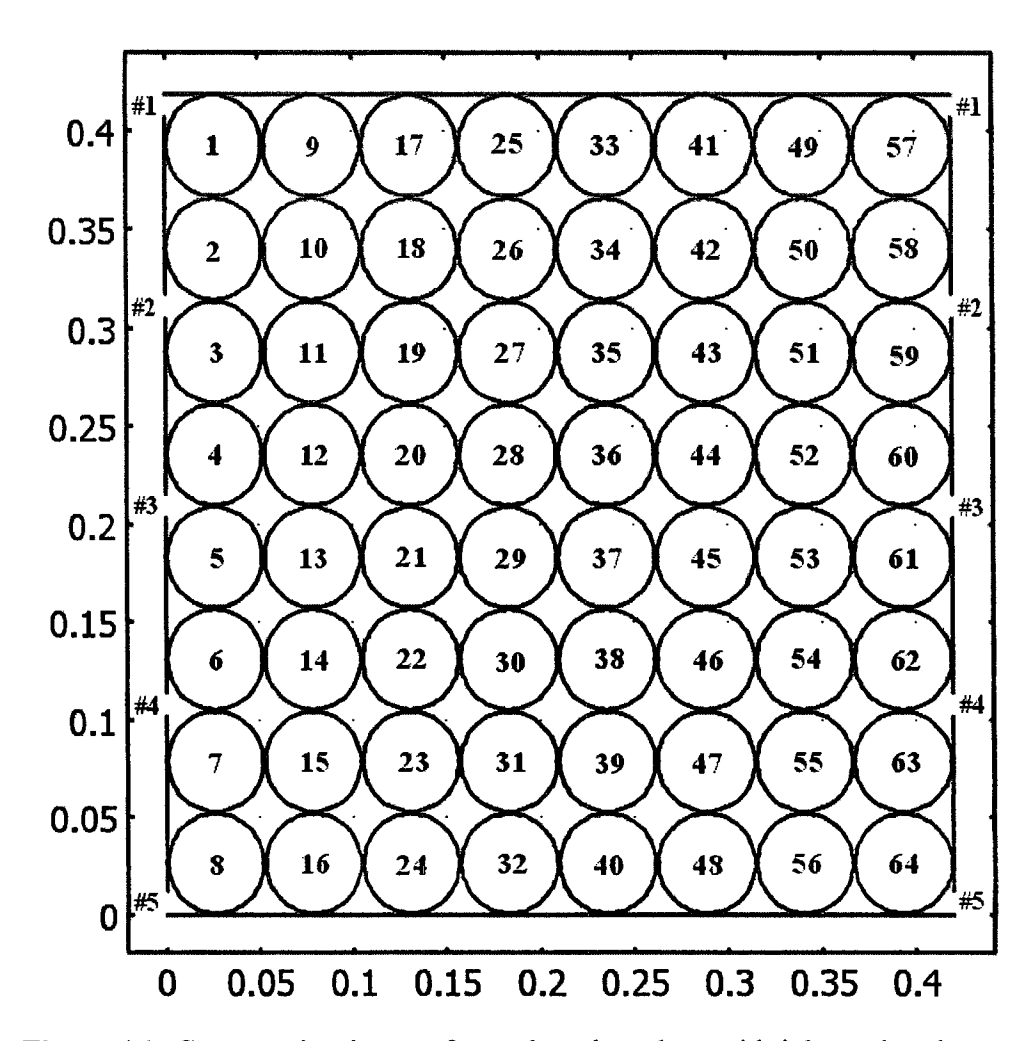


Figure 4.1: Cross-sectional area of a packaged produce with inlet and outlet vent positions shown in left and right sides, respectively (Table 3.1)

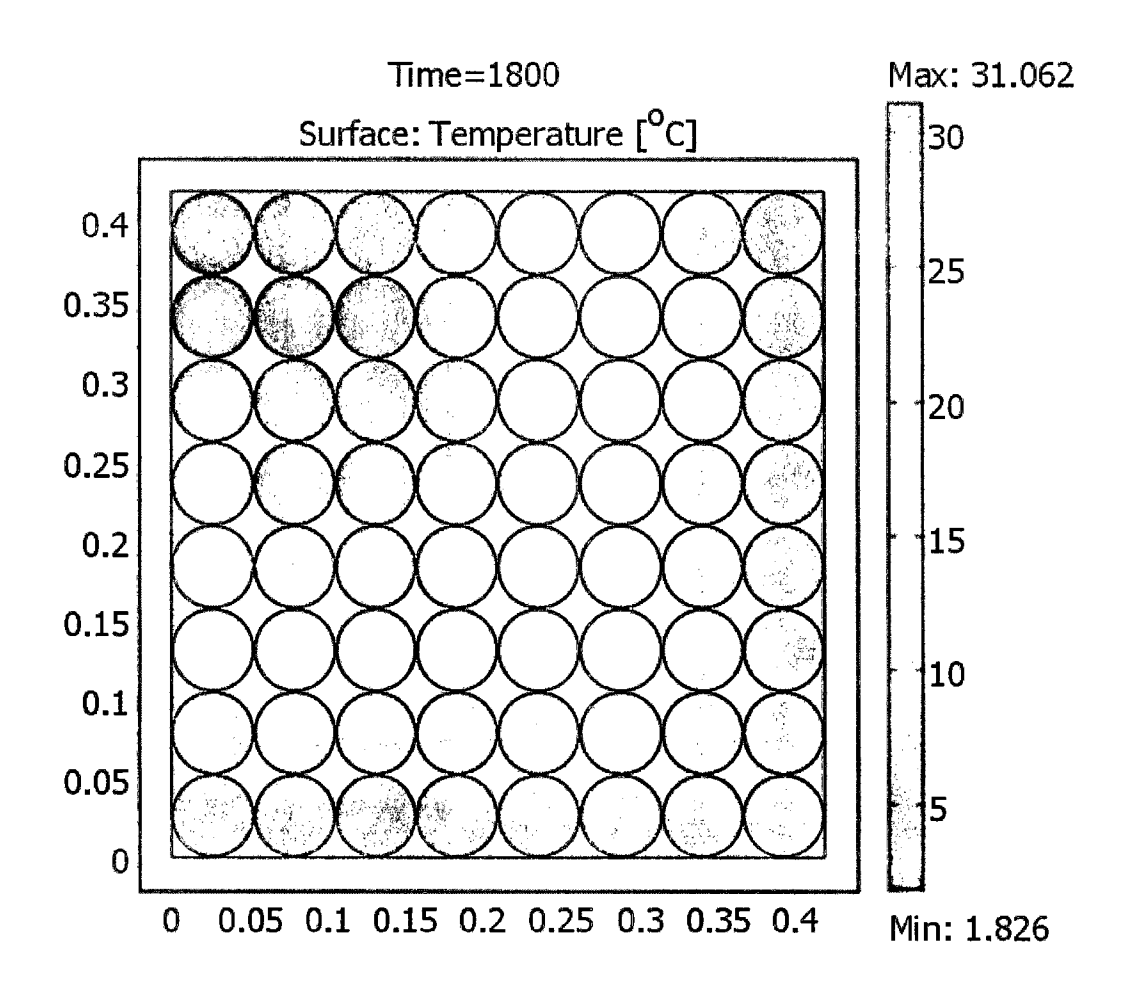


Figure 4.2 (a): Produce temperature distribution after 30 min cooling in the package with one vent

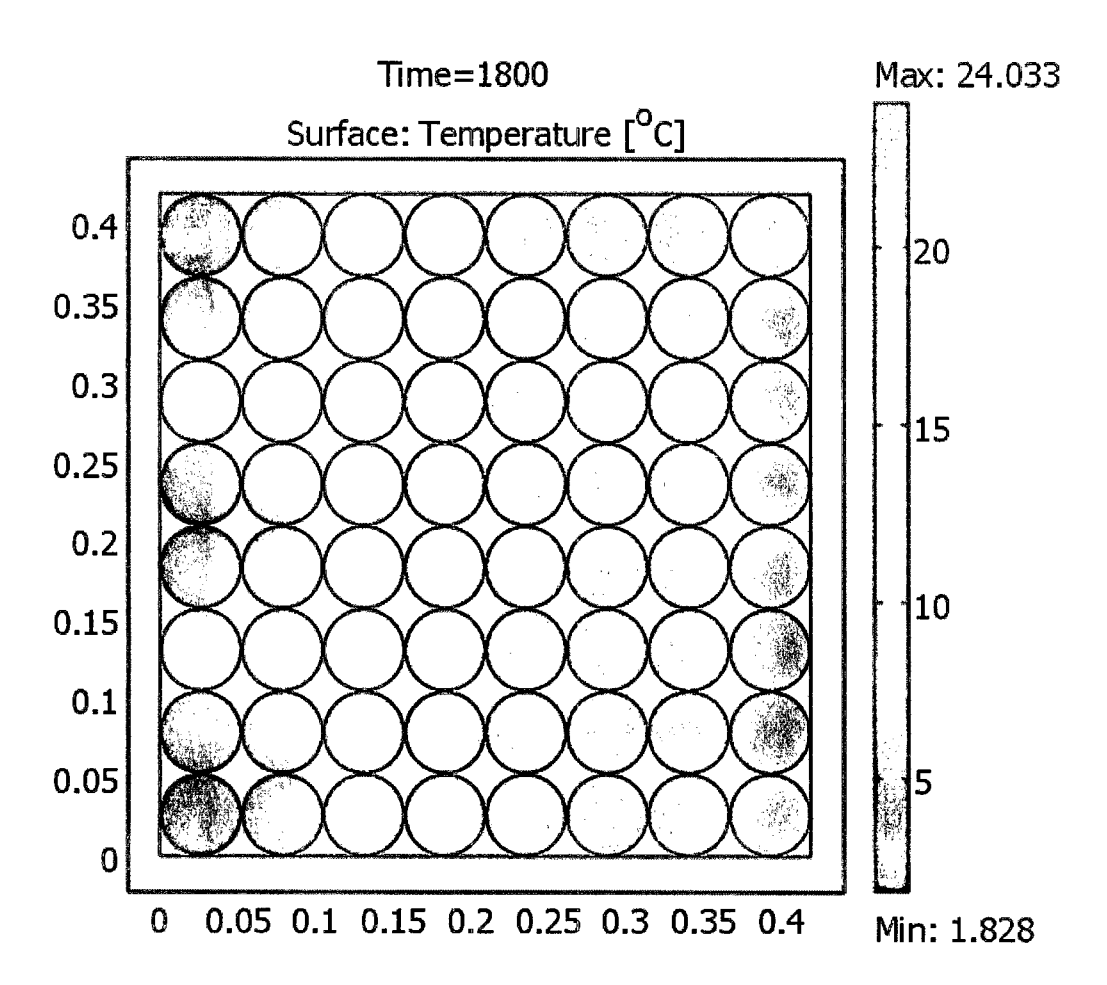


Figure 4.2 (b): Produce temperature distribution after 30 min cooling in the package with three vents

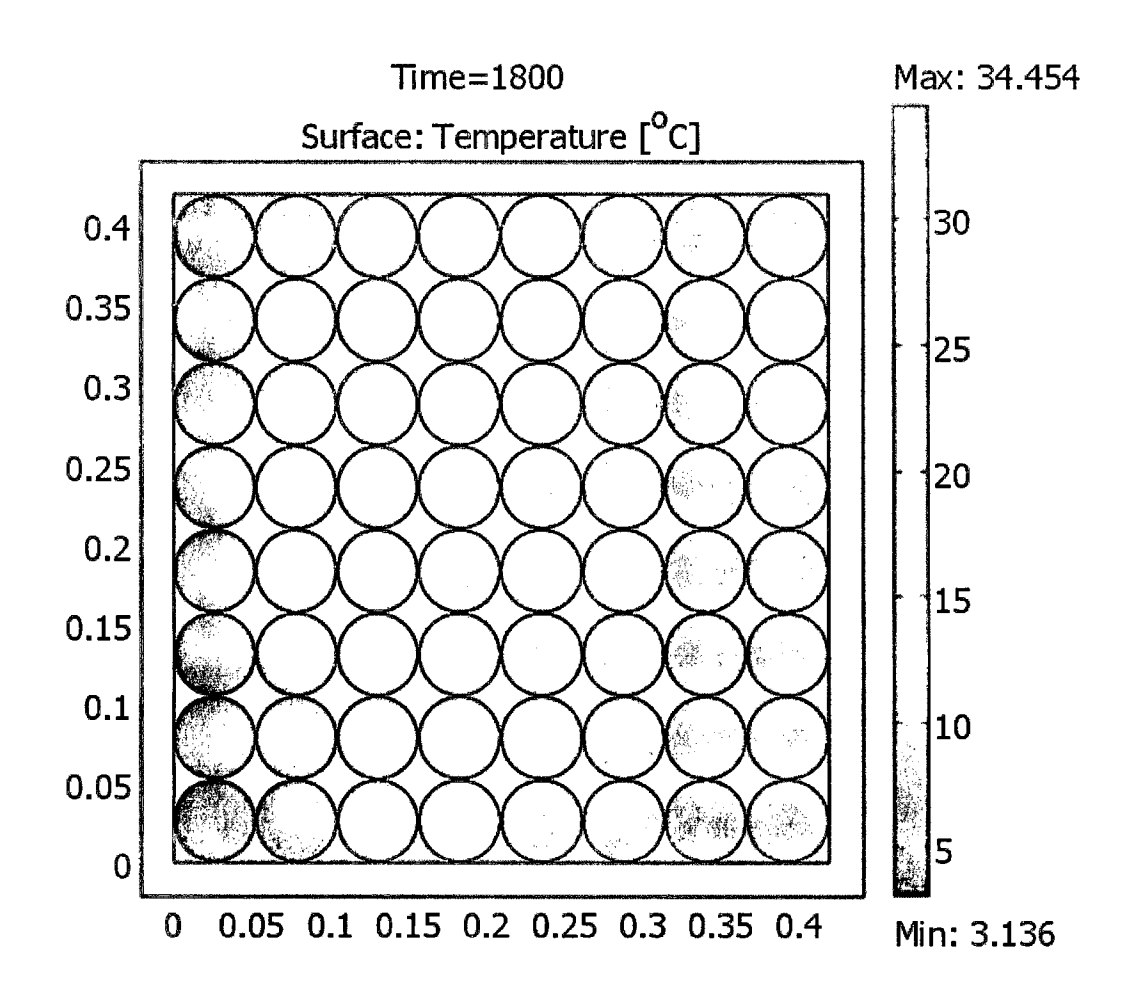


Figure 4.2 (c): Produce temperature distribution after 30 min cooling in the package with five vents

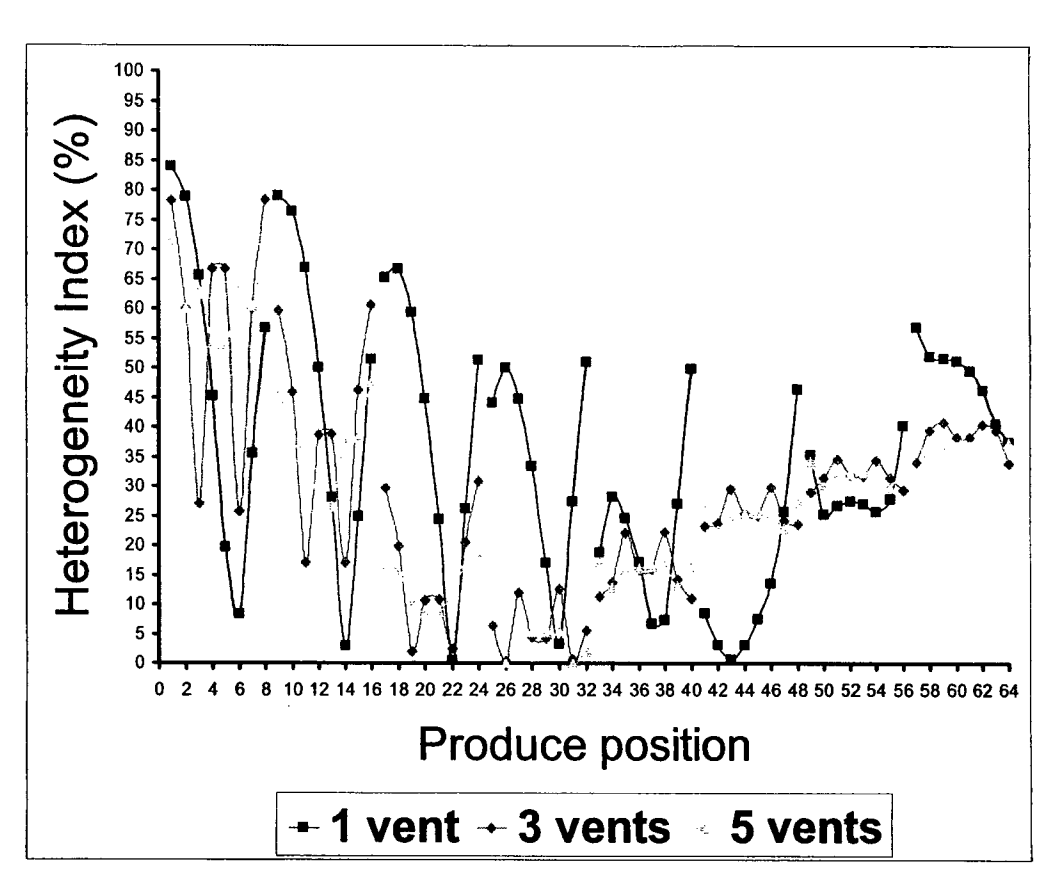


Figure 4.3: Heterogeneity indexes at 64 positions, shown in Figure 4.1, for three different package vent configurations after 30 min cooling

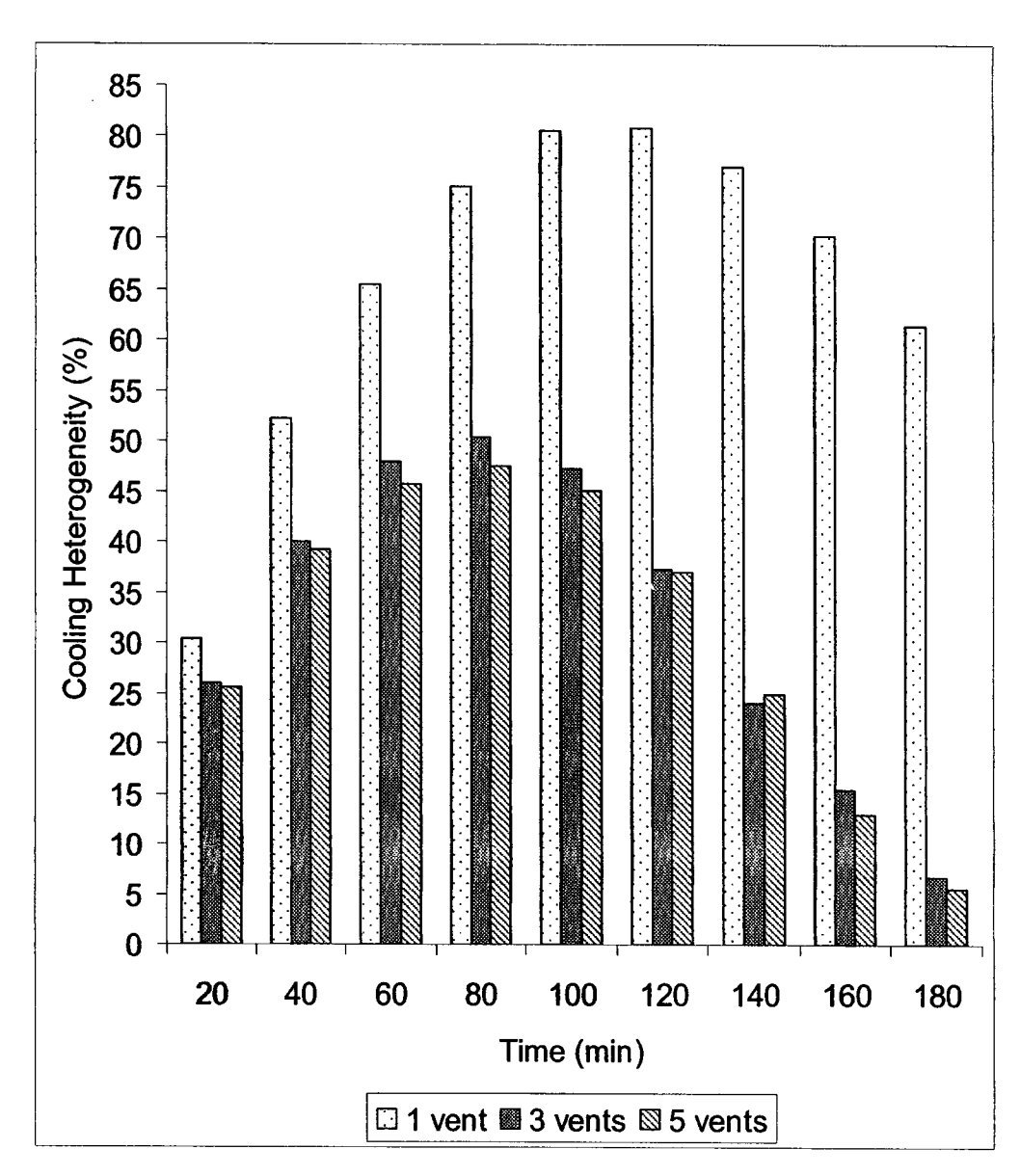


Figure 4.4: Cooling heterogeneities at different cooling times in three different package vent configurations

CONNECTING TEXT

The results of the investigation in Chapter IV confirmed that produce temperature distribution is influenced by different ventilated package designs. It was shown that produce cooling uniformity is increased by increasing number of vents. In Chapter V, a sensitivity analysis will be conducted. In addition to packages with different number of vents, packages with the same number of vents but different vent distributions on package walls will be considered. This is to investigate the simultaneous effect of the vent numbers and the vent distribution on produce cooling efficiency during the forced-air precooling process.

V. SENSITIVITY OF PRODUCE COOLING EFFICIENCY AS INFLUENCED BY DIFFERENT PACKAGE VENT CONFIGURATIONS

5.1 ABSTRACT

Produce cooling sensitivity with respect to various package vent designs during forced convection cooling process was studied by direct numerical simulation. For this purpose, 9 different vent designs including 1, 2, 3 and 5 vents corresponding to 4 different vent areas of 2.4, 4.8, 7.2 and 12.1%, respectively, were simulated. More uniform produce cooling at less cooling time was obtained when the vents were uniformly distributed on package walls with at least 4.8% opening areas. The study showed that vent areas and positions on package walls must be taken into account in designing ventilated packages in order to improve cooling efficiency regarding both produce cooling time as well as cooling uniformity during the cooling operation.

Keywords: Mathematical simulation; airflow and heat transfer modeling; package design; vent configuration; cooling time; cooling uniformity

5.2 INTRODUCTION

Forced convection cooling process is commonly used to decrease agricultural produce temperature after harvest (Kader, 2002; de Castro et al., 2005; Kumar et al., 2008). To maintain optimum quality of the commodities during storage or transportation (Rodriguez-Bermejo et al., 2007), the process should provide a uniform cooling throughout stacked produce during the treatment (Goyette et al., 1996). However, heterogeneous airflow distribution at different locations of the package is created resulting in produce deterioration and shriveling during storage (Alvarez and Flick, 1999; Alvarez et al., 2003; de Castro et al., 2004; Smale et al.,

2006). In practice, the experiential combinations of air temperature and velocity are chosen by designers to rapidly cool the produce to a suitable temperature. This is because the thermal performance of containers are neither supplied nor considered in the package design by manufacturers due to the lack of available tools. A more logical approach in designing new packages is to develop a model that would be able to predict package performance rather than requiring costly experiments.

The airflow and heat transfer models in the literature during forced convection cooling process have not considered the effects of package vent design including percent vent area and its position on produce cooling uniformity (Zou et al., 2006; Opara and Zou, 2007; Ferrua and Singh, 2008). Opara and Zou (2007) applied sensitivity analysis of a CFD model to study the effect of variation in package vent area and position during forced convection cooling process. The authors noticed some considerable effects of the variation on produce cooling rate; however, the effect of multiple vents on cooling uniformity considering different vent area and position was not reflected in the study. More recently, Dehghannya et al. (2008) developed and experimentally validated a mathematical model of airflow and heat transfer for aerodynamic analysis during forced-air precooling inside ventilated packages. The authors applied direct numerical simulation and analyzed velocity distributions and their resultant airflow heterogeneity indexes inside different ventilated packages. Dehghannya et al. (submitted for publication) also performed a thermal analysis by simulating and analyzing temperature distribution inside different ventilated packages to provide uniform cooling during the process.

The aim of this study was to assess sensitivity of produce cooling uniformity and cooling time with respect to package vent design during forced convection cooling of produce. The effect of different package designs including various vent areas and positions on produce cooling were considered.

5.3 MATERIALS AND METHODS

A transient two-phase air-produce mathematical model of simultaneous airflow and heat transfer inside ventilated packages containing spherical produce (Figure 5.1 and Table 5.1) was developed and validated using experimental data (Dehghannya et al., 2008). Model description including the governing equations for air and produce domains, numerical method and experimental model validation are referred to Sections 3.3.1, 3.3.2 and 3.3.3, respectively.

5.4 RESULTS AND DISCUSSIONS

5.4.1 Temperature Distribution inside Different Package Vent Designs

Figure 5.2 (from A to I) illustrates produce temperature distribution after 120 min cooling considering air temperature of 4°C and initial produce temperature of 28°C in 9 different package vent configurations (Table 5.1). As can be seen from the figure, considerable differences were obtained for different package vent configurations regarding the maximum and minimum temperatures after 120 min cooling. In all the 9 vent designs, the commodities near to airflow inlet were generally cooled faster compared to the commodities far from the inlet.

Figure 5.2 (A) demonstrates that the cold air entering from the only inlet of the package with 2.4% vent area creates a slower cooling rate for commodities located in the bottom and right sides of the package. In the package with one central vent (Figure 5.2 (B)), a slower cooling was obtained in the top and bottom parts of the package. On the other hand, a slower cooling rate was obtained in the package vent configuration of C for commodities in the top and right sides of the package (Figure 5.2 (C)). After 120 min cooling, the difference between the maximum and minimum temperature of about 15°C was obtained for all the 3 packages with 2.4% vent area indicating a heterogeneous cooling during forced convection cooling process.

In the packages with 2 vents and 4.8% vent area (Figure 5.2 (D, E and F)), the vent configuration of E created much better cooling uniformity in comparison with configurations of D and F. While the difference between the maximum and minimum produce temperature was less than 8°C in the configuration of E, the difference was more than 17°C in the vent configurations of D and F. Therefore, more uniform cooling operation is expected in the package vent configuration of E

compared to D and F. It should also be noted that a higher package vent area with improper vent distribution can provide more heterogeneous cooling operation compared to the packages with lower vent areas. For example, as can be seen from Figure 5.2, the vent designs of D and F with 4.8% vent area creates a higher difference between the maximum and minimum temperatures (more than 17°C) compared to the designs of A, B and C with 2.4% vent area (about 15°C) suggesting more heterogeneous cooling in configurations of D and F. This result shows that package vent area is not the only significant factor influencing the efficiency of the forced convection cooling process; rather, package vent area should be respected together with vent distribution on package walls.

The importance of the vent distribution on package walls was further confirmed in the case of the packages with 3 vents and 7.2% vent area. While the difference between the maximum and minimum temperatures in the vent configuration of G was less than 5°C, the difference of more than 9°C was obtained in the configuration of H explaining more uniform cooling operation for the case of G. Additionally, by comparing the configurations of E (4.8% vent area) and H (7.2% vent area), it was shown that the maximum and minimum temperature differences of 7.8 and 9.2°C were obtained in the configurations of E and H, respectively. This result shows that increasing vent area does not necessarily provide a homogeneous cooling and it can even increase cooling heterogeneity, if vents are not properly distributed on package walls.

Finally, in the package with 5 vents and vent area of 12.1%, the least difference between the maximum and minimum temperatures in comparison with all other package vent configurations was obtained with the magnitude of 4.7°C after 120 min cooling. However, this difference was lower only about 0.2°C compared to the configuration of G explaining no considerable difference between these two packages with 7.2 and 12.1% vent areas.

Figure 5.3 (a, b, c and d) illustrates temperature profiles based on center temperature of the 4 positions demonstrated in Figure 5.1 in 9 different package vent configurations (Table 5.1). The figure shows that the temperature profiles obtained at a particular position (P1, P2, P3 or P4) are strongly influenced by

different package vent configurations. By analyzing the temperature profile of a specific position, for example P2, it can be seen that considerable differences were obtained regarding 9 different package vent configurations. For instance, after 30 min cooling, the produce center temperature (P2) was 18.3, 17.6, 17.1, 15.3, 13.0, 12.5, 11.8, 10.6 and 9.8°C in vent configurations of E, I, G, H, F, A, D, B and C, respectively. The difference could be explained due to different air pathways created in different package vent configurations and therefore influencing the temperature profiles in different positions inside ventilated packages during forced convection cooling process. It should be emphasized that these different temperature profiles were obtained with the same air velocity, air temperature as well as produce initial temperature during the process establishing the high importance of package vent configuration on produce cooling.

Additionally, by considering a typical vent configuration such as vent configuration of A, four different temperature profiles were obtained at 4 different positions. For example, after 30 min cooling, produce center temperature located in positions P1, P2, P3 and P4 was 17.7, 12.5, 23.6 and 20.7°C, respectively, illustrating the heterogeneous nature of the process in the vent configuration of A.

5.4.2 Cooling Heterogeneity Obtained in Different Package Vent Configurations

Produce temperature distribution inside 9 different package vent configurations was further investigated considering a cooling heterogeneity index during 180 min cooling (Figure 5.4). The cooling heterogeneity index was calculated based on the ratio of the standard deviation to the mean instantaneous temperature (i.e., essentially coefficient of variation of cooling) obtained at the center of all the 64 positions demonstrated in Figure 5.1. As can be seen from the figure, the cooling heterogeneity is increased until about 90 min cooling and then decreased by increasing cooling time in all vent configurations. The package vent configuration of A, B, C, D and F created the highest cooling heterogeneity with the heterogeneity indexes of more than 30% after 180 min cooling and therefore, the worst cooling operation in terms of cooling uniformity compared to the other configurations.

The cooling heterogeneity indexes in the vent configurations of E, G, H and I after 180 min cooling were 9.1, 6.8, 12.2 and 6.2%, respectively. In these configurations, after an initial increase in the cooling heterogeneity until about 90 min cooling, more uniform cooling was obtained by increasing cooling time. The initial increase in cooling heterogeneity can be explained by the very fast cooling of the commodities located in the columns near inlet vents. After a certain period of time, however, the temperature of the commodities located far from the package inlets, reaches to the temperature of the commodities located near inlet vents and therefore, the cooling heterogeneity is decreased.

Additionally, the lower cooling heterogeneity of the vent configuration of E after 180 min cooling (9.1%) compared to the other two-ventilated packages (D: 37.3% and F: 37.0%) implies that a certain package vent area obtained from certain number of properly distributed vents is capable of providing uniform air pathways and the resultant homogeneous temperature distribution without any need to increase the number of vents; which can compromise structural resistance of the ventilated packages during storage or transport. On the other hand, in case of the packages with 3 vents, the cooling heterogeneity of 6.8 and 12.2% was obtained after 180 min cooling for the vent configurations of G and H, respectively, explaining a better cooling uniformity of the case G compared to H. The cooling heterogeneity obtained in the package vent configuration of G after 180 min cooling (6.8%) is almost the same as the case I with 5 vents (6.2%). Vigneault et al. (2006) also showed that cooling heterogeneity was not significantly different at an alpha level of 5% between packages with 7.2 and 12.1% opening areas.

5.4.3 Cooling Time Obtained in Different Ventilated Packages

Figure 5.5 shows produce cooling time in different package vent configurations based on the maximum time required for cooling of the slowest cooled produce to reach 7°C. The temperature of 7°C was chosen as an index temperature since it is the temperature after the 7/8 cooling time (air temperature: 4°C and produce temperature: 28°C). The positions of the slowest cooled produce were 57, 57, 64,

64, 57, 59, 64 and 57, demonstrated in Figure 5.1, in the vent configurations of A, B, C, D, E, F, G, H and I, respectively. Figure 5.5 demonstrates considerable differences in cooling times in different package vent configurations. The package vent configurations of D (4.8% vent area) and I (12.1% vent area) produced the highest and lowest cooling time, respectively, required for cooling of the slowest cooled produce to reach 7°C. Additionally, as the case with cooling uniformity, by comparing the results obtained for the vent configurations such as B and D or E and H, it is apparent that for the different package vent configurations, increasing vent area does not necessarily shorten the cooling time but could indeed increase the time of cooling depending on vent positions on the package walls.

It should also be noted that a desirable forced convection cooling process requires an operation with less cooling time together with less cooling heterogeneity regarding different produce needs. Therefore, vent configurations of D and I could be selected as the worst and best choices among other vent configurations with regard to both produce cooling time as well as produce cooling heterogeneity.

5.5 CONCLUSIONS

Produce cooling during forced convection cooling process considering 9 different package vent configurations was investigated. Considerable differences were obtained for different package vent configurations regarding produce temperature distribution, cooling heterogeneity and cooling time. It was shown that a certain number of vents together with their distributions on package walls can provide suitable air pathways and therefore a uniform cooling operation. Additionally, it was confirmed that for different package vent configurations, increasing vent area does not necessarily shorten the cooling time but could indeed increase the time of cooling depending on vent positions on the package walls. Consequently, increasing vent area may not necessarily have a positive effect on cooling uniformity and time. Cooling time and cooling heterogeneity can be reduced by suitable package designs to provide efficient forced convection cooling.

5.6 REFERENCES

- Alvarez, G., and D. Flick. 1999. Analysis of heterogeneous cooling of agricultural products inside bins Part II: Thermal study. Journal of Food Engineering 39:239-245.
- Alvarez, G., P.E. Bournet, and D. Flick. 2003. Two-dimensional simulation of turbulent flow and transfer through stacked spheres. International Journal of Heat and Mass Transfer 46:2459-2469.
- de Castro, L.R., C. Vigneault, and L.A.B. Cortez. 2004. Effect of container opening area on air distribution during precooling of horticultural produce.

 Transactions of the ASABE 47:2033-2038.
- de Castro, L.R., C. Vigneault, and L.A.B. Cortez. 2005. Cooling performance of horticultural produce in containers with peripheral openings. Postharvest Biology and Technology 38:254-261.
- Dehghannya, J., M. Ngadi, and C. Vigneault. 2008. Simultaneous aerodynamic and thermal analysis during cooling of stacked spheres inside ventilated packages. Chemical Engineering and Technology 31(11): 1651-1659.
- Dehghannya, J., M. Ngadi, and C. Vigneault. Mathematical modeling of airflow and heat transfer during forced convection cooling of produce intended for optimal package design. Transactions of the Institution of Chemical Engineers (IChemE) Part C, Food and Bioproducts Processing. Submitted for publication.
- Ferrua, M.J., and R.P. Singh. 2008. A nonintrusive flow measurement technique to validate the simulated laminar fluid flow in a packed container with vented walls. International Journal of Refrigeration-Revue Internationale Du Froid 31:242-255.

- Goyette, B., C. Vigneault, B. Panneton, and G.S.V. Raghavan. 1996. Method to evaluate the average temperature at the surface of a horticultural crop. Canadian Agricultural Engineering 38:291-295.
- Kader, A.A. 2002. Postharvest technology of horticultural crops, 3rd ed. University of California, Division of Agriculture and Natural Resources, Oakland, California.
- Kumar, R., A. Kumar, and U.N. Murthy. 2008. Heat transfer during forced air precooling of perishable food products. Biosystems Engineering 99:228-233.
- Opara, L.U., and Q. Zou. 2007. Sensitivity analysis of a CFD modelling system for airflow and heat transfer of fresh food packaging: Inlet air flow velocity and inside-package configurations. International Journal of Food Engineering 3: Article 16.
- Rodriguez-Bermejo, J., P. Barreiro, J.I. Robla, and L. Ruiz-Garcia. 2007. Thermal study of a transport container. Journal of Food Engineering 80:517-527.
- Smale, N.J., J. Moureh, and G. Cortella. 2006. A review of numerical models of airflow in refrigerated food applications. International Journal of Refrigeration-Revue Internationale Du Froid 29:911-930.
- Vigneault, C., B. Goyette, and L.R. De Castro. 2006. Maximum slat width for cooling efficiency of horticultural produce in wooden crates. Postharvest Biology and Technology 40:308-313.
- Zou, Q., L.U. Opara, and R. McKibbin. 2006. A CFD modeling system for airflow and heat transfer in ventilated packaging for fresh foods: I. Initial analysis

and development of mathematical models. Journal of Food Engineering 77:1037-1047.

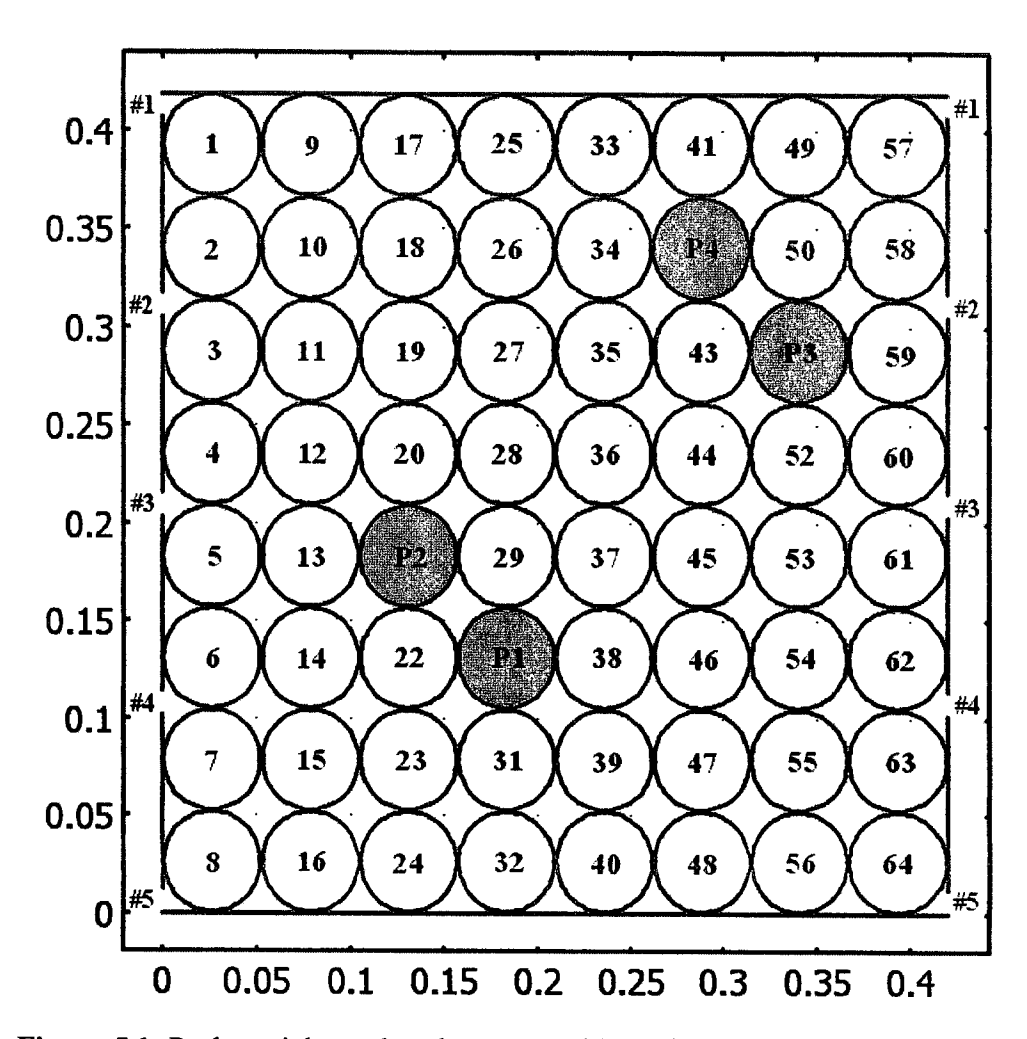


Figure 5.1: Package inlet and outlet vent positions shown in left and right sides, respectively (Table 5.1) as well as produce positions (P1, P2, P3 and P4) used for investigation of produce temperature distributions at nine different package vent configurations

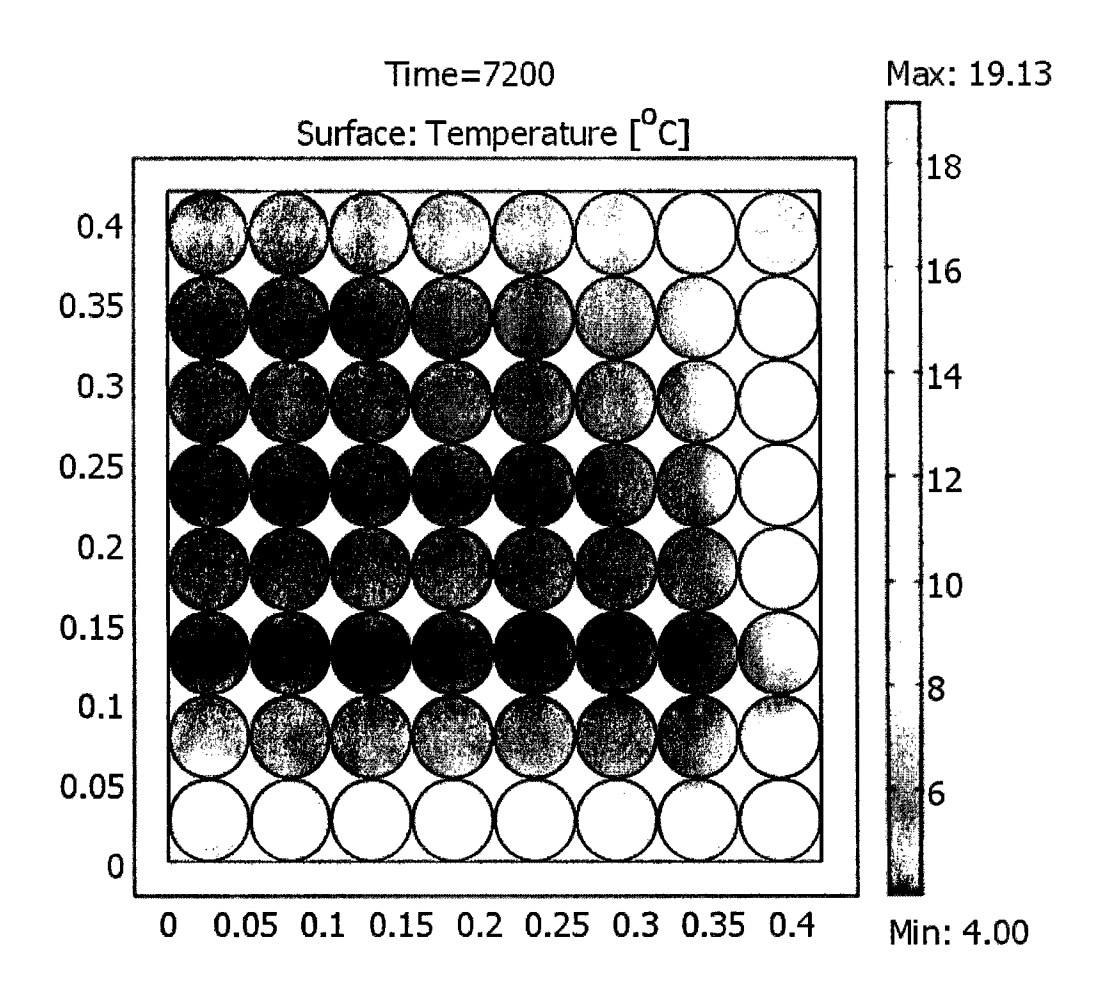


Figure 5.2 (A): Produce temperature distribution after 120 min cooling in the package vent configuration of "A" described in Table 5.1

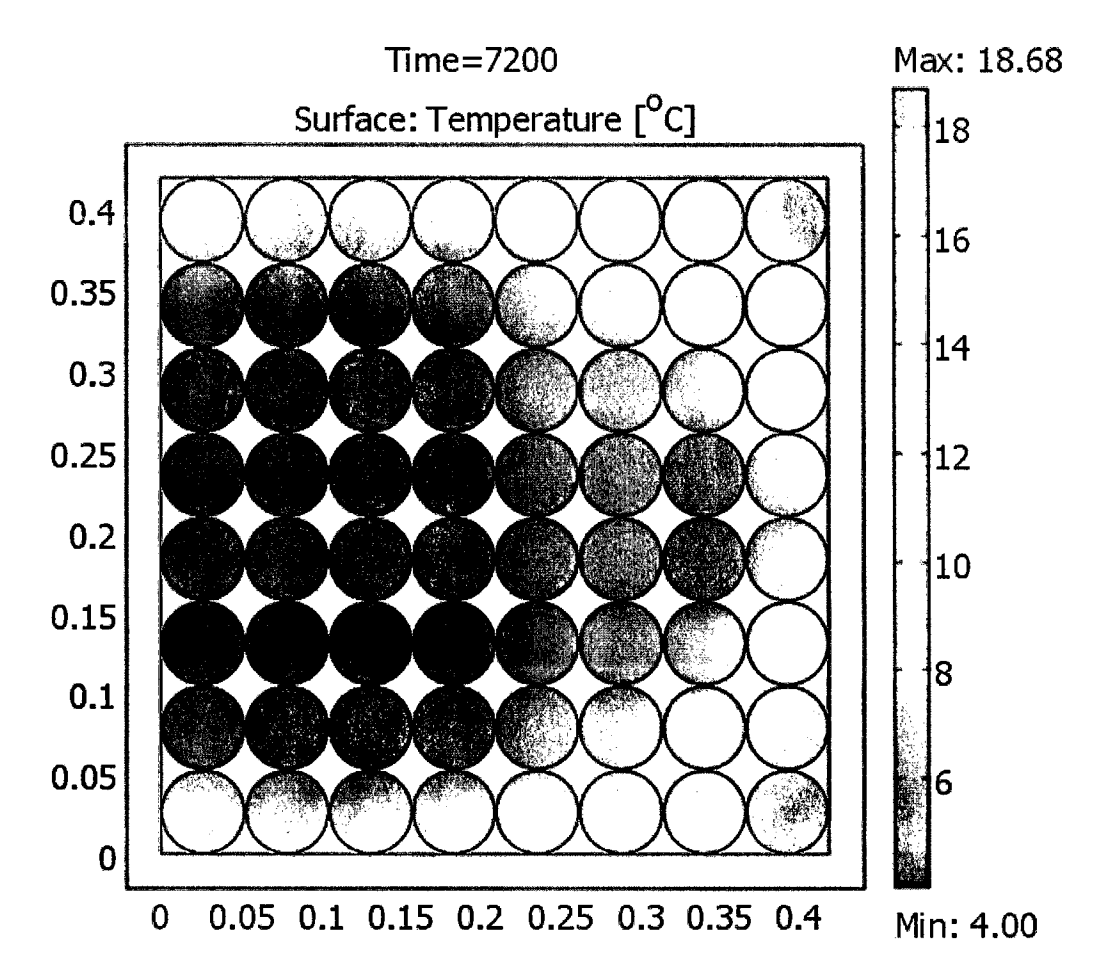


Figure 5.2 (B): Produce temperature distribution after 120 min cooling in the package vent configuration of "B" described in Table 5.1

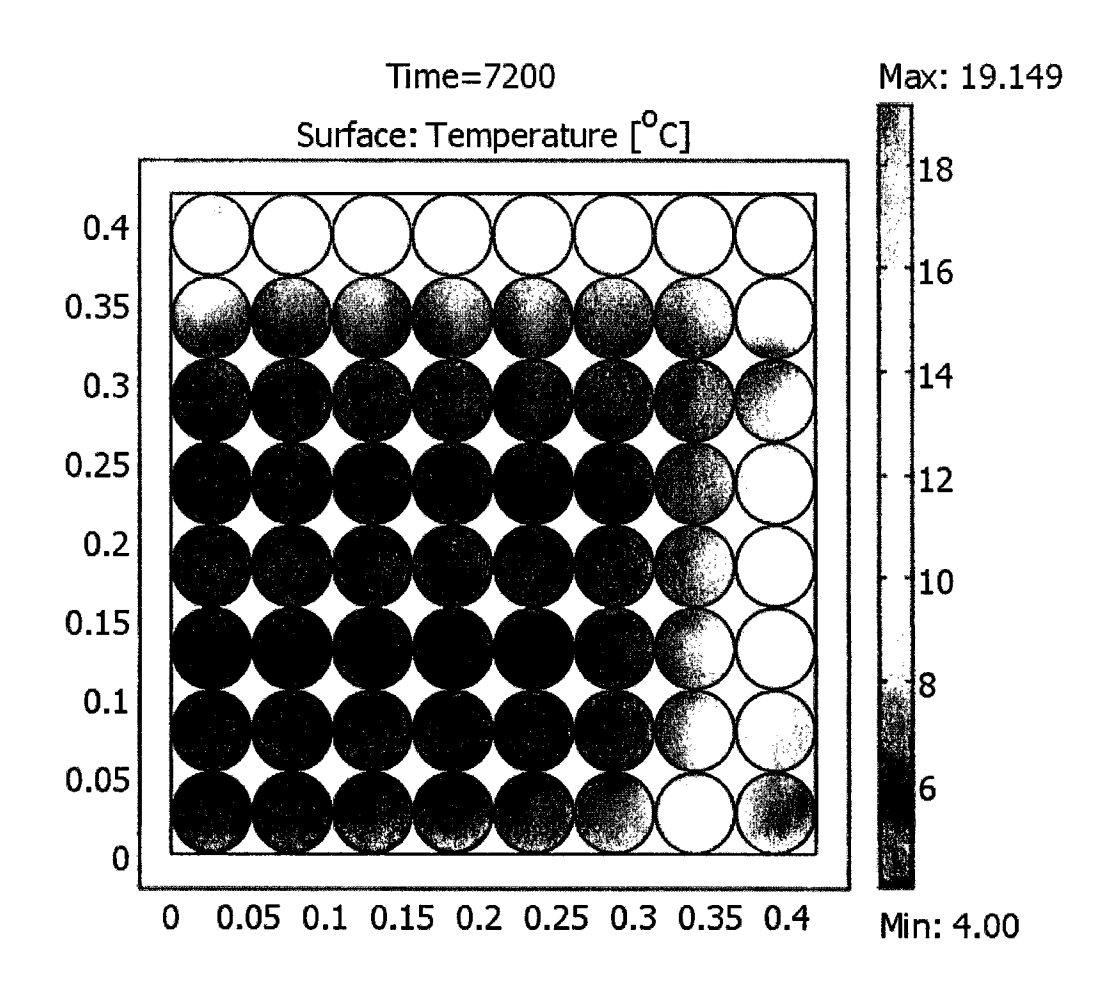


Figure 5.2 (C): Produce temperature distribution after 120 min cooling in the package vent configuration of "C" described in Table 5.1

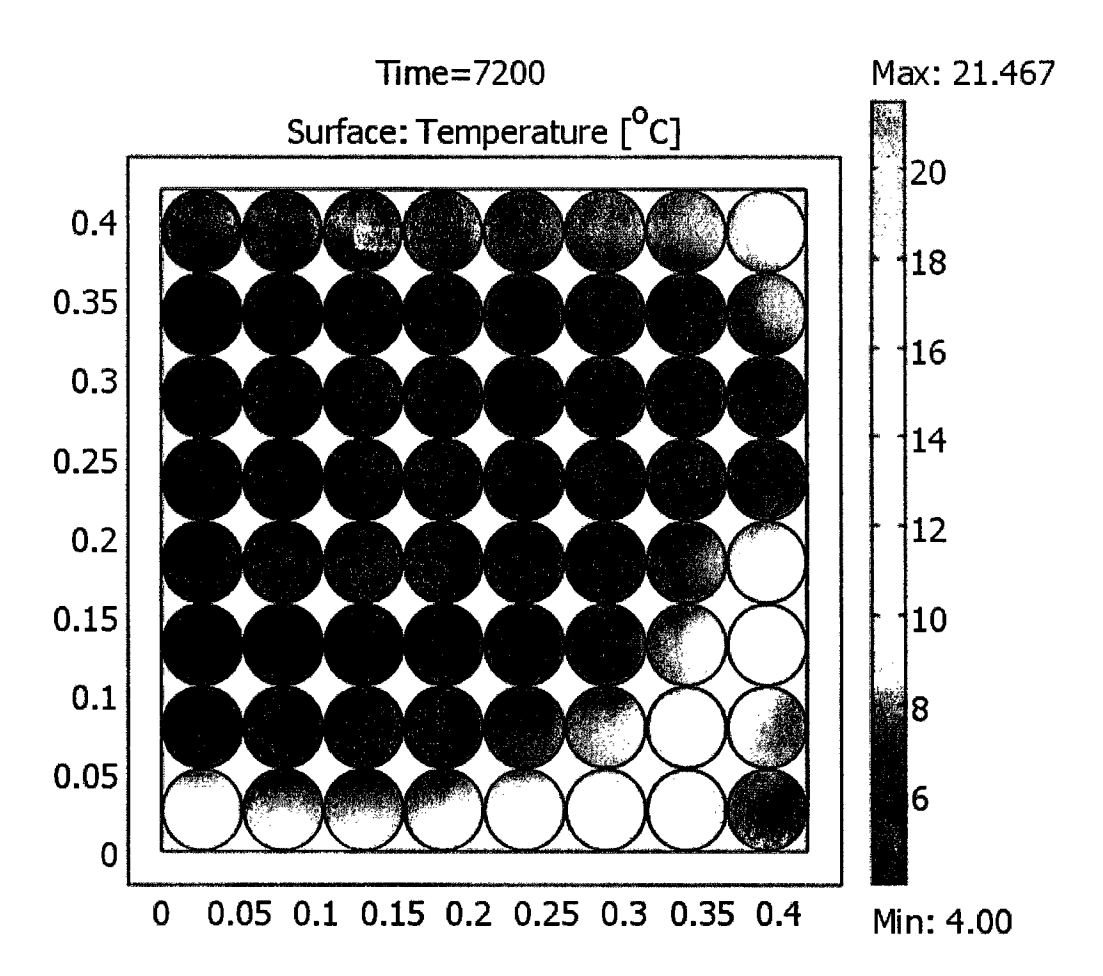


Figure 5.2 (D): Produce temperature distribution after 120 min cooling in the package vent configuration of "D" described in Table 5.1

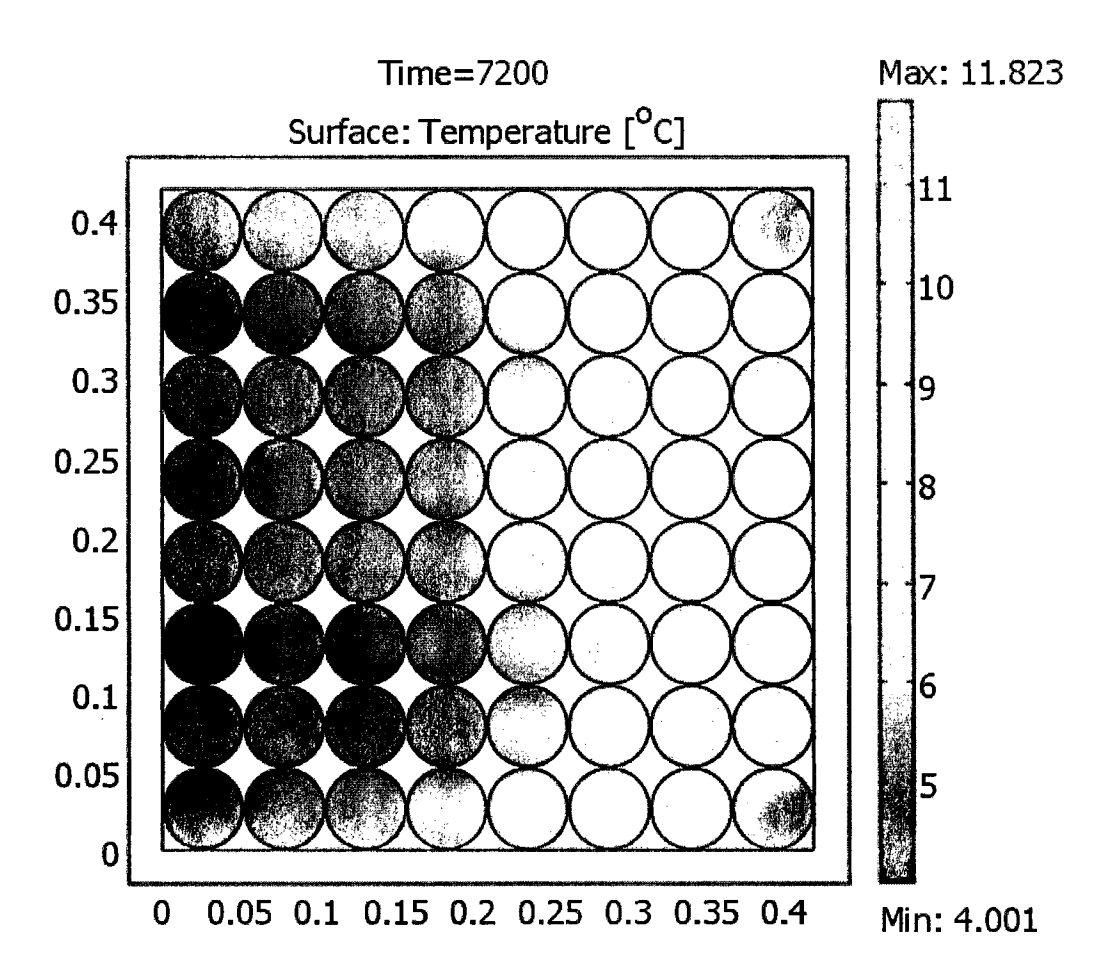


Figure 5.2 (E): Produce temperature distribution after 120 min cooling in the package vent configuration of "E" described in Table 5.1

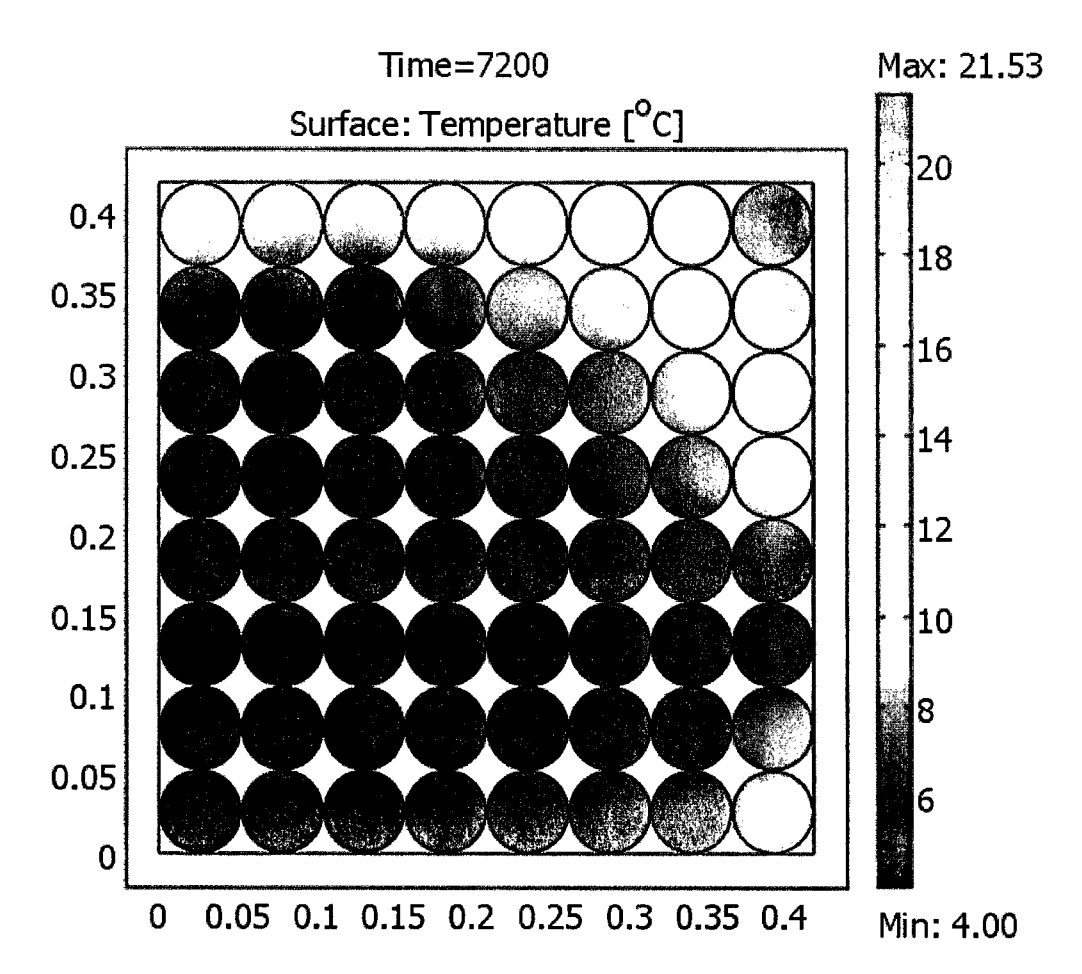


Figure 5.2 (F): Produce temperature distribution after 120 min cooling in the package vent configuration of "F" described in Table 5.1

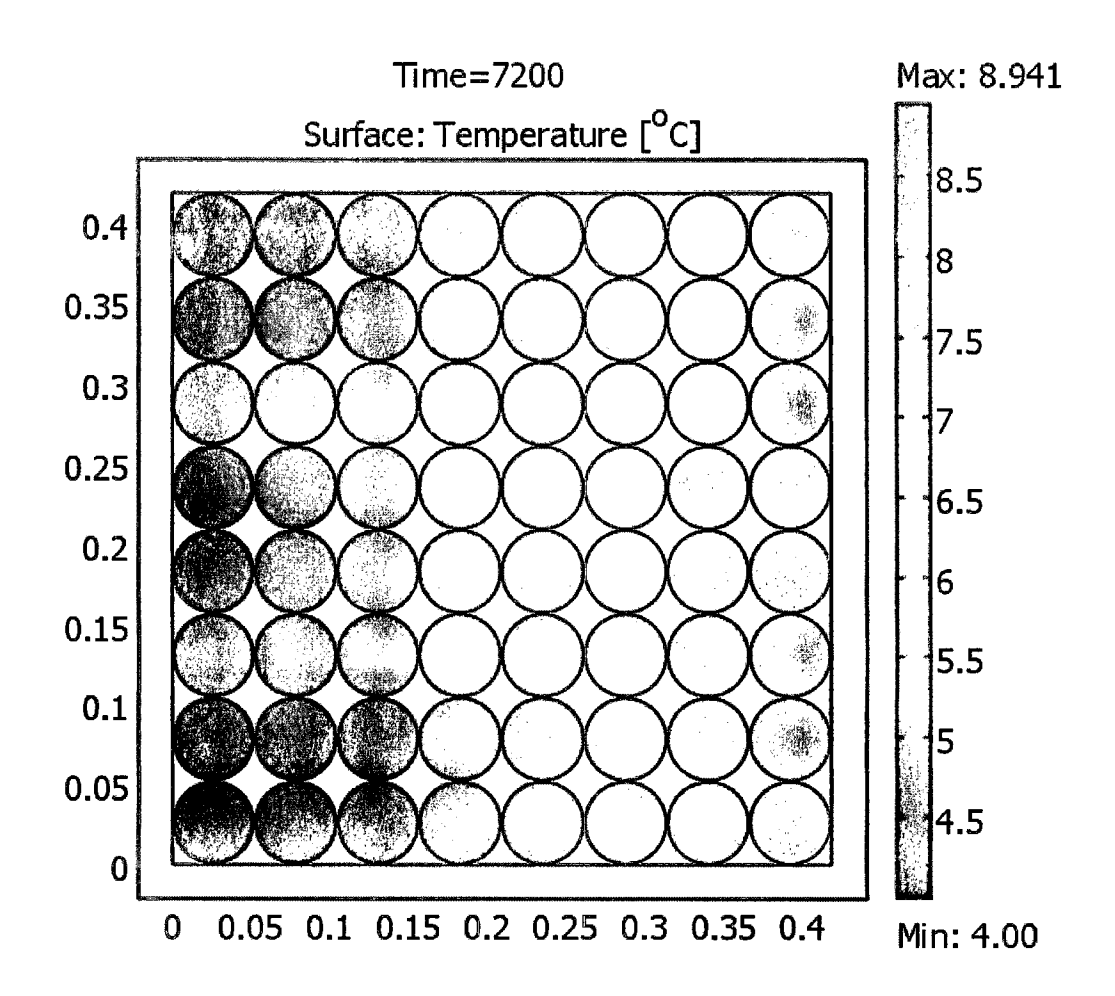


Figure 5.2 (G): Produce temperature distribution after 120 min cooling in the package vent configuration of "G" described in Table 5.1

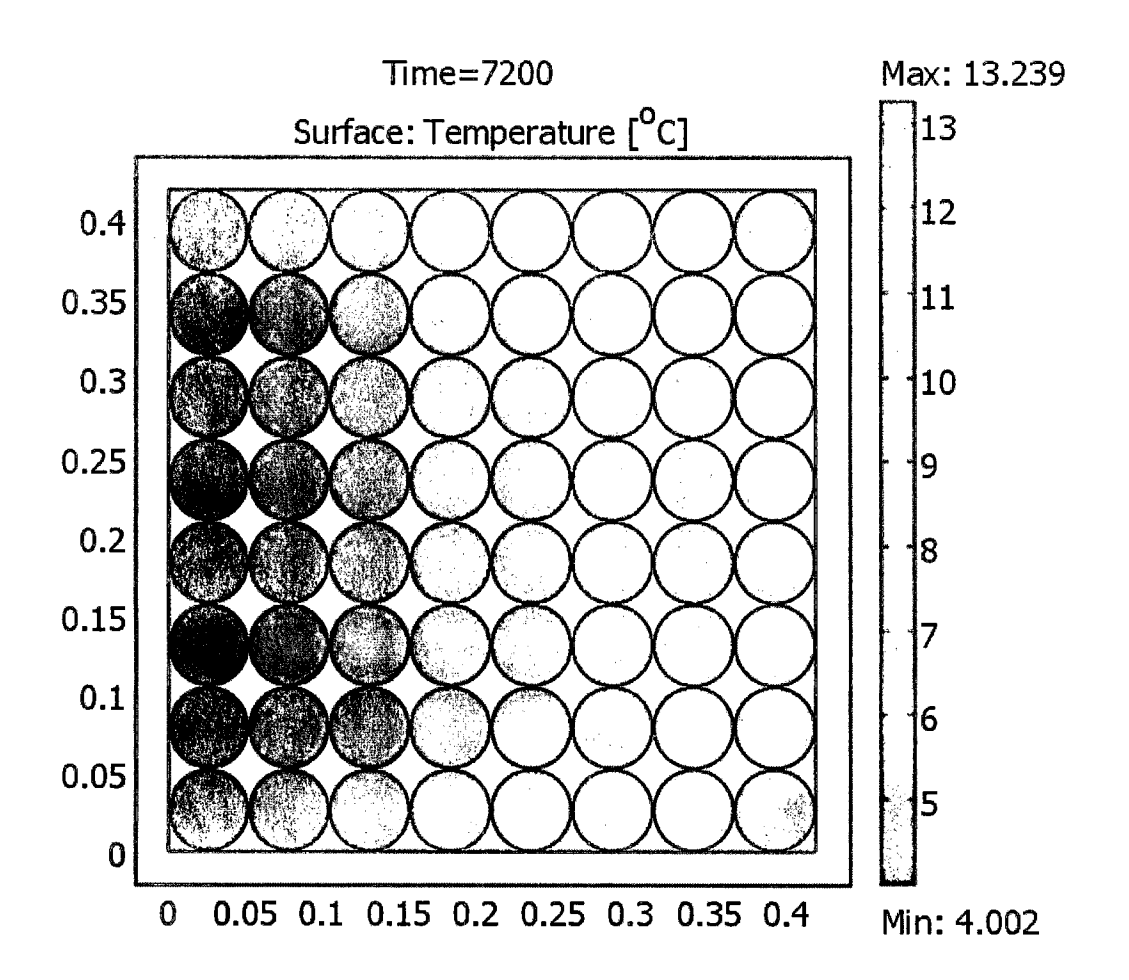


Figure 5.2 (H): Produce temperature distribution after 120 min cooling in the package vent configuration of "H" described in Table 5.1

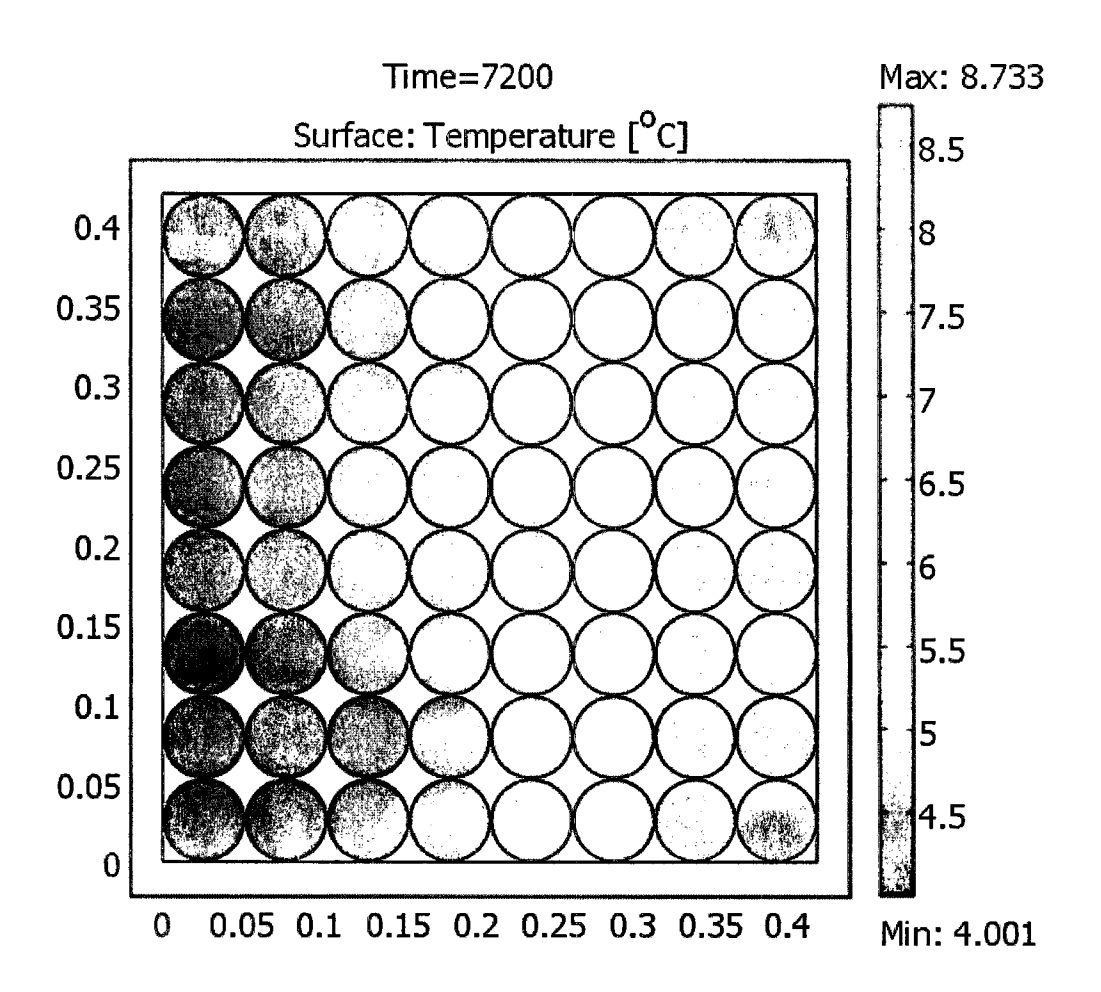


Figure 5.2 (I): Produce temperature distribution after 120 min cooling in the package vent configuration of "I" described in Table 5.1

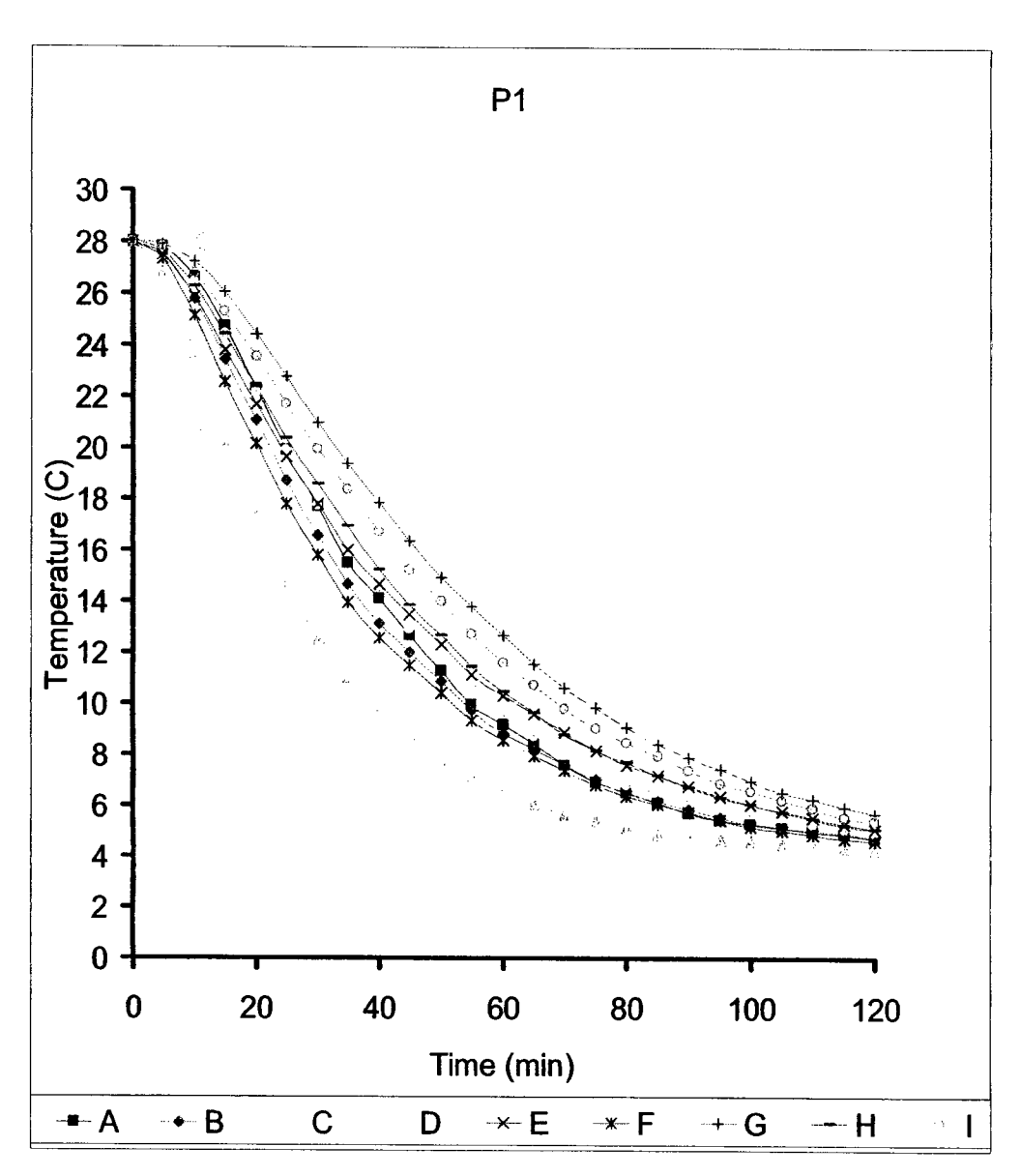


Figure 5.3 (a): Produce temperature profiles based on center temperature of the positions P1 demonstrated in Figure 5.1 considering various vent configurations

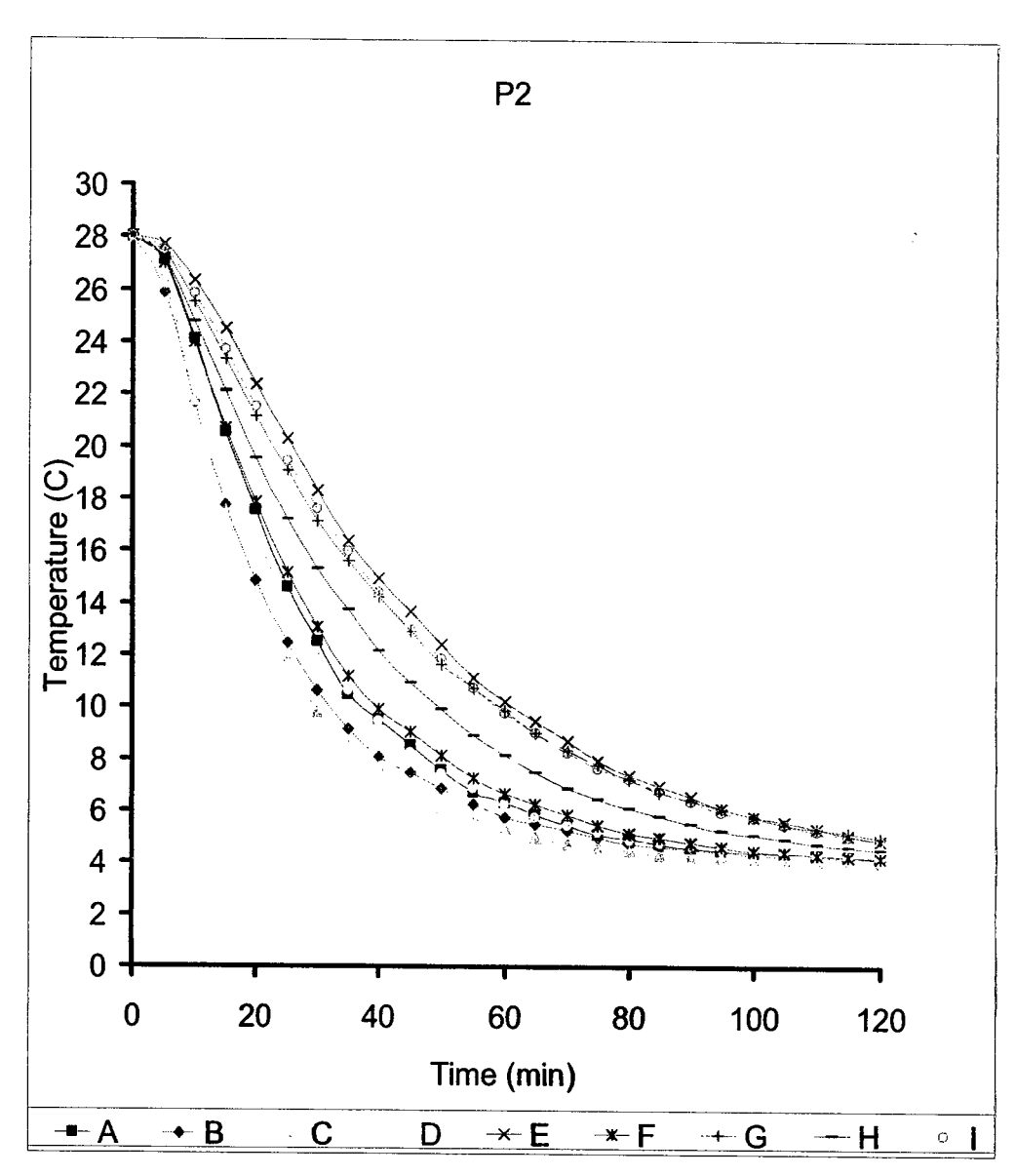


Figure 5.3 (b): Produce temperature profiles based on center temperature of the positions P2 demonstrated in Figure 5.1 considering various vent configurations

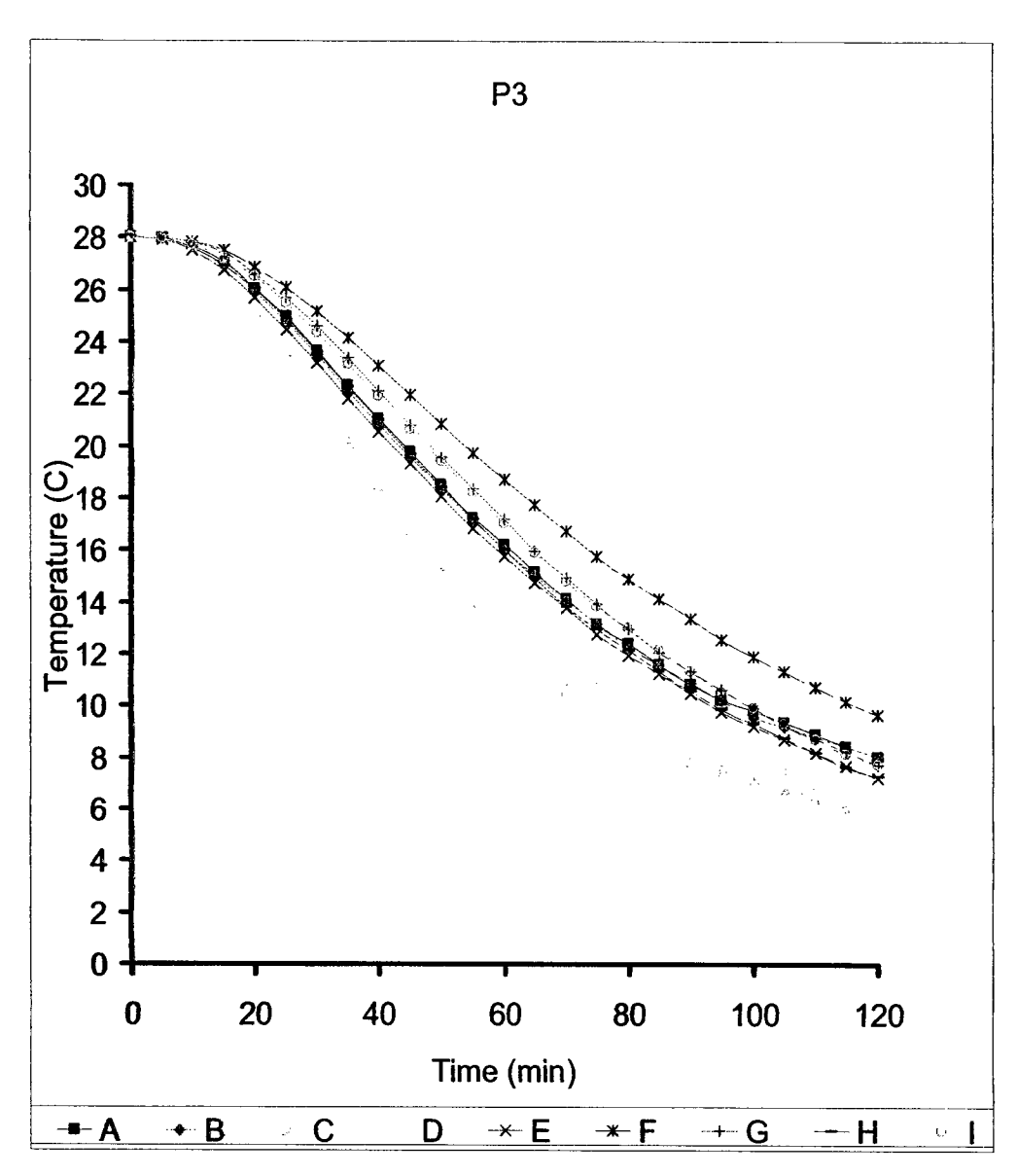


Figure 5.3 (c): Produce temperature profiles based on center temperature of the positions P3 demonstrated in Figure 5.1 considering various vent configurations

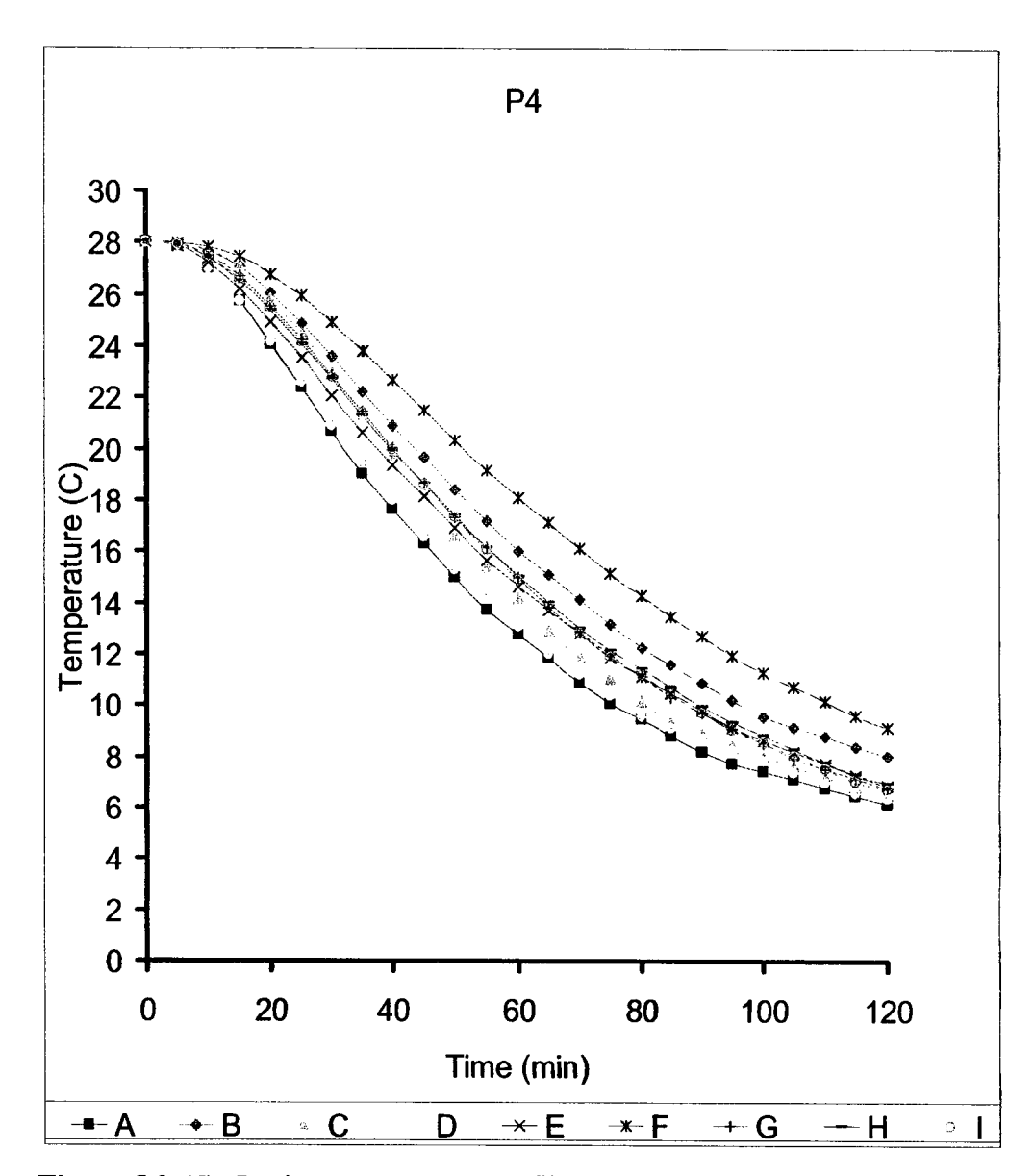


Figure 5.3 (d): Produce temperature profiles based on center temperature of the positions P4 demonstrated in Figure 5.1 considering various vent configurations

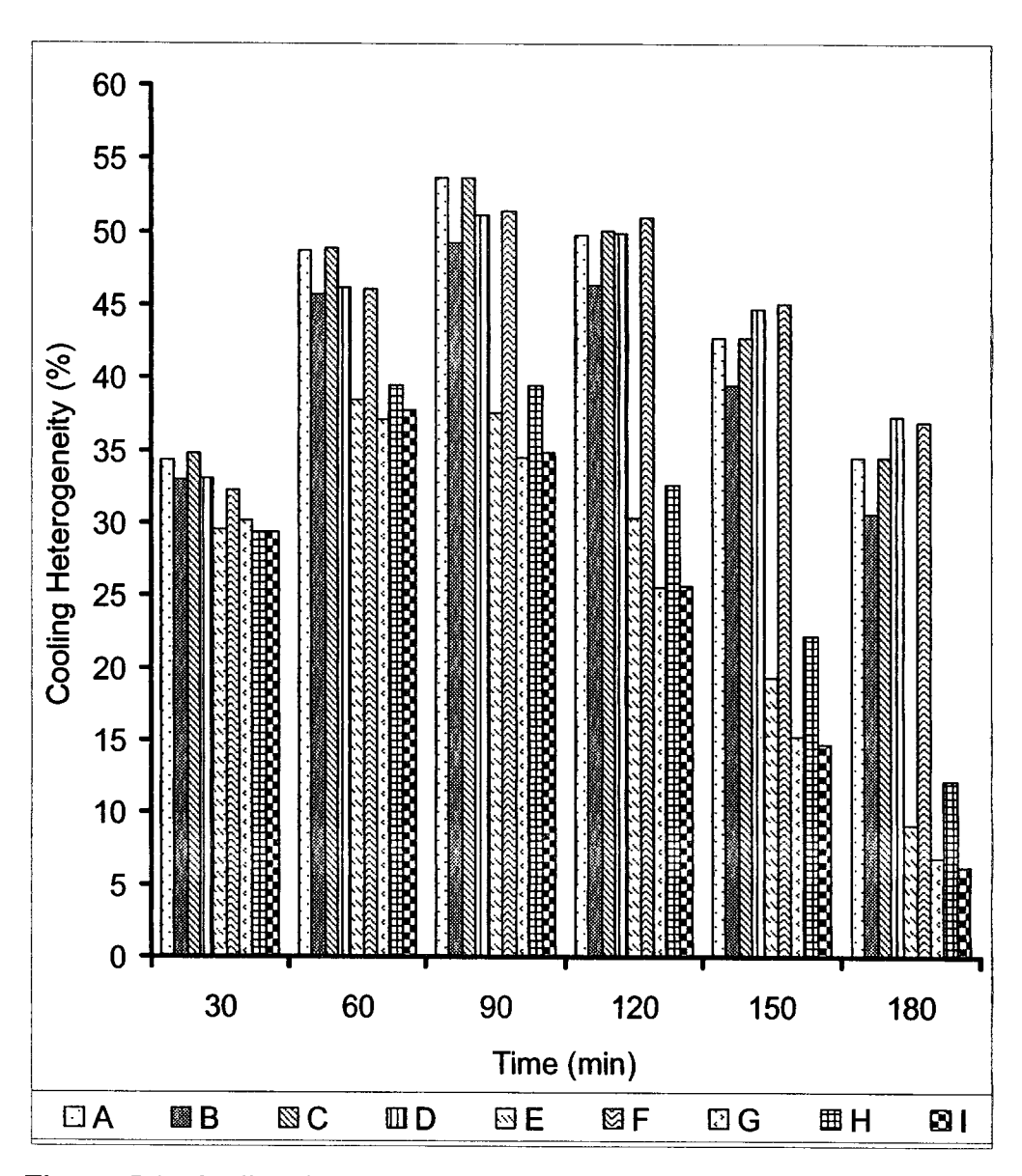


Figure 5.4: Cooling heterogeneity in 9 different package vent designs, as demonstrated in Table 5.1, during 180 min cooling

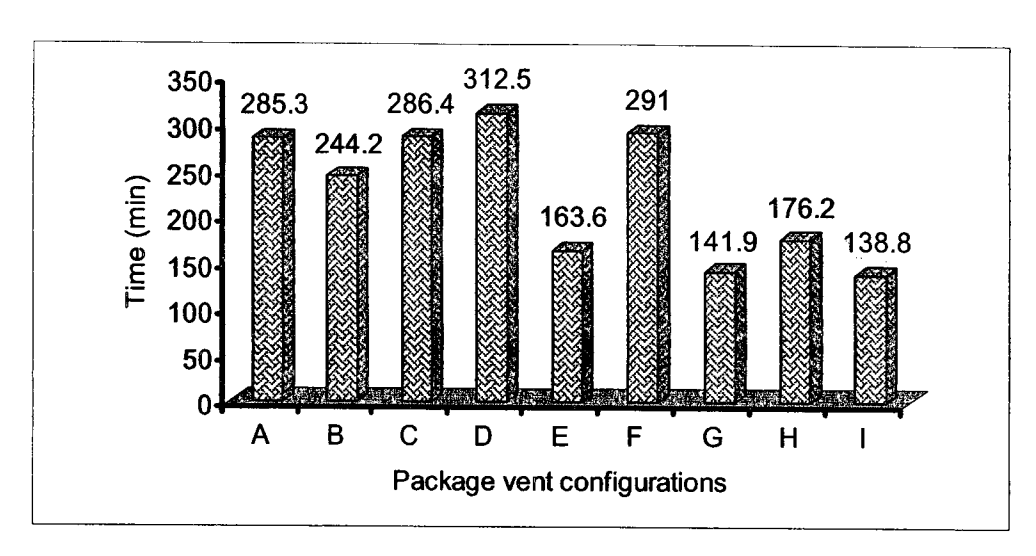


Figure 5.5: Maximum time required for cooling of the slowest cooled produce to reach 7°C in different ventilated packages

Table 5.1: Package vent configurations considered for different simulations based on different vent positions demonstrated in Figure 5.1

Vent configuration	Number of vent(s)	Inlet vent position(s)	Outlet vent position(s)	Vent area (%)
A	1	#2	#4	2.4
В	1	#3	#3	2.4
С	1	#4	#2	2.4
D	2	#2, #3	#2, #3	4.8
E	2	#2, #4	#2, #4	4.8
F	2	#3, #4	#3, #4	4.8
G	3	#1, #3, #5	#1, #3, #5	7.2
Н	3	#2, #3, #4	#2, #3, #4	7.2
I	5	#1, #2, #3, #4, #5	#1, #2, #3, #4, #5	12.1

CONNECTING TEXT

In Chapter V, the importance of package design to be used during forced-air precooling process and its effect on produce cooling efficiency were observed. There have been some discrepancies in the literature regarding the effects of produce evaporative cooling (EC) and heat generation by respiration (HG) on produce cooling efficiency. While some researchers have recognized the importance of EC and HG, some other researchers do not agree with the conclusion. In Chapter VI, the magnitudes of EC and HG as well as the interactive effects of EC, HG and package vent design on produce cooling efficiency during forced-air precooling will be studied.

VI. INFLUENCE OF VENTILATED PACKAGE DESIGN, EVAPORATIVE COOLING AND HEAT GENERATION ON PRODUCE COOLING

6.1 ABSTRACT

The magnitudes of produce evaporative cooling (EC) and heat generation by respiration (HG) as well as the interactive effects of EC, HG and package vent design on produce cooling time during forced-air precooling was investigated using simultaneous modeling of airflow, heat and mass transfer. Different EC and HG values were obtained at various produce positions in different ventilated packages with 1, 3 and 5 vents. Additionally, considerable differences in cooling times were obtained with regard to independent and simultaneous effects of EC and HG in different package vent configurations. Cooling time was increased to about 47% in the package with 1 vent compared to the packages with 3 and 5 vents considering simultaneous effects of EC and HG. The results showed that the effects of EC and HG can be influential in designing the forced-air precooling system and therefore, in the accurate determination of cooling time and the corresponding refrigeration load.

Keywords: Direct numerical simulation; Forced convection cooling; Package vent configuration; Evaporative cooling; Heat generation by respiration; Cooling time

6.2 INTRODUCTION

Forced-air precooling process is a rapid removal of field heat immediately after harvest to extend produce storage life. To ensure optimum produce quality, different variables influencing produce temperature such as evaporative cooling, heat generation by respiration and package vent configuration should be taken into account during the process (Sastry et al., 1978; Holdredge and Wyse, 1982; Dincer,

1993; Gowda et al., 1997; Xu and Burfoot, 1999; Campanone et al., 2002; Hoang et al., 2003; Hoang et al., 2004; Vigneault et al., 2006). Produce is normally cooled faster at a low air temperature, low relative humidity and high air velocity due to the effect of coupled heat and mass transfer. However, practically, low relative humidity is not generally favorable due to a high produce moisture loss (Tassou and Xiang, 1998; Chourasia and Goswami, 2007). Moisture transpires continuously from fruits and vegetables whenever the water vapor pressure of the surrounding air is lower than the water vapor pressure at the produce surface. When moisture evaporates at the produce surface due to a water vapor pressure gradient between the produce and the surrounding air, the heat required to evaporate the moisture is removed from the produce surface, thus providing a cooling effect (Gaffney et al., 1985a).

On the other hand, produce heat generation by respiration may have some influence on produce cooling rate during forced-air precooling (Gowda et al., 1997; Hoang et al., 2004; Jooste and Khumalo, 2005). For products with high respiration rates and for conditions of low cooling rate, considerations of the respiratory heat generation may be important (Gaffney et al., 1985b). However, some researchers have recognized that produce respiration is unlikely to significantly affect the rate of cooling during forced-air precooling (Awberry, 1927; Gan and Woods, 1989; Campanone et al., 1995; Tanner et al., 2002). Gowda et al. (1997) studied forced-air precooling of spherical foods in bulk and found that heat generation by respiration did affect the cooling time; however, this effect was negligible when a high cooling rate was achieved.

In addition to the evaporative cooling and heat generation, package vent design is also a very critical factor that influences airflow and heat transfer phenomena during the process due to different vent areas and locations on package walls (Baird et al., 1988; Vigneault et al., 2006), which in turn affects produce temperature and moisture loss. Therefore, in order to design an effective forced-air precooling system, the designer must have knowledge of the complex interactions of various thermophysical processes which occur around and within produce, such as evaporative cooling and heat generation as well as package vent design. A better

understanding of the effects of produce evaporative cooling, heat generation and package vent configuration should help in improving present forced-air precooling systems and accurate determination of cooling time and the corresponding refrigeration load.

To our knowledge, there is no model in the literature on the simultaneous effects of different package vent configurations, evaporative cooling and heat generation on produce cooling. Recently, Dehghannya et al. (2008) developed and experimentally validated a mathematical model of airflow and heat transfer for simultaneous aerodynamic and thermal analysis during forced-air precooling inside ventilated packages. The authors applied direct numerical simulation and analyzed velocity distributions and their resultant airflow heterogeneity indexes inside different ventilated packages. Dehghannya et al. (submitted for publication 1) also simulated and analyzed temperature distribution inside different ventilated packages to provide uniform cooling during the process. In addition, Dehghannya et al. (submitted for publication 2) assessed the sensitivity of produce cooling uniformity and cooling time as influenced by different package vent designs including various vent areas and positions during forced convection cooling of produce. However, the simultaneous effects of evaporative cooling, heat generation and package vent design on produce temperature and cooling time were not considered in any of these studies.

The aim of this study was to investigate the magnitudes of produce evaporative cooling and heat generation considering different package vent configurations as well as to assess the interactive effects of evaporative cooling, heat generation and package vent design on produce temperature and cooling time during forced-air precooling using simultaneous modeling of airflow, heat and mass transfer. The model was to predict produce transient temperature, evaporative cooling and heat generation at any position inside different ventilated packages.

6.3. MATERIALS AND METHODS

6.3.1 Model Overview

A transient two-phase air-produce mathematical model of simultaneous airflow, heat and mass transfer inside different ventilated packages containing spherical produce (Figure 6.1 and Table 3.1) was developed and validated using experimental data (Dehghannya et al., 2008). For the model description, including the governing equations for the air and produce domains, the numerical method and experimental model validation, refer to Sections 3.3.1, 3.3.2 and 3.3.3, respectively.

6.3.1.1 Model parameters

6.3.1.1.1 Heat generation by respiration

Becker et al. (1996) developed correlations that relate a commodity's rate of carbon dioxide production to its temperature. The carbon dioxide production rate can then be related to the commodity's heat generation rate due to respiration. An interpretation of the correlation is as follows:

$$Q_{resp} = \rho_p q_{resp} \tag{6.1}$$

where q_{resp} is given by:

$$q_{resp} = \frac{10.7f}{3600} (1.8 T_p - 459.67)^g$$
 (6.2)

T_p is transient produce temperature in K and the respiration constants (f and g) have been given in Becker et al. (1996) for different crops.

6.3.1.1.2 Mass transfer

The rate of moisture loss from fruits and vegetables was expressed by the basic equation of the following form:

$$\dot{\mathbf{m}} = \mathbf{k}(\mathbf{p}_{s} - \mathbf{p}_{a}) \tag{6.3}$$

6.3.1.1.2.1 Calculation of k

The mass transfer coefficient (k) was given as follows (Becker et al., 1996):

$$k = \frac{1}{\frac{1}{k_{air}} + \frac{1}{k_{skin}}} \tag{6.4}$$

The air film mass transfer coefficient (k_{air}) was estimated by using the Sherwood-Reynolds-Schmidt correlations (Sastry and Buffington, 1982; Gaffney et al., 1985a; Becker et al., 1996; Geankoplis, 2003):

$$Sh = 2 + 0.552 Re^{0.53} Sc^{0.33}$$
 (6.5)

Note that the Sherwood number yields k'_{air} with a driving force in concentration unit (kg/m³); however, the driving force in the mass transfer model is vapor pressure. Therefore, a conversion from concentration to vapor pressure was made by use of the ideal gas law:

$$k_{air} = \frac{1}{R_{H,O}T} k'_{air} \tag{6.6}$$

where T is the transient boundary layer temperature in K.

The skin mass transfer coefficient, \mathbf{k}_{skin} , describing the resistance to moisture migration through the skin of a produce, is related to the structure and properties of the produce skin. Becker et al. (1996) have tabulated skin mass transfer coefficients for different commodities.

6.3.1.1.2.2 Calculation of pw, pa and ps

The saturation partial water vapor pressure (p_w) was approximated from the Antoine equation (Chuntranuluck et al., 1998; Hu and Sun, 2000):

$$p_{w} \approx \exp\left[23.4795 - \frac{3990.5}{T - 39.317}\right] \tag{6.7}$$

where T is the transient boundary layer temperature in K.

Assuming water vapor to follow the ideal gas law, the partial pressure of water vapor in the air (p_a) is given by the standard psychrometric principle:

$$p_{a} = RH \cdot p_{w} \tag{6.8}$$

where RH denotes the relative humidity.

The partial pressure of water vapor at the evaporating surface (p_s) was defined as (Becker et al., 1996):

$$p_s = VPL \cdot p_w \tag{6.9}$$

where VPL is vapor pressure lowering effect of the produce. The water vapor pressure lowering effect for various fruits and vegetables has also been provided in Becker et al. (1996) obtained from Chau et al. (1987).

6.3.1.1.3 Latent heat of evaporation

The latent heat of evaporation (L) was calculated as a transient function of the boundary layer temperature, as follows (Hoang et al., 2003):

$$L = C_1 T^2 + C_2 T + C_3 (6.10)$$

where $C_1 = 0.0091 \times 10^3$, $C_2 = -7.5129 \times 10^3$, $C_3 = 3875.1 \times 10^3$, and T is in K.

6.3.1.2 Simulation setups

Brussels sprouts was chosen as a representative produce with a very high respiration rate so that it can better represent the effect of produce heat generation on produce cooling, if any. The respiration rate of Brussels sprouts has been classified in the range of 40-60 mg CO₂/kg hr at 5°C (Kader, 2002). It should be noted that the primary objective of this study was to find not absolute but relative values of the effect of evaporative cooling and heat generation on cooling time to allow comparison among different vent areas and positions during forced-air precooling. These results were obtained under comparable circumstances in terms of both simulation and experiment. In simulation, different input parameters, including respiration constants (f and g), skin mass transfer coefficient (k_{skin}), water vapor pressure lowering effect (VPL) and diffusivity of water vapor in air (D) were considered as follows (Becker et al., 1996):

$$f = 2.7238 \times 10^{-3}$$
; $g = 2.5728$; $k_{skin} = 1.33 \times 10^{-8} \text{ kg/m}^2$.s. Pa; VPL = 0.99; $D = 2.6 \times 10^{-5} \text{ m}^2/\text{s}$.

Other simulation setups have been provided in Section 3.3.3.

6.4 RESULTS AND DISCUSSIONS

6.4.1 Effect of Different Package Vent Designs and Relative Humidity on Produce Evaporative Cooling

Figure 6.2 (a, b, c and d) shows produce evaporative cooling at 4 different positions at RH=60% and RH=95% in 3 different package vent configurations with air and initial produce temperature of 4 and 28°C, respectively. A higher evaporative cooling was obtained at RH=60% compared to RH=95% at various positions in all the 3 vent configurations. For example, in the package with 5 vents after 60 min cooling, the evaporative cooling values of 108.1, 98.0, 146.9 and 130.4 mW at RH=60% compared to 11.9, 10.6, 17.1 and 14.8 mW at RH=95% were obtained at positions P1, P2, P3 and P4, respectively. The difference in the

evaporative cooling values at different positions explains the importance of considering moisture loss (and its resultant evaporative cooling) at a specific location rather than considering a mean value of the whole bulk produce inside ventilated packages (Gaffney et al., 1985a).

On the other hand, different evaporative cooling values were obtained at a particular position in different packages before reaching steady state. For instance, by considering position P3 and RH=60%, the values of 127.5, 148.0 and 146.9 mW were obtained after 60 min cooling in the packages with 1, 3 and 5 vents, respectively. The higher evaporative cooling in the packages with 3 and 5 vents, compared to the package with 1 vent, could be related to a higher water vapor pressure gradient between the produce surface and the air in the vicinity of the produce location (P3), which in turn could be related to various air pathways in different ventilated packages (Dehghannya et al., 2008). The difference in produce evaporative cooling obtained at a particular position is more pronounced at position P4 compared to the other 3 positions after a few minutes from the start of the cooling (Figure 6.2). After 60 min cooling, the magnitudes of 99.0, 131.2 and 130.4 mW were obtained at RH=60% in the packages with 1, 3 and 5 vents, respectively. These evaporative cooling values correspond to about 32% lower evaporative cooling in the package with 1 vent compared to the packages with 3 and 5 vents. The similar evaporative cooling magnitudes in the packages with 3 and 5 vents could be attributed to the specific vent distribution on the package walls and therefore a similar air circulation through the commodities during the process (Vigneault et al., 2006; Dehghannya et al., submitted for publication 2).

It should be noted that the evaporative cooling rates shown in Figure 6.2 (a, b, c and d) are the initial evaporative cooling rates and are valid only until the amount of moisture loss begins to affect the physical characteristics of the produce. For example, after a produce has lost a certain amount of moisture, shriveling of the skin will result in a reduced mass transfer coefficient, which in turn will reduce the rate of moisture loss. Also, removal of moisture from the produce may dilute the solution at the evaporating surface, thus changing the magnitude of the vapor pressure lowering effect. It should also be noted that the evaporative cooling rates

are not necessarily those for all Brussels sprouts, since the values for VPL and k_{skin} used in this study were taken as representative values given in the literature.

6.4.2 Effect of Different Package Vent Designs on Produce Heat Generation

Figure 6.3 (a, b, c and d) shows produce heat generation at 4 various positions at RH=60% and RH=95% in 3 different package vent configurations with air and initial produce temperature of 4 and 28°C, respectively. A steep decrease in produce heat generation was generally obtained during about the first 90 min cooling considering all the 3 package configurations and 4 different positions after which a relatively steady state heat generation was reached due to produce cooling. By comparing different produce positions, it can be seen that positions that are near to airflow inlet in different packages, reached the steady state heat generation faster compared to positions that are located far from inlet. This trend can be seen, for instance, by comparing Positions P2 (near inlet) and P3 (far from inlet) in different packages (Figure 6.3). Additionally, the heat generation rates were slightly higher at RH=95% compared to RH=60% before reaching steady state considering 3 different ventilated packages (Figure 6.3). This could be related to a lower temperature at RH=60% due to the evaporative cooling effect. Also, different heat generation rates were obtained at a specific position considering different package vent configurations due to different air pathways from package inlet to outlet vents. For example, the heat generation rates of 32.2, 39.9 and 39.5 mW was obtained at position P3 (RH=95%) in the packages with 1, 3 and 5 vents, respectively.

On the other hand, different heat generation rates were obtained at different positions in different ventilated packages considering a specific relative humidity. For example, while heat generation was 19.9, 24.5 and 22.5 mW for the produce at position P1, the magnitudes of 28.4, 34.4 and 34.0 mW were obtained at position P3 after 60 min cooling at RH=60% in the packages with 1, 3 and 5 vents, respectively. These heat generation magnitudes correspond to the mean produce temperature of 8.6, 10.8 and 9.9°C at position P1 compared to 12.5, 14.9 and 14.7°C at position P3 after 60 min cooling in the packages with 1, 3 and 5 vents, respectively. This result

shows that positions P1 and P3 in the package with 1 vent cools faster and therefore lower heat is generated by respiration compared to the packages with 3 and 5 vents. This phenomenon probably seems to be controversial at first, especially for position P1, because it is far from the inlet in the package with 1 vent compared to the packages with 3 and 5 vents, and therefore it might be expected to cool faster in the packages with 3 and 5 vents. This could be explained by the fact that the produce surface at position P1 in the packages with 3 and 5 vents was cooled faster due to the position's nearness to the inlet vents of the packages compared to the package with 1 vent. However, the produce center (P1) took sometime to reach to its surface temperature in the packages with 3 and 5 vents. Therefore, its mean temperature is higher in the package with 3 (10.8°C) and 5 vents (9.9°C) compared to the package with 1 vent (8.6°C).

6.4.3 Effect of Evaporative Cooling and Heat Generation on Cooling Time

In order to investigate independent and simultaneous effects of evaporative cooling (EC) and heat generation (HG) on produce temperature, 18 different cases were simulated in 3 different packages with air and initial produce temperature of 4 and 28°C, respectively. The simulated cases included no EC and no HG, only HG (without EC), only EC (without HG) at the relative humidity of 60 and 95% and both EC (at the relative humidity of 60 and 95%) and HG. Table 6.1 shows the results of the simulations based on the center temperature of 4 different positions shown in Figure 6.1 as well as the maximum temperature in different cases after 60 min cooling. Generally, evaporative cooling and heat generation decreased and increased produce temperature, respectively, at all the positions inside all the ventilated packages. When both EC and HG was considered, produce center temperature was generally lower compared to the mean value of the cases with only HG and only EC (Table 6.1). For example, in the package with 3 vents at position P1, the produce center temperature was 12.6, 13.2, 11.3 and 11.9°C when no EC and no HG, only HG, only EC (RH=60%) and both EC (RH=60%) and HG was

considered. This phenomenon could be related to the effect of respiration on evaporative cooling. The respiratory heat generation tends to raise produce temperature, increasing the water vapor pressure deficit, thereby increasing moisture loss and evaporative cooling (Sastry et al., 1978).

Table 6.1 shows that different produce center temperatures were obtained at different positions inside different ventilated packages. For example, when both EC (RH=60%) and HG were considered, the maximum temperature was 15.9°C at position P3 in the package with 3 vents and the minimum temperature was 7.1°C at position P2 in the package with 1 vent. These different temperatures were obtained by applying the same conditions in terms of produce initial temperature, air velocity and air temperature, explaining the importance of package vent design in produce cooling at different positions (Dehghannya et al., submitted for publication 1).

To better illustrate the importance of package vent design on produce cooling time, Figure 6.4 shows produce cooling time in different package vent configurations based on the maximum time required for cooling of the slowestcooled produce to 7°C regarding the independent and simultaneous effects of EC and HG. The temperature of 7°C was chosen as an index temperature since it is the temperature after the 7/8 cooling time (air temperature: 4°C and produce temperature: 28°C) which is normally used during forced-air precooling (Kader, 2002). The positions of the slowest-cooled produce in different situations are shown in Table 6.1. Figure 6.4 demonstrates considerable differences in cooling times with regard to independent and simultaneous effects of EC and HG in different package vent configurations. For example, in the package with 3 vents, 13.2 min increase, 35.3 min decrease, 2.6 min decrease, 29.8 min decrease and 8.6 min increase were obtained when only HG, only EC (RH=60%), only EC (RH=95%), both EC (RH=60%) and HG, and both EC (RH=95%) and HG, respectively, were compared to the case with no EC and no HG. This result shows that the effects of evaporative cooling and heat generation can be influential in designing the forced-air precooling system and therefore, in the accurate determination of cooling time.

Additionally, by considering a specific case such as the case with both EC (RH=95%) and HG, the necessary cooling times for cooling of the slowest-cooled

produce to 7°C were 297.7, 157.7 and 156.9 min in the packages with 1, 3 and 5 vents, respectively. These values correspond to about 47% increase in cooling time in the package with 1 vent compared to the packages with 3 and 5 vents. However, in terms of the cooling time, no considerable difference (0.8 min) was found between the packages with 3 (7.2% vent area) and 5 vents (12.1% vent area). This could be related to the better vent distribution on the package walls with 3 and 5 vents and therefore, uniform air circulation through the commodities. This result could suggest that a certain vent area is capable of providing uniform cooling with no need to increase vent area, which in turn can compromise package structural resistance (Vigneault et al., 2006).

6.5 CONCLUSIONS

Simultaneous models of airflow, heat and mass transfer during forced-air precooling were developed to investigate the magnitudes of produce evaporative cooling and heat generation by respiration as well as the interactive effects of evaporative cooling, heat generation and package vent design on produce cooling time. It was shown that package vent configuration has considerable influence on produce evaporative cooling, heat generation and cooling time and, consequently, the effects of evaporative cooling and heat generation can be influential in designing forced-air precooling systems and therefore, accurate determination of cooling time and the corresponding refrigeration load. The methodology developed in this study can be a useful tool to study produce cooling rate as influenced by different parameters, to improve forced-air precooling efficiency.

6.6 REFERENCES

- Awberry, J.H. 1927. The flow of heat in a body generating heat. Phil Mag 4:629-638.
- Baird, C., J. Gaffney, and M. Talbot. 1988. Design criteria for efficient and cost effective forced air cooling systems for fruits and vegetables. ASHRAE Transactions 94:1434-1454.
- Becker, B.R., A. Misra, and B.A. Fricke. 1996. Bulk refrigeration of fruits and vegetables Part I: Theoretical considerations of heat and mass transfer. HVAC&R Research 2:122-134.
- Campanone, L.A., S.A. Giner, and R.H. Mascheroni. 1995. The use of a simulation software to optimize cooling times and to lower weight losses in fruit refrigeration, pp. 121-128 Proceedings of the 19th International Congress of Refrigeration Vol. 1.
- Campanone, L.A., S.A. Giner, and R.H. Mascheroni. 2002. Generalized model for the simulation of food refrigeration. Development and validation of the predictive numerical method. International Journal of Refrigeration-Revue Internationale Du Froid 25:975-984.
- Chau, K.V., R.A. Romero, C.D. Baird, and J.J. Gaffney. 1987. Transpiration coefficients of fruits and vegetables in refrigerated storage. ASHRAE Report: 370-RP. Atlanta: ASHRAE.
- Chourasia, M.K., and T.K. Goswami. 2007. CFD simulation of effects of operating parameters and product on heat transfer and moisture loss in the stack of bagged potatoes. Journal of Food Engineering 80:947-960.

- Chuntranuluck, S., C.M. Wells, and A.C. Cleland. 1998. Prediction of chilling times of foods in situations where evaporative cooling is significant Part 1. Method development. Journal of Food Engineering 37:111-125.
- Dehghannya, J., M. Ngadi, and C. Vigneault. 2008. Simultaneous aerodynamic and thermal analysis during cooling of stacked spheres inside ventilated packages. Chemical Engineering and Technology 31(11): 1651-1659.
- Dehghannya, J., M. Ngadi, and C. Vigneault. Mathematical modeling of airflow and heat transfer during forced convection cooling of produce intended for optimal package design. Transactions of the Institution of Chemical Engineers (IChemE) Part C, Food and Bioproducts Processing. Submitted for publication 1.
- Dehghannya, J., M. Ngadi, and C. Vigneault. Direct numerical simulation of produce cooling in ventilated packages. Journal of Food Engineering. Submitted for publication 2.
- Dincer, I. 1993. An exact heat transfer analysis of spherical products subjected to forced-air cooling. International Journal of Energy Research 17:9-18.
- Gaffney, J.J., C.D. Baird, and K.V. Chau. 1985a. Influence of airflow rate, respiration, evaporative cooling, and other factors affecting weight loss calculations for fruits and vegetables. ASHRAE Transactions 91:690-707.
- Gaffney, J.J., C.D. Baird, and K.V. Chau. 1985b. Methods for calculating heat and mass transfer in fruits and vegetables individually and in bulk. ASHRAE Transactions 91:333-352.
- Gan, G., and J.L. Woods. 1989. A deep bed simulation of vegetable cooling, pp. 2301-2308, *In* V. A. Dodd and P. M. Grace, (eds.) Agricultural Engineering:

- Proceedings of the Eleventh International Congress on Agricultural Engineering. A.A. Balkema, Rotterdam, Netherlands; Brookfield, VT., Dublin, 4-8 September.
- Geankoplis, C.J. 2003. Transport processes and separation process principles: (includes unit operations). Prentice Hall Professional Technical Reference, Upper Saddle River, New Jersey
- Gowda, B.S., G.S.V.L. Narasimham, and M.V.K. Murthy. 1997. Forced-air precooling of spherical foods in bulk: A parametric study. International Journal of Heat and Fluid Flow 18:613-624.
- Hoang, M.L., P. Verboven, M. Baelmans, and B.M. Nicolai. 2003. A continuum model for airflow, heat and mass transfer in bulk of chicory roots.

 Transactions of the ASABE 46:1603-1611.
- Hoang, M.L., P. Verboven, M. Baelmans, and B.M. Nicolai. 2004. Sensitivity of temperature and weight loss in the bulk of chicory roots with respect to process and product parameters. Journal of Food Engineering 62:233-243.
- Holdredge, R.M., and R.E. Wyse. 1982. Computer simulation of the forced convection cooling of sugarbeets. Transactions of the ASABE 25:1425-1430.
- Hu, Z.H., and D.W. Sun. 2000. CFD simulation of heat and moisture transfer for predicting cooling rate and weight loss of cooked ham during air-blast chilling process. Journal of Food Engineering 46:189-197.
- Jooste, M.M., and P. Khumalo. 2005. Effect of the rate and duration of forced air cooling on the quality of 'Imperial' apricots and 'Pioneer' and 'Songold' plums. Acta Horticulturae (ISHS) 682:1633-1638.

- Kader, A.A. 2002. Postharvest technology of horticultural crops, 3rd ed. University of California, Division of Agriculture and Natural Resources, Oakland, California.
- Sastry, S.K., C.D. Baird, and D.E. Buffington. 1978. Transpiration rates of certain fruits and vegetables. ASHRAE Transactions 84:237-255.
- Sastry, S.K., and D.E. Buffington. 1982. Transpiration rates of stored perishable commodities: A mathematical model and experiments on tomatoes. ASHRAE Transactions 88:159-184.
- Tanner, D.J., A.C. Cleland, L.U. Opara, and T.R. Robertson. 2002. A generalised mathematical modelling methodology for design of horticultural food packages exposed to refrigerated conditions: part 1, formulation. International Journal of Refrigeration 25:33-42.
- Tassou, S.A., and W. Xiang. 1998. Modelling the environment within a wet air-cooled vegetable store. Journal of Food Engineering 38:169-187.
- Vigneault, C., B. Goyette, and L.R. De Castro. 2006. Maximum slat width for cooling efficiency of horticultural produce in wooden crates. Postharvest Biology and Technology 40:308-313.
- Xu, Y.F., and D. Burfoot. 1999. Simulating the bulk storage of foodstuffs. Journal of Food Engineering 39:23-29.

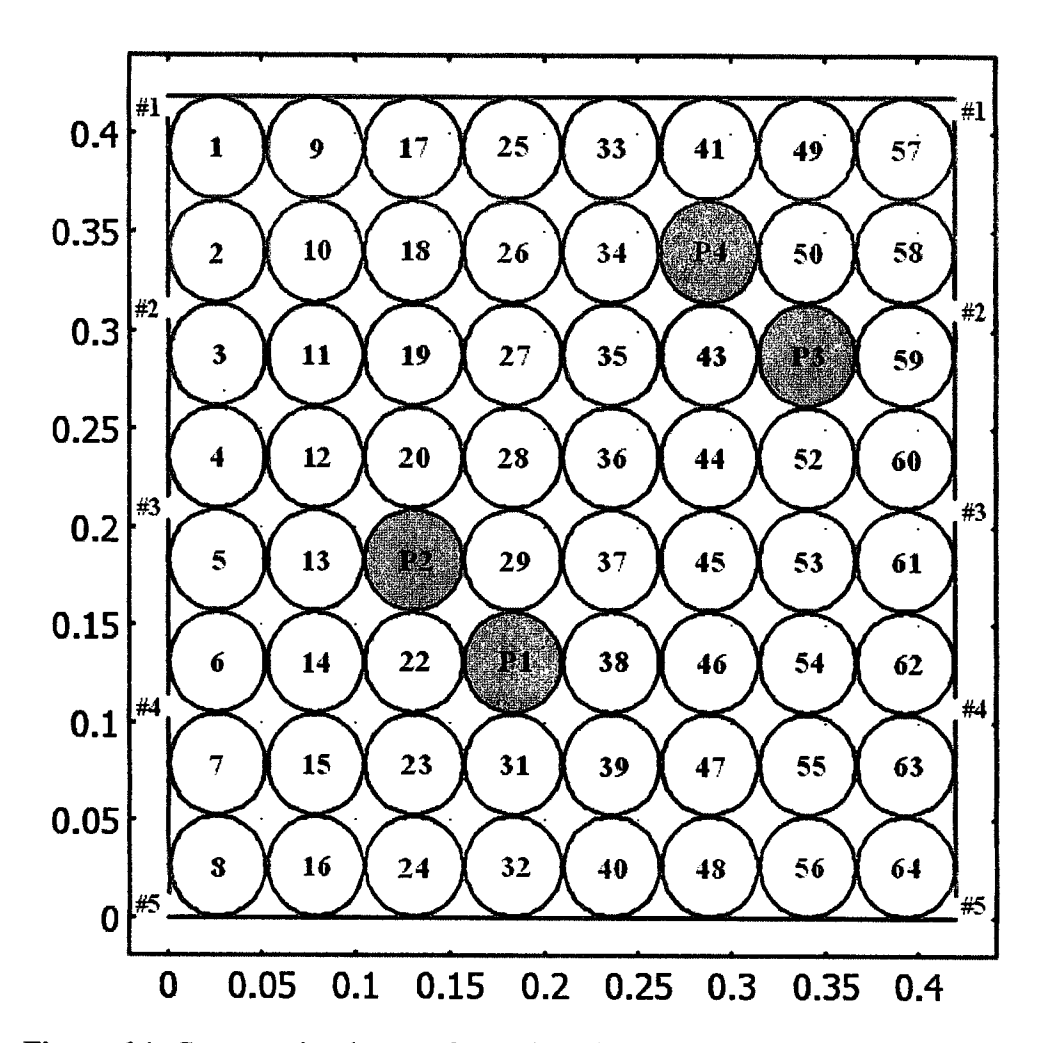


Figure 6.1: Cross-sectional area of a packaged produce with inlet and outlet vent positions shown in left and right sides, respectively (Table 3.1) as well as produce positions (P1, P2, P3 and P4) used for investigation of evaporative cooling and heat generation

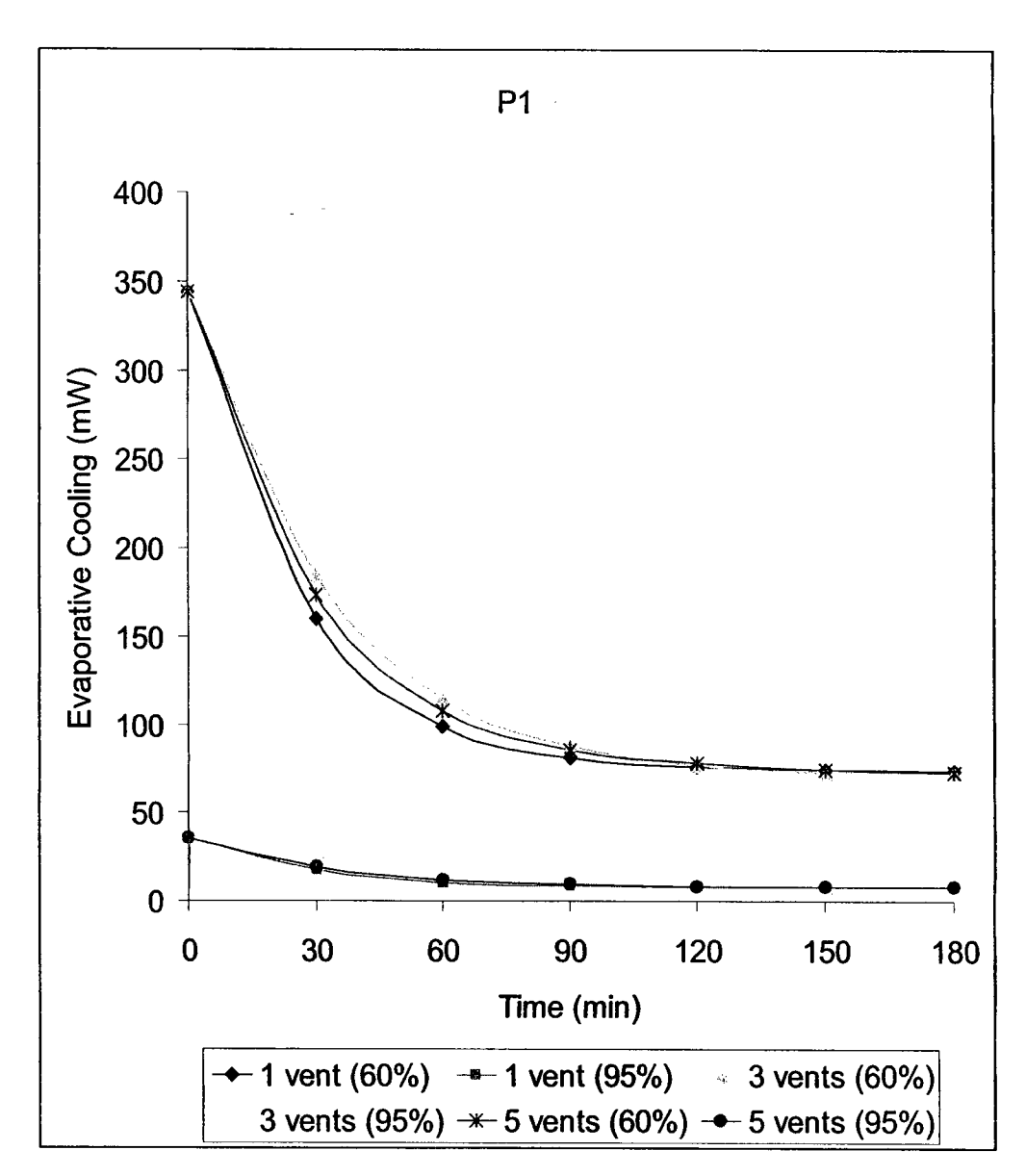


Figure 6.2 (a): Produce evaporative cooling at the position P1 shown in Figure 6.1 at RH=60% and RH=95% in different package vent configurations

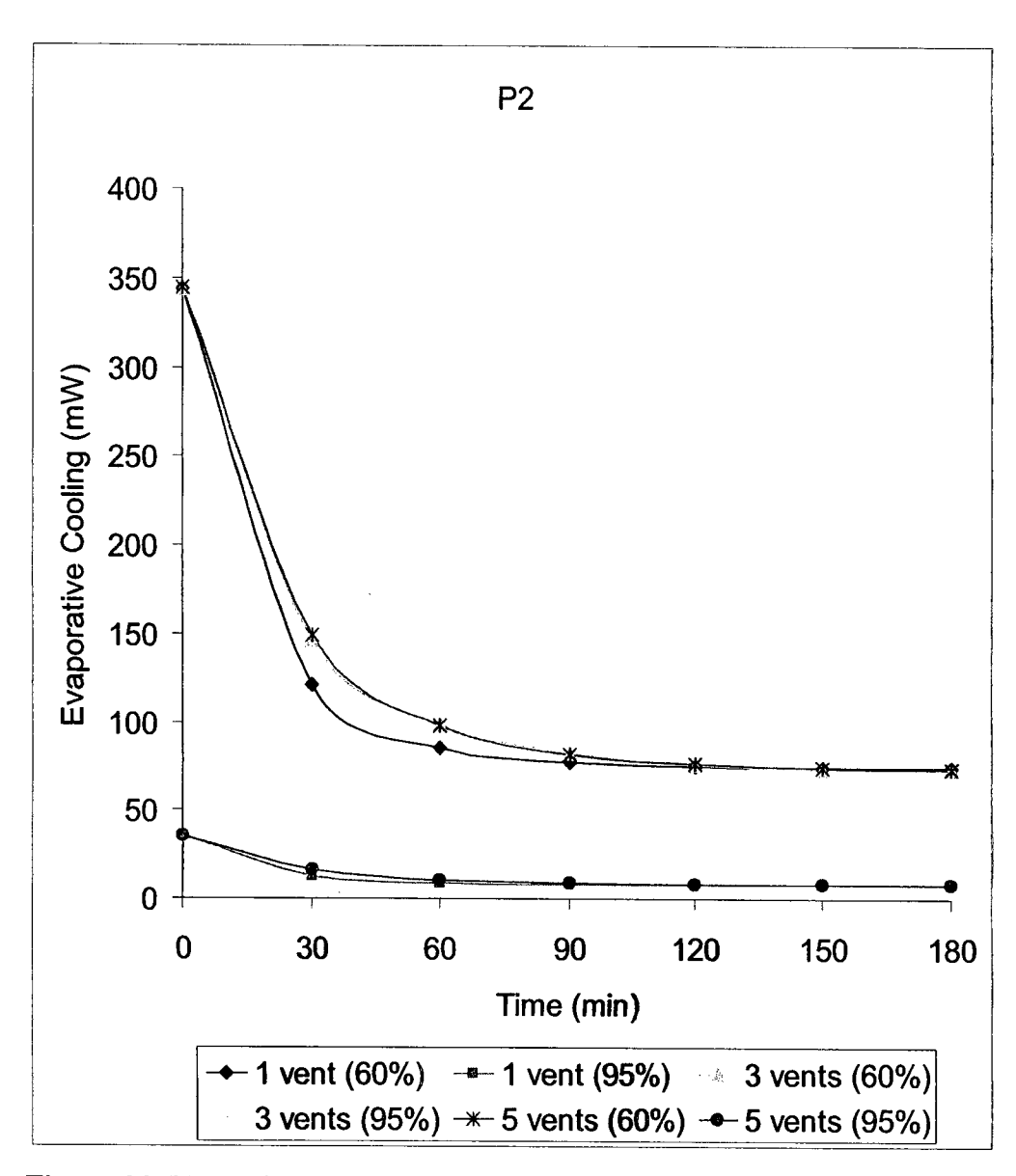


Figure 6.2 (b): Produce evaporative cooling at the position P2 shown in Figure 6.1 at RH=60% and RH=95% in different package vent configurations

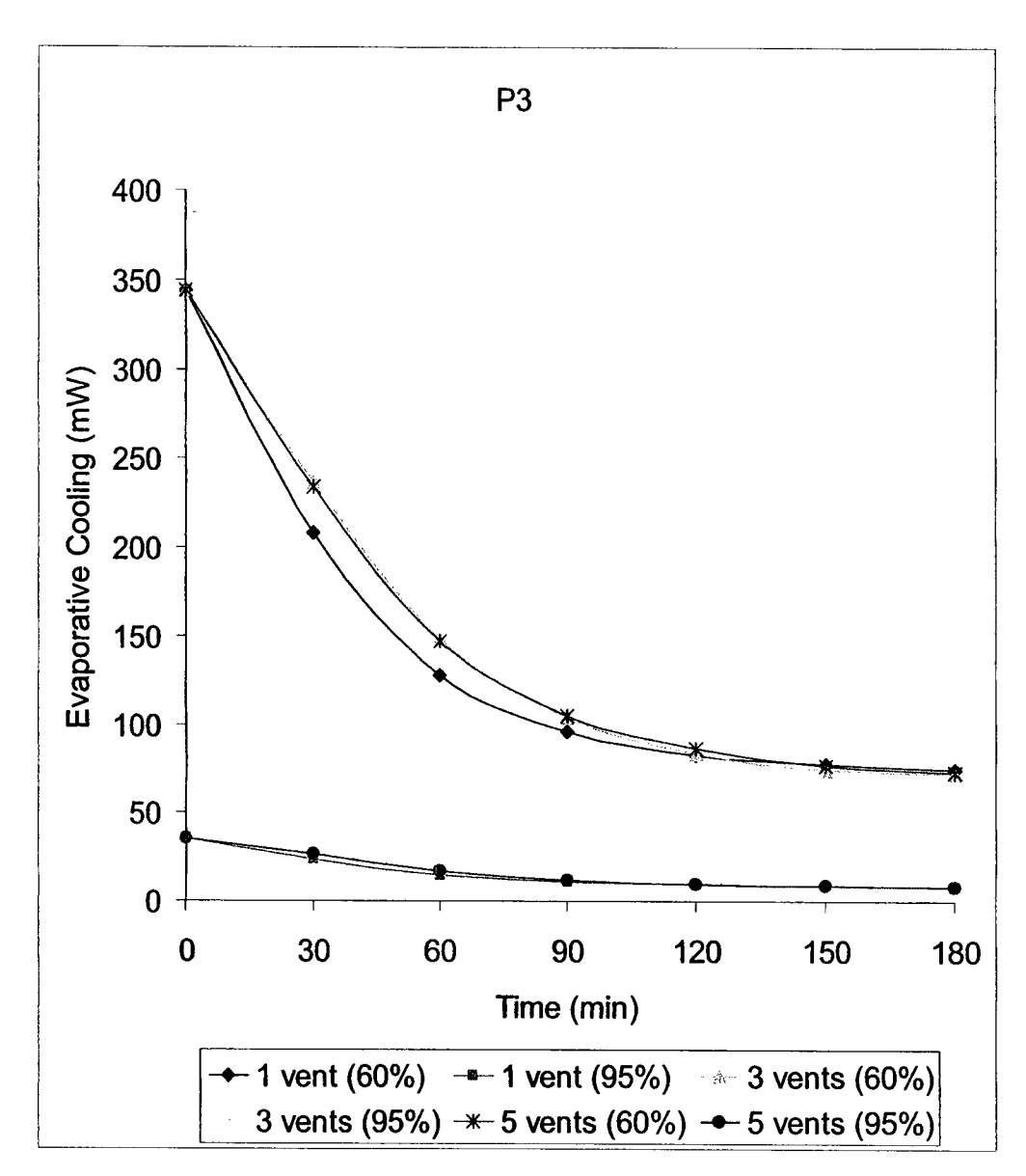


Figure 6.2 (c): Produce evaporative cooling at the position P3 shown in Figure 6.1 at RH=60% and RH=95% in different package vent configurations

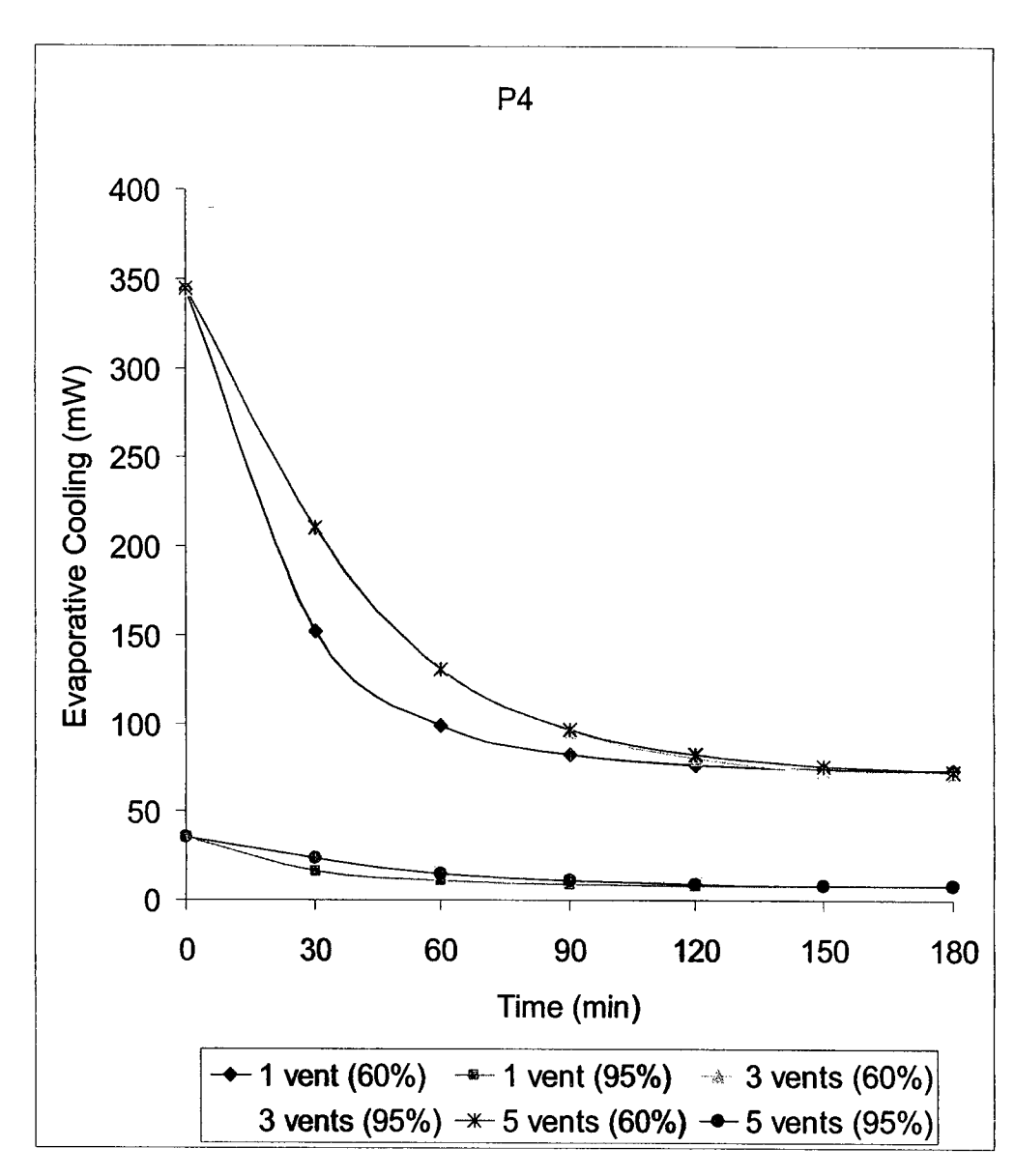


Figure 6.2 (d): Produce evaporative cooling at the position P4 shown in Figure 6.1 at RH=60% and RH=95% in different package vent configurations

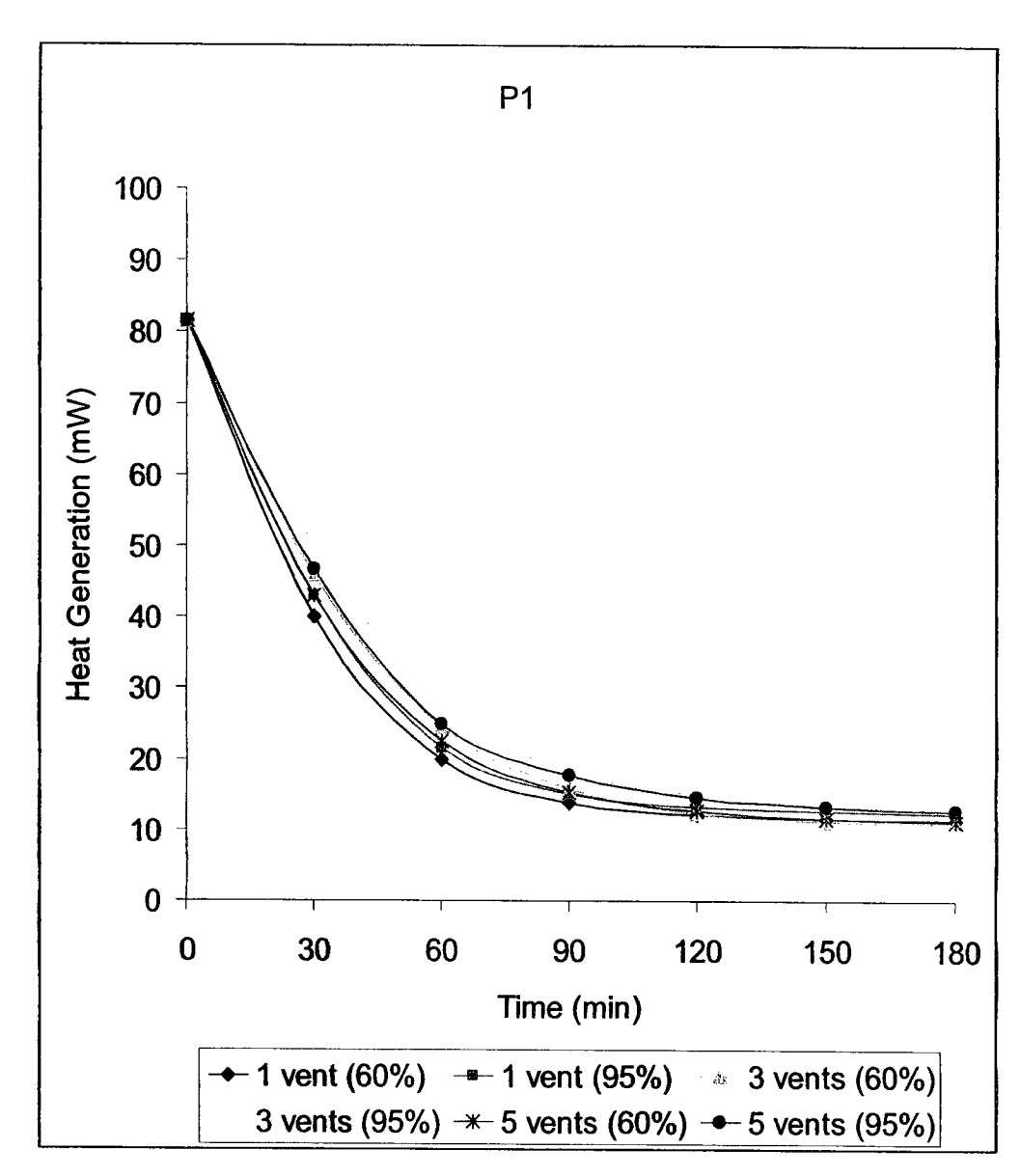


Figure 6.3 (a): Produce heat generation at the position P1 shown in Figure 6.1 at RH=60% and RH=95% in different package vent configurations

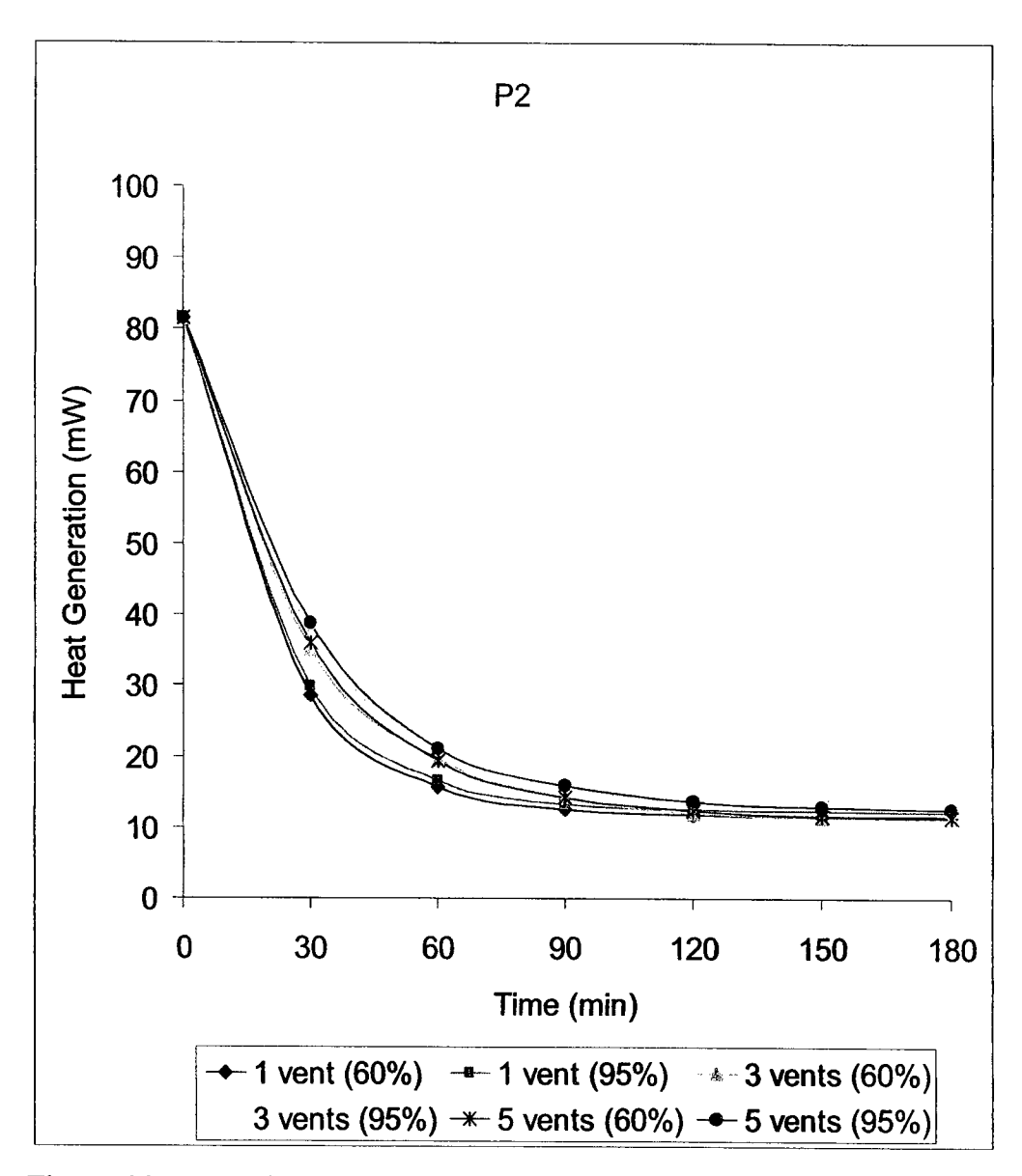


Figure 6.3 (b): Produce heat generation at the position P2 shown in Figure 6.1 at RH=60% and RH=95% in different package vent configurations

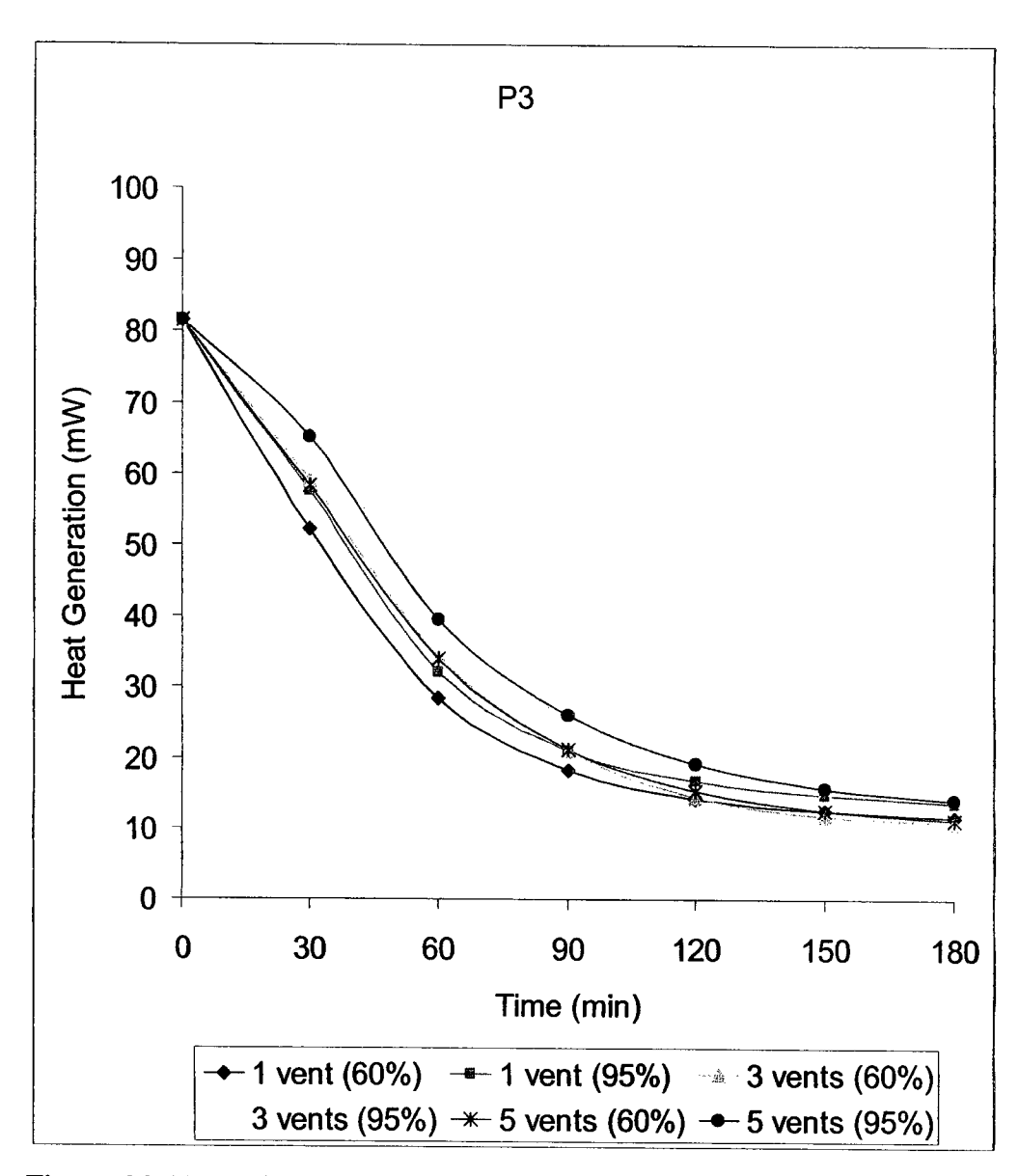


Figure 6.3 (c): Produce heat generation at the position P3 shown in Figure 6.1 at RH=60% and RH=95% in different package vent configurations

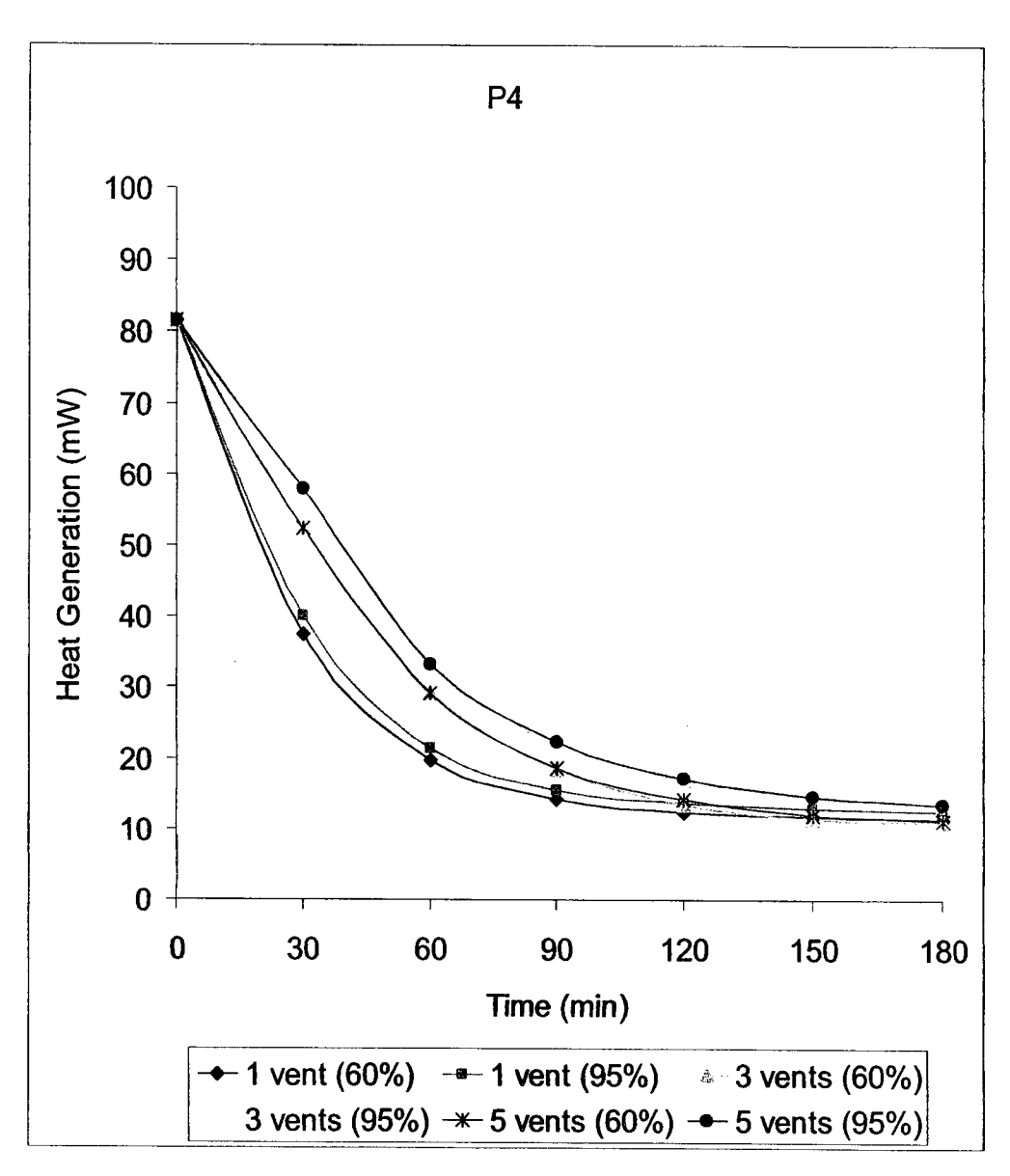


Figure 6.3 (d): Produce heat generation at the position P4 shown in Figure 6.1 at RH=60% and RH=95% in different package vent configurations

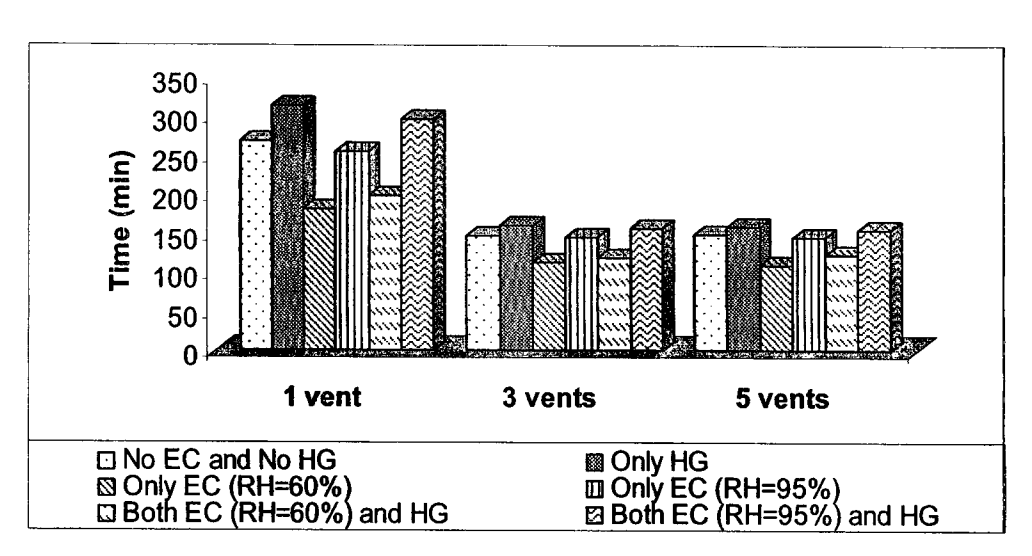


Figure 6.4: Maximum time required for cooling of the slowest-cooled produce to reach 7°C in different ventilated packages regarding independent and simultaneous effects of evaporative cooling (EC) and heat generation (HG)

Table 6.1: Effect of evaporative cooling (EC), heat generation (HG) and package vent configuration on produce temperature (°C) at different positions after 60 min cooling

Parameter ¹	Vent	Produce Positions ³					
	Configuration ²	P1	P2	P3	P4	T_{Max}^4	P _{Max} ⁴
No EC and No HG	1 vent	10.2	7.4	14.5	10.0	25.1	57
	3 vents	12.6	9.9	17.2	15.0	19.1	59
	5 vents	11.6	9.8	17.0	14.9	18.7	57
Only HG	1 vent	10.6	7.7	15.3	10.5	27.0	57
	3 vents	13.2	10.3	18.1	15.8	20.2	59
	5 vents	12.2	10.2	18.0	15.7	19.8	57
Only EC	1 vent (RH=60%)	9.3	6.9	12.9	9.1	21.0	57
	1 vent (RH=95%)	10.1	7.4	14.3	9.9	24.6	57
	3 vents (RH=60%)	11.3	9.0	15.1	13.3	16.7	59
	3 vents (RH=95%)	12.5	9.8	16.9	14.8	18.8	59
	5 vents (RH=60%)	10.4	8.8	14.9	13.2	16.3	57
	5 vents (RH=95%)	11.5	9.7	16.8	14.7	18.4	57
Both EC and HG	1 vent (RH=60%)	9.7	7.1	13.6	9.5	22.3	57
	1 vent (RH=95%)	10.5	7.6	15.1	10.4	26.4	57
	3 vents (RH=60%)	11.9	9.3	15.9	14.0	17.6	59
	3 vents (RH=95%)	13.1	10.2	17.9	15.6	20.0	59
	5 vents (RH=60%)	10.9	9.2	15.8	13.9	17.2	57
	5 vents (RH=95%)	12.0	10.1	17.7	15.5	19.5	57

¹EC: Evaporative Cooling; HG: Heat Generation

² As shown in Figure 6.1 and Table 3.1

³ As shown in Figure 6.1

 $^{^4}$ Maximum produce temperature (T_{Max}) at a particular position (P_{Max}) shown in Figure 6.1

VII. SUMMARY AND GENERAL CONCLUSIONS

Coupled mathematical models of airflow, heat and mass transfer were developed for simultaneous aerodynamic and thermal analysis during forced convection cooling of produce, intended for optimal package design. Air velocity, heterogeneity indexes and produce temperature profiles were investigated in 3 different package vent configurations. Predicted temperature profiles were compared with experimental data for model validation. Good agreement between model prediction and measured data was obtained.

The results showed that airflow distribution during forced convection cooling is not homogeneous. The highest cooling heterogeneity index (108%) was recorded at 2.4% vent area whereas the lowest heterogeneity index (0%) was detected in a package with 12.1% vent area. Therefore, the higher the vent area the better the air uniformity during the process; however, the vent area can not exceed a certain point due to the risk of compromising package structural resistance. On the other hand, produce cooling uniformity was increased by increasing the number of vents from 1 to 5. In addition, produce cooling heterogeneity increased until about 90 min cooling and subsequently decreased with further cooling regarding different package vent designs.

For further analysis of the effect of package vent design on produce cooling efficiency, 9 different vent designs including 1, 2, 3 and 5 vents corresponding to 4 different vent areas of 2.4, 4.8, 7.2 and 12.1%, respectively, were simulated. Considerable differences were obtained for different package vent configurations regarding produce temperature distribution, cooling heterogeneity and cooling time. It was shown that a certain number of vents together with their distributions on package walls can provide suitable air pathways and therefore a uniform cooling operation. Additionally, it was confirmed that for different package vent configurations, increasing vent area does not necessarily shorten the cooling time but could indeed increase the time of cooling depending on vent positions on the

package walls. Consequently, increasing vent area may not necessarily have a positive effect on cooling efficiency and its negative impact on package structural resistance would remain a major concern. Cooling time and cooling heterogeneity can be reduced by suitable package designs to provide efficient forced convection cooling.

The magnitudes of produce evaporative cooling (EC) and heat generation by respiration (HG) as well as the interactive effects of EC, HG and package vent design on produce cooling time were also investigated using the developed model. Different EC and HG values were obtained at various produce positions in different ventilated packages. Additionally, considerable differences in cooling times were obtained with regard to independent and simultaneous effects of EC and HG in different package vent configurations. Cooling time was increased to about 47% in the package with 1 vent compared to the packages with 3 and 5 vents when considering the simultaneous effects of EC and HG. Consequently, the effects of evaporative cooling and heat generation can be influential in designing forced-air precooling systems and, therefore, accurate determination of cooling time and the corresponding refrigeration load.

By simulating different vent configurations, the methodology developed in this study can be used as a package design tool to provide homogeneous temperature distribution in ventilated packages during forced convection cooling of produce. Using the mathematical model, produce temperature distribution during forced-air precooling can be predicted at any position as influenced by different package vent designs. The tool can simulate velocity and temperature distributions for various combinations of package size and shape; size, number and location of vents; produce packing arrangements; size and shape of produce; airflow rate and air temperature.

VIII. CONTRIBUTIONS TO KNOWLEDGE AND SUGGESTIONS FOR FUTURE RESEARCH

8.1 CONTRIBUTIONS TO KNOWLEDGE

This is the first study to develop and validate mathematical models of coupled airflow, heat and mass transfer for design optimization of ventilated packages to be used during the forced convection cooling process. Achieving homogeneous produce cooling inside ventilated packages is a serious challenge during the process. The model developed in the study can be used as a package design tool to provide uniform cooling and, therefore, to increase produce shelf life.

The specific contributions to knowledge from this study are as follows:

- 1) Prediction of local airflow inside different ventilated packages during forced convection cooling of produce was achieved considering various vent areas and positions on package walls. By simulating different combinations of package vent area and position, uniform airflow distribution can be reached during the process.
- 2) Prediction of produce temperature at any position inside various packages during the process was achieved. The influence of different package vent designs including various vent distributions with the same or different vent area on produce cooling efficiency was investigated.
- 3) The interactive effects of evaporative cooling, heat generation and package vent design on produce temperature distribution and cooling time were assessed. The magnitudes of produce evaporative cooling and heat generation at any position inside different ventilated packages can be predicted using the developed model.

8.2 SUGGESTIONS FOR FUTURE RESEARCH

In direct numerical simulation (DNS), the governing equations for the fluid flow and heat transfer include both laminar and turbulent flows, and are not restricted by fluid type or by flow rate; however, the geometric modeling and grid generation become complicated and the computational demands increase significantly. The enhanced computational requirements are mainly due to the extremely fine mesh necessary to carry out the simulation. Because of the significant computing costs, DNS is typically performed at low and moderate Reynolds numbers near laminar and transition regimes.

Additionally, three-dimensional (3-D) modeling of airflow and heat transfer inside a ventilated package containing few hundred spheres extensively increases the computational demands both in mesh size and iteration process. To be able to solve for certain details in a 3-D model, such as areas where spheres are close to each other or to package walls, a high level of detail is necessary for the required accuracy of the simulation. Such a large computational requirement is currently neither affordable nor manageable. Although the computational requirement is at the limit of today's computing power, it is predictable that within a few years, 3-D modeling of fluid flow and heat transfer for some hundred spheres at high Reynolds numbers will be considered a normal situation.

GENERAL REFERENCES

- Allais, I., G. Alvarez, and D. Flick. 2006. Modelling cooling kinetics of a stack of spheres during mist chilling. Journal of Food Engineering 72:197-209.
- Alvarez, G., and G. Trystram. 1995. Design of a new strategy for the control of the refrigeration process: Fruit and vegetables conditioned in a pallet. Food Control 6:347-355.
- Alvarez, G., and D. Flick. 1999a. Analysis of heterogeneous cooling of agricultural products inside bins Part I: Aerodynamic study. Journal of Food Engineering 39:227-237.
- Alvarez, G., and D. Flick. 1999b. Analysis of heterogeneous cooling of agricultural products inside bins Part II: Thermal study. Journal of Food Engineering 39:239-245.
- Alvarez, G., P.E. Bournet, and D. Flick. 2003. Two-dimensional simulation of turbulent flow and transfer through stacked spheres. International Journal of Heat and Mass Transfer 46:2459-2469.
- Alvarez, G., and D. Flick. 2007. Modelling turbulent flow and heat transfer using macro-porous media approach used to predict cooling kinetics of stack of food products. Journal of Food Engineering 80:391-401.
- Amirante, R., P. Catalano, F. Fucci, and G. La Fianza. 2000. Planning and automated management of a horticultural station. Energy Conversion and Management 41:1237-1246.
- Amos, N.D., D.J. Cleland, and N.H. Banks. 1993. Effect of pallet stacking arrangement on fruit cooling rates within forced-air pre-coolers. Refrigeration Science and Technology 3:232-241.

- Anderson, B.A., A. Sarkar, J.F. Thompson, and R.P. Singh. 2004. Commercial-scale forced-air cooling of packaged strawberries. Transactions of the ASAE 47:183-190.
- Arifin, B.B., and K.V. Chau. 1988. Cooling of strawberries in cartons with new vent hole designs. ASHRAE Transactions 92:1415-1426.
- Baird, C.D., and J.J. Gaffney. 1976. A numerical procedure for calculating heat transfer in bulk loads of fruits and vegetables. ASHRAE Transactions 82:525-540.
- Baird, C., J. Gaffney, and M. Talbot. 1988. Design criteria for efficient and cost effective forced air cooling systems for fruits and vegetables. ASHRAE Transactions 94:1434-1454.
- Banks, N.H., K.M. Maguire, and D.J. Tanner. 2000. Innovation in postharvest handling systems. Journal of Agricultural Engineering Research 76:285-295.
- Bear, J. 1972. Dynamics of fluids in porous media American Elsevier Pub. Co., New York.
- Becker, B.R., A. Misra, and B.A. Fricke. 1996a. Bulk refrigeration of fruits and vegetables Part I: Theoretical considerations of heat and mass transfer. HVAC&R Research 2:122-134.
- Becker, B.R., A. Misra, and B.A. Fricke. 1996b. Bulk refrigeration of fruits and vegetables Part 2: Computer algorithm for heat loads and moisture loss. HVAC&R Research 2:215-230.

- Ben Amara, S., O. Laguerre, and D. Flick. 2004. Experimental study of convective heat transfer during cooling with low air velocity in a stack of objects.

 International Journal of Thermal Sciences 43:1213-1221.
- Beukema, K.J., S. Bruin, and J. Schenk. 1982. Heat and mass transfer during cooling and storage of agricultural products. Chemical Engineering Science 37:291-298.
- Bird, R.B., W.E. Stewart, and E.N. Lightfoot. 2002. Transport phenomena J. Wiley, New York.
- Brosnan, T., and D.W. Sun. 2001. Precooling techniques and applications for horticultural products a review. International Journal of Refrigeration-Revue Internationale Du Froid 24:154-170.
- Campanone, L.A., S.A. Giner, and R.H. Mascheroni. 1995. The use of a simulation software to optimize cooling times and to lower weight losses in fruit refrigeration, pp. 121-128 Proceedings of the 19th International Congress of Refrigeration Vol. 1.
- Campanone, L.A., S.A. Giner, and R.H. Mascheroni. 2002. Generalized model for the simulation of food refrigeration. Development and validation of the predictive numerical method. International Journal of Refrigeration-Revue Internationale Du Froid 25:975-984.
- Carbonell, R.G., and S. Whitaker. 1984. Heat and mass transfer in porous media, *In*J. Bear and M. Y. Corapcioglu, eds. Fundamentals of Transport Phenomena in Porous Media. Springer, New York.

- Carroll, N., R. Mohtar, and L.J. Segerlind. 1996. Predicting the cooling time for irregular shaped food products. Journal of Food Process Engineering 19:385-401.
- Chau, K.V., J.J. Gaffney, C.D. Baird, and G.A. Church. 1985. Resistance to air flow of oranges in bulk and in cartons. Transactions of the ASABE 28:2083-2088.
- Chau, K.V., R.A. Romero, C.D. Baird, and J.J. Gaffney. 1987. Transpiration coefficients of fruits and vegetables in refrigerated storage. ASHRAE Report: 370-RP. Atlanta: ASHRAE.
- Chourasia, M.K., and T.K. Goswami. 2007. CFD simulation of effects of operating parameters and product on heat transfer and moisture loss in the stack of bagged potatoes. Journal of Food Engineering 80:947-960.
- Chuntranuluck, S., C.M. Wells, and A.C. Cleland. 1998. Prediction of chilling times of foods in situations where evaporative cooling is significant Part 1.

 Method development. Journal of Food Engineering 37:111-125.
- Codina, R. 1993. A discontinuity-capturing crosswind-dissipation for the finite element solution of the convection-diffusion equation. Computer Methods in Applied Mechanics and Engineering 110:325-342.
- Comiti, J., and M. Renaud. 1989. A New Model for Determining Mean Structure Parameters of Fixed Beds from Pressure Drop Measurements Application to Beds Packed with Parallelepipedal Particles. Chemical Engineering Science 44:1539-1545.
- COMSOL MultiphysicsTM. 2007. COMSOL Multiphysics User's Guide. COMSOL Inc., Burlington, Massachusetts.

- Cortbaoui, P., B. Goyette, Y. Gariépy, M.T. Charles, G.S.V. Raghavan, and C. Vigneault. 2006. Forced air cooling system for Zea mays. Journal of Food, Agriculture & Environment 4:100-104.
- Datta, A.K. 2007. Porous media approaches to studying simultaneous heat and mass transfer in food processes. I: Problem formulations. Journal of Food Engineering 80:80-95.
- de Castro, L.R., C. Vigneault, and L.A.B. Cortez. 2004a. Container opening design for horticultural produce cooling efficiency. Journal of Food, Agriculture & Environment 2:135-140.
- de Castro, L.R., C. Vigneault, and L.A.B. Cortez. 2004b. Effect of container opening area on air distribution during precooling of horticultural produce.

 Transactions of the ASABE 47:2033-2038.
- de Castro, L.R., C. Vigneault, and L.A.B. Cortez. 2005a. Cooling performance of horticultural produce in containers with peripheral openings. Postharvest Biology and Technology 38:254-261.
- de Castro, L.R., C. Vigneault, and L.A.B. Cortez. 2005b. Effect of container openings and airflow on energy required for forced air cooling of horticultural produce. Canadian Biosystems Engineering 47:3.1-3.9.
- Dehghannya, J., M. Ngadi, and C. Vigneault. 2008. Simultaneous aerodynamic and thermal analysis during cooling of stacked spheres inside ventilated packages. Chemical Engineering and Technology 31(11): 1651-1659.
- Dehghannya, J., M. Ngadi, and C. Vigneault. Mathematical modeling of airflow and heat transfer during forced convection cooling of produce intended for optimal package design. Transactions of the Institution of Chemical

- Engineers (IChemE) Part C, Food and Bioproducts Processing. Submitted for publication 1.
- Dehghannya, J., M. Ngadi, and C. Vigneault. Direct numerical simulation of produce cooling in ventilated packages. Journal of Food Engineering. Submitted for publication 2.
- Delele, M.A., E. Tijskens, Y.T. Atalay, Q.T. Ho, H. Ramon, B.M. Nicolai, and P. Verboven. 2008. Combined discrete element and CFD modelling of airflow through random stacking of horticultural products in vented boxes. Journal of Food Engineering 89:33-41.
- Dincer, I. 1993. An exact heat transfer analysis of spherical products subjected to forced-air cooling. International Journal of Energy Research 17:9-18.
- Dincer, I. 1995. An Effective Method for Analyzing Precooling Process Parameters.

 International Journal of Energy Research 19:95-102.
- Edeogu, I., J. Feddes, and J. Leonard. 1997. Comparison between vertical and horizontal airflow for fruit and vegetable precooling. Canadian Agricultural Engineering 39:107-112.
- Eisfeld, B., and K. Schnitzlein. 2001. The influence of confining walls on the pressure drop in packed beds. Chemical Engineering Science 56:4321-4329.
- Elman, H.C., and A. Ramage. 2002. An analysis of smoothing effects of upwinding strategies for the convection-diffusion equation. SIAM Journal on Numerical Analysis 40:254-281.

- Emond, J.P., F. Mercier, S.O. Sadfa, M. Bourre, and A. Gakwaya. 1996. Study of parameters affecting cooling rate and temperature distribution in froced-air precooling of strawberry. Transactions of the ASAE 39:2185-2191.
- Ergun, S. 1952. Fluid Flow through Packed Columns. Chemical Engineering Progress 48:89-94.
- Faubion, D.F., and A.A. Kader. 1997. Influence of place packing or tray packing on the cooling rate of palletized 'Anjou' pears. Hort Technology 7:378-382.
- Ferrua, M.J., and R.P. Singh. 2007. Modelling airflow through vented packages containing horticultural products, *In* D.-W. Sun, ed. Computational Fluid Dynamics in Food Processing. CRC Press, Florida.
- Ferrua, M.J., and R.P. Singh. 2008. A nonintrusive flow measurement technique to validate the simulated laminar fluid flow in a packed container with vented walls. International Journal of Refrigeration-Revue Internationale Du Froid 31:242-255.
- Fikiin, A.G., K.A. Fikiin, and S.D. Triphonov. 1999. Equivalent thermophysical properties and surface heat transfer coefficient of fruit layers in trays during cooling. Journal of Food Engineering 40:7-13.
- Fricke, B.A. 2006. Precooling fruits & vegetables. ASHRAE Journal 48:20-28.
- Gaffney, J.J., C.D. Baird, and K.V. Chau. 1985a. Influence of airflow rate, respiration, evaporative cooling, and other factors affecting weight loss calculations for fruits and vegetables. ASHRAE Transactions 91:690-707.

- Gaffney, J.J., C.D. Baird, and K.V. Chau. 1985b. Methods for calculating heat and mass transfer in fruits and vegetables individually and in bulk. ASHRAE Transactions 91:333-352.
- Galeao, A.C., R.C. Almeida, S.M.C. Malta, and A.E. Loula. 2004. Finite element analysis of convection dominated reaction-diffusion problems. Applied Numerical Mathematics 48:205-222.
- Gan, G., and J.L. Woods. 1989. A deep bed simulation of vegetable cooling, pp. 2301-2308, In V. A. Dodd and P. M. Grace, (eds.) Agricultural Engineering: Proceedings of the Eleventh International Congress on Agricultural Engineering. A.A. Balkema, Rotterdam, Netherlands; Brookfield, VT., Dublin, 4-8 September.
- Geankoplis, C.J. 2003. Transport processes and separation process principles: (includes unit operations). Prentice Hall Professional Technical Reference, Upper Saddle River, New Jersey.
- Gowda, B.S., G.S.V.L. Narasimham, and M.V.K. Murthy. 1997. Forced-air precooling of spherical foods in bulk: A parametric study. International Journal of Heat and Fluid Flow 18:613-624.
- Goyette, B., C. Vigneault, B. Panneton, and G.S.V. Raghavan. 1996. Method to evaluate the average temperature at the surface of a horticultural crop. Canadian Agricultural Engineering 38:291-295.
- Hass, E., G. Felsenstein, A. Shitzer, and G. Manor. 1976. Factors affecting resistance to airflow through packed fresh fruit. ASHRAE Transactions 82:548-554.

- He, S.Y., and Y.F. Li. 2003. Theoretical simulation of vacuum cooling of spherical foods. Applied Thermal Engineering 23:1489-1501.
- Hetsroni, G., C.F. Li, A. Mosyak, and I. Tiselj. 2001. Heat transfer and thermal pattern around a sphere in a turbulent boundary layer. International Journal of Multiphase Flow 27:1127-1150.
- Hoang, M.L., P. Verboven, J. De Baerdemaeker, and B.M. Nicolai. 2000. Analysis of the air flow in a cold store by means of computational fluid dynamics. International Journal of Refrigeration-Revue Internationale Du Froid 23:127-140.
- Hoang, M.L., P. Verboven, M. Baelmans, and B.M. Nicolai. 2003. A continuum model for airflow, heat and mass transfer in bulk of chicory roots. Transactions of the ASABE 46:1603-1611.
- Hoang, M.L., P. Verboven, M. Baelmans, and B.M. Nicolai. 2004. Sensitivity of temperature and weight loss in the bulk of chicory roots with respect to process and product parameters. Journal of Food Engineering 62:233-243.
- Holdredge, R.M., and R.E. Wyse. 1982. Computer simulation of the forced convection cooling of sugarbeets. Transactions of the ASABE 25:1425-1430.
- Hu, Z.H., and D.W. Sun. 2000. CFD simulation of heat and moisture transfer for predicting cooling rate and weight loss of cooked ham during air-blast chilling process. Journal of Food Engineering 46:189-197.
- Janick, J. 1986. Horticultural science. 4th ED W.H. Freeman, New York.

- John, V., and P. Knobloch. 2007. On spurious oscillations at layers diminishing (SOLD) methods for convection-diffusion equations: Part I A review. Computer Methods in Applied Mechanics and Engineering 196:2197-2215.
- Jooste, M.M., and P. Khumalo. 2005. Effect of the rate and duration of forced air cooling on the quality of 'Imperial' apricots and 'Pioneer' and 'Songold' plums. Acta Horticulturae (ISHS) 682:1633-1638.
- Kader, A.A. 2002. Postharvest technology of horticultural crops, 3rd ed. University of California, Division of Agriculture and Natural Resources, Oakland, California.
- Kaviany, M. 1995. Principles of heat transfer in porous media Springer-Verlag, New York.
- Kim, J., P. Moin, and R. Moser. 1987. Turbulence Statistics in Fully-Developed Channel Flow at Low Reynolds-Number. Journal of Fluid Mechanics 177:133-166.
- Kumar, R., A. Kumar, and U.N. Murthy. 2008. Heat transfer during forced air precooling of perishable food products. Biosystems Engineering 99:228-233.
- Ladaniya, M.S., and S. Singh. 2000. Influence of ventilation and stacking pattern of corrugated fibre board containers on forced-air pre-cooling of 'Nagpur' mandarins. Journal of Food Science and Technology-Mysore 37:233-237.
- Liu, S.J., and J.H. Masliyah. 1996. Single fluid flow in porous media. Chemical Engineering Communications 150:653-732.

- Lube, G., and G. Rapin. 2006. Residual-based stabilized higher-order FEM for advection-dominated problems. Computer Methods in Applied Mechanics and Engineering 195:4124-4138.
- Macdonald, I.F., M.S. Elsayed, K. Mow, and F.A.L. Dullien. 1979. Flow through Porous Media Ergun Equation Revisited. Industrial and Engineering Chemistry Fundamentals 18:199-208.
- Nahor, H.B., M.L. Hoang, P. Verboven, M. Baelmans, and B.M. Nicolai. 2005. CFD model of the airflow, heat and mass transfer in cool stores. International Journal of Refrigeration-Revue Internationale Du Froid 28:368-380.
- Natarajan, R., and A. Acrivos. 1993. The Instability of the Steady Flow Past Spheres and Disks. Journal of Fluid Mechanics 254:323-344.
- Nijemeisland, M., and A.G. Dixon. 2004. CFD study of fluid flow and wall heat transfer in a fixed bed of spheres. AICHE Journal 50:906-921.
- Opara, L.U., and Q. Zou. 2007. Sensitivity analysis of a CFD modelling system for airflow and heat transfer of fresh food packaging: Inlet air flow velocity and inside-package configurations. International Journal of Food Engineering 3: Article 16.
- Portela, L.M., P. Cota, and R.V.A. Oliemans. 2002. Numerical study of the near-wall behaviour of particles in turbulent pipe flows. Powder Technology 125:149-157.
- Quintard, M., M. Kaviany, and S. Whitaker. 1997. Two-medium treatment of heat transfer in porous media: Numerical results for effective properties.

 Advances in Water Resources 20:77-94.

- Ranade, V. 2002. Computational Flow Modeling for Chemical Reactor Engineering. Academic Press, New York.
- Rennie, T.J., G.S.V. Raghavan, C. Vigneault, and Y. Gariepy. 2001. Vacuum cooling of lettuce with various rates of pressure reduction. Transactions of the ASABE 44:89-93.
- Rennie, T.J., C. Vigneault, J.R. Deell, and G.S.V. Raghavan. 2003. Cooling and storage, p. 505-538, *In A. Chakraverty*, et al., eds. Handbook of Postharvest Technology, ed. Marcel Dekker, New York.
- Rodriguez-Bermejo, J., P. Barreiro, J.I. Robla, and L. Ruiz-Garcia. 2007. Thermal study of a transport container. Journal of Food Engineering 80:517-527.
- Sastry, S.K., C.D. Baird, and D.E. Buffington. 1978. Transpiration rates of certain fruits and vegetables. ASHRAE Transactions 84:237-255.
- Sastry, S.K., and D.E. Buffington. 1982. Transpiration rates of stored perishable commodities: A mathematical model and experiments on tomatoes. ASHRAE Transactions 88:159-184.
- Smale, N.J., J. Moureh, and G. Cortella. 2006. A review of numerical models of airflow in refrigerated food applications. International Journal of Refrigeration-Revue Internationale Du Froid 29:911-930.
- Smale, N.J., D.J. Tanner, N.D. Amos, and D.J. Cleland. 2003. Airflow properties of packaged horticultural produce a practical study Acta Horticulturae (ISHS) 599:443-450.

- Stanley, R. 1989. The influence of temperature and packaging material on the post harvest quality of iceberg lettuce. Acta Horticulturae 244:171-177.
- Sullivan, G., L. Davenport, and J. Julian. 1996. Progress in new crops: Precooling: key factor for assuring quality in new fresh market vegetable crops. ASHS Press, Arlington: Virginia
- Talbot, M.T., C.C. Oliver, and J.J. Gaffney. 1990. Pressure and velocity distribution for air flow through fruits packed in shipping containers using porous media flow analysis. ASHRAE Transactions 96:406-417.
- Tanner, D.J., A.C. Cleland, L.U. Opara, and T.R. Robertson. 2002a. A generalised mathematical modelling methodology for design of horticultural food packages exposed to refrigerated conditions: part 1, formulation. International Journal of Refrigeration 25:33-42.
- Tanner, D.J., A.C. Cleland, and L.U. Opara. 2002b. A generalised mathematical modelling methodology for the design of horticultural food packages exposed to refrigerated conditions Part 2. Heat transfer modelling and testing. International Journal of Refrigeration-Revue Internationale Du Froid 25:43-53.
- Tanner, D.J., A.C. Cleland, and T.R. Robertson. 2002c. A generalised mathematical modelling methodology for design of horticultural food packages exposed to refrigerated conditions: Part 3, mass transfer modelling and testing. International Journal of Refrigeration-Revue Internationale Du Froid 25:54-65.
- Tashtoush, B. 2000. Natural losses from vegetable and fruit products in cold storage. Food Control 11:465-470.

- Tassou, S.A., and W. Xiang. 1998. Modelling the environment within a wet air-cooled vegetable store. Journal of Food Engineering 38:169-187.
- Tezduyar, T.E. 1992. Stabilized finite element formulations for incompressible flow computations, p. 1-44 Advances in Applied Mechanics, Vol. 28.
- Thompson, A.K. 1996. Postharvest technology of fruit and vegetables Blackwell Science, Oxford, England
- Turek, S. 1999. Efficient solvers for incompressible flow problems / an algorithmic and computational approach. Springer-Verlag, Berlin, New York.
- Vafai, K., and C.L. Tien. 1982. Boundary and Inertia Effects on Convective Mass Transfer in Porous Media. International Journal of Heat and Mass Transfer 25:1183-1190.
- Van der Sman, R.G.M. 2002. Prediction of airflow through a vented box by the Darcy-Forchheimer equation. Journal of Food Engineering 55:49-57.
- Verboven, P., M.L. Hoang, M. Baelmans, and B.M. Nicolai. 2004. Airflow through beds of apples and chicory roots. Biosystems Engineering 88:117-125.
- Verboven, P., D. Flick, B.M. Nicolai, and G. Alvarez. 2006. Modelling transport phenomena in refrigerated food bulks, packages and stacks: basics and advances. International Journal of Refrigeration-Revue Internationale Du Froid 29:985-997.
- Vigneault, C., and B. Goyette. 2002. Design of plastic container opening to optimize forced-air precooling of fruits and vegetables. Applied Engineering in Agriculture 18:73-76.

- Vigneault, C., B. Goyette, N.R. Markarian, C.K.P. Hui, S. Cote, M.T. Charles, and J.P. Emond. 2004. Plastic container opening area for optimum hydrocooling. Canadian Biosystems Engineering 46:3.41-3.44.
- Vigneault, C., and L.R. de Castro. 2005. Produce-simulator property evaluation for indirect airflow distribution measurement through horticultural crop package. Journal of Food, Agriculture & Environment 3:67-72.
- Vigneault, C., and L.R. de Castro. 2006. Indirect measurement method for laminar to turbulent airflow through horticultural produce simulators. Transactions of the ASABE 49:1455-1461.
- Vigneault, C., B. Goyette, and L.R. De Castro. 2006. Maximum slat width for cooling efficiency of horticultural produce in wooden crates. Postharvest Biology and Technology 40:308-313.
- Wakao, N., and S. Kaguei. 1982. Heat and Mass Transfer in Packed Beds Routledge, New York.
- Wilcox, D.C. 1993. Turbulence modeling for CFD. DCW Industries, Inc., La Canada, California.
- Wills, R.B.H. 1998. Postharvest: an introduction to the physiology & handling of fruit, vegetables & ornamentals UNSW Press; Cab International, Sydney, Australia: Wallingford, Oxon, UK; New York.
- Xu, Y.F., and D. Burfoot. 1999. Simulating the bulk storage of foodstuffs. Journal of Food Engineering 39:23-29.
- Zou, Q., L.U. Opara, and R. McKibbin. 2006a. A CFD modeling system for airflow and heat transfer in ventilated packaging for fresh foods: I. Initial analysis

and development of mathematical models. Journal of Food Engineering 77:1037-1047.

Zou, Q.A., L.U. Opara, and R. McKibbin. 2006b. A CFD modeling system for airflow and heat transfer in ventilated packaging for fresh foods: II. Computational solution, software development, and model testing. Journal of Food Engineering 77:1048-1058.